# Optimization of Charging Stations on a Route with Electric Buses

RIKKE HELENE BÆKKEN

SUPERVISOR

Mohan Lal Kolhe

**University of Agder, 2019**

Faculty of Engineering and Science

Department of Engineering Sciences

# ABSTRACT

This study considers placement of electric charging stations for a public electric bus system with the intention of minimizing the charging power. This is an optimization problem where fully electric buses with opportunity charging strategy are considered. The developed strategies are proposed for an existing bus route in Oslo city, Norway.

Battery and charging specifications were determined based on a literature review. Measurements regarding velocity of the bus and altitude of the route were performed. This data where further used to determine the energy needs for an electric bus. Four cases were formed regarding different battery capacities, desired end battery levels, maximum charging powers and end stop regulation times. Further, a mathematical model was developed and verified in order to solve the optimization. The optimization model was developed in terms of an objective function with the intention of minimizing the charging power subject to constraints regarding battery operation ranges and charging power restrictions.

The four optimized cases showed that electric buses with opportunity charging strategy is possible for the selected route. Three of the cases were optimized to have two charging stations at each end stop. The charging power at each station was reduced by having lower desired end battery level and lower battery capacity. The optimized placement of the charging stations was at those bus stops where the bus stand for the longest time. To minimize the charging power each station should be distributed with equal charging powers. Another measure may be to include external batteries connected to the charging stations.

Bus route characteristics, driving cycles and available grid capacity are essential considerations when planning an electric bus system. As for further works, it will be interesting to develop the optimization model to have the possibility of operating with multiple electric bus routes. By doing so, the system will be considered in a wider perspective giving the opportunity to plan a more accurate an effective electric bus system.

# PREFACE

This report is a result of my master's thesis in the study program Renewable Energy at the University of Agder in Grimstad, Norway. The master program is a two yearlong study and before this I finished a bachelor's degree in Renewable Energy at the Norwegian University of Science and Technology in Gjøvik, Norway.

The master's thesis corresponds to 30 study credits which is equivalent to one semester lasting from 07.01.2019 until 24.05.2019. The report considers optimization of placement of electric charging stations on a route with electric buses in Oslo city, Norway. The target group for which this thesis was written for are those that are involved in planning electric bus systems, electric bus and charging infrastructure owners and operators as well as everyone that is interesting in optimization of charging station placement.

My interest of the electric bus technology started when writing the bachelor's thesis. In the bachelor, a pilot project on electric buses was considered and evaluated for a bus route in Hamar, Norway. Because of this, it was desirable to continue the learning and get a more complex understanding of the challenges and considerations related to electric buses. The master's thesis period has been an exciting, challenging and interesting time. The semester has given a steep learning curve regarding optimization, independent work and electric bus and infrastructure knowledge.

I wish to thank my supervisor Mohan Lal Kolhe, professor at UiA Grimstad, for guidance and valuable inputs regarding my thesis. Further, I wish to thank my external supervisor Kristine Ristad, engineer at COWI, together with the rest of the people at COWI for ideas, contact network and discussions. I also want to thank Sandun Yasantha Konara Konara Mudiyanselage, PhD research fellow at UiA Grimstad, for useful assistance. In addition, a thanks to Werner Klausen, my contact person in Hafslund Nett As, for providing data on electrical substations. I also wish to thank family and friends for support and encouragement.

*Rikke Helene Bækken*

University of Agder, Grimstad, May 24, 2019

## INDIVIDUAL DECLARATION

The individual student or group of students is responsible for the use of legal tools, guidelines for using these and rules on source usage. The statement will make the students aware of their responsibilities and the consequences of cheating. Missing statement does not release students from their responsibility.

| 1. | I hereby declare that my thesis is my own work and that I have not used any other sources or have received any other help than mentioned in the thesis. | ☒ |
|----|----|----|
| 2. | I further declare that this thesis:<br><br>- has not been used for another exam at another department/university/university college in Norway or abroad;<br>- does not refer to the work of others without it being stated;<br>- does not refer to own previous work without it being stated;<br>- have all the references given in the literature list;<br>- is not a copy, duplicate or copy of another's work or manuscript. | ☒ |
| 3. | I am aware that violation of the above is regarded as cheating and may result in cancellation of exams and exclusion from universities and colleges in Norway, see Universitets- og høgskoleloven §§4-7 og 4-8 og Forskrift om eksamen §§ 31. | ☒ |
| 4. | I am aware that all submitted theses may be checked for plagiarism. | ☒ |
| 5. | I am aware that the University of Agder will deal with all cases where there is suspicion of cheating according to the university's guidelines for dealing with cases of cheating. | ☒ |
| 6. | I have incorporated the rules and guidelines in the use of sources and references on the library's web pages. | ☒ |

## PUBLISHING AGREEMENT

Authorization for electronic publishing of the thesis.

Author(s) have copyrights of the thesis. This means, among other things, the exclusive right to make the work available to the general public (Åndsverkloven. §2).

All theses that fulfill the criteria will be registered and published in Brage Aura and on UiA's web pages with author's approval.

Theses that are not public or are confidential will not be published.

I hereby give the University of Agder a free right to

make the task available for electronic publishing:     ☒YES   ☐NO

Is the thesis confidential?     ☐YES   ☒NO

 (confidential agreement must be completed)

   - If yes:

Can the thesis be published when the confidentiality period is over?   ☐YES   ☐NO

Is the task except for public disclosure?     ☐YES   ☒NO

(contains confidential information. see Offl. §13/Fvl. §13)

**UiA** University of Agder

# UNIVERSITETET I AGDER
## FAKULTET FOR TEKNOLOGI OG REALFAG

By order of Dean of Faculty of Engineering and Science: 30.01.2018

## STANDARD AGREEMENT

**concerning work on a bachelor's thesis/master's thesis/project assignment (academic work) done in cooperation with a company/external organization (organization).**

This is the authoritative agreement that governs academic work by students at the UiA Faculty of Engineering and Science that is carried out in cooperation with an organization.

The involved parties have the responsibility to clarify whether or not a third party (that is not a party to this agreement) may have intellectual property rights to the project background before the latter is used in connection with the academic work.

Agreement between

| Student: Rikke Helene Bækken | Date of birth: 09-08-1994 |
|---|---|

| Supervisor(s) at UiA: Mohan Lal Kolhe | |
|---|---|

| Company/external organization: COWI | |
|---|---|

and

| University of Agder (UiA), represented by the Head of Department: | |
|---|---|

concerning the use and exploitation of the results from a bachelor's thesis/master's thesis/project assignment.

### 1. Description of the academic work
The student is to carry out

| Bachelor's thesis | ☐ |
|---|---|
| Master's thesis | ☒ |
| Project assignment | ☐ |

(insert cross)

In cooperation with

| COWI |
|---|

company/external organization:

| 07-01-2019 – 24-05-2019 |
|---|

starting date – completion date (dd-mm-yyyy)

Title of the academic work:

| Implementation of electric bus charger stations into the distribution net |
|---|

UiA 2018-01-30          Page 1 of 4

The responsible supervisor at UiA has overall academic responsibility for structuring and approving the description of the academic work and the student's learning.

**2. Responsibilities of the organization**

The organization is to appoint a contact person who has the necessary experience in supervision and will give the student adequate supervision in cooperation with the supervisor at UiA. The contact person at the organization is:

The organization is to appoint a contact person who shall provide the student with the necessary work resources at the organization and, if possible, contribute in supervision in cooperation with supervisor at UiA. The organization's contact person is:

Kristine Ristad

The purpose of completing the academic work is academic training for the student. The academic work is part of a student's course of study and the student is not to receive wages or similar compensation from the organization. The organization agrees to cover the following expenses that are associated with carrying out the academic work:

Access to PC if necessary

**3. Rights of the parties**

**a) The student**

The student holds the copyright to his/her academic work. All intellectual property rights to the results of the academic work done by the student alone during the academic work are held by the student with the reservations stated in points b) and c) below.

The student has the right to enter into an agreement with UiA concerning the publication of his/her academic work in UiA's institutional archive on the Internet. The student has also the right to publish his/her academic work or parts of it in other media providing the present agreement has not imposed restriction concerning publication, cf. Clause 4.

**b) The organization**

If the academic work is based on or develops materials and/or methods (project background) that are owned by the organization, the project background is owned by the organization. If the development work that includes the project background can be commercially exploited, it is assumed that a separate agreement will be drawn up concerning this between the student and the organization.

The organization is to have the right to use the results of the academic work in its own activities providing the commercial exploitation falls within the activities of the organization. This is to be interpreted in accordance with the terminology used in Section 4 of the Act Respecting the Right to Employees' Inventions (Arbeidstakeroppfinnelsesloven). This right is non-exclusive.

The use of the results of the academic work outside of the activities of the organization, cf. the last paragraph above, assumes that a separate agreement will be drawn up between the student and the organization. The agreement between the student and the organization concerning the rights to the results of the academic work produced by the student is to be in writing and the agreement is invalid until UiA has received a copy of the agreement in writing.

If the value of the results of the academic work is considerable, i.e. it is more than NOK 100 000, the student is entitled to receive reasonable compensation. Section 7 of the Act Respecting the Right to Employees' Inventions states how the amount of compensation is to be calculated. This right to compensation also applies to non-patentable results. Section 7 of the Act also states the applicable deadlines.

### c) UiA
All copies of the submitted academic work/files containing the academic work and any appendices that are necessary for determining a grade and for the records at UiA, are the property of UiA.
The academic work and any appendices to it can be used by UiA for educational and scientific purposes free of charge, except when the restrictions specified in Clause 4 are applicable.

### 4. Delayed publication
The general rule is that academic work by students is to be available in the public domain. If there are specific circumstances, the parties can agree to delay the publication of all or part of the academic work for a maximum of 5 years, i.e. the work is not available for other students or organizations during this period.

The academic work is subject to delayed publication for:

| | |
|---|---|
| one year | ☐ |
| two years | ☐ |
| three years | ☐ |
| five years | ☐ |

(insert cross next to the number of years if this clause applies)

The reasons for delayed publication are as follows:

| |
|---|
| |

The parts of the academic work that are not subject to delayed publication can be published in UiA's institutional archive, cf. Clause 3 a) second paragraph.

Even if the academic work is subject to delayed publication, the organization is to make it possible for the student to use all or part of his/her academic work in connection with a job application or follow-up work in connection with doctoral study.
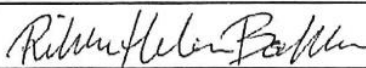
## 5. General

This agreement takes precedence over any other agreements that are or will be entered into by two of the parties mentioned above. In case the student and the organization are to enter into a confidentiality agreement concerning information the student obtains while he/she is at the organization, UiA's template for a confidentiality agreement is to be used for this purpose. If there is such an agreement, it is to be appended to the present agreement.

Should there be any dispute relating to this agreement, it should be resolved by negotiation. If this does not lead to a solution, the parties agree to the matter being resolved by arbitration in accordance with Norwegian law. Any such dispute is to be decided by Agder District Court or a body appointed by this court.

This agreement is signed in 4 - four - copies, where each party to this agreement is to keep one copy. The agreement comes into effect when it has been approved and signed by UiA represented by the Head of Department.

Note that the Norwegian version of this standard agreement is the authoritative version.

Grimstad, 25-01-2019

place, date (dd-mm-yyyy) — student

31/01/2019 Grimstad

place, date (dd-mm-yyyy) — supervisor at UiA

GRIMSTAD 04 MAR 2019

place, date (dd-mm-yyyy) — Head of Department, UiA

UNIVERSITY OF AGDER
Department of engineering

Oslo, 01/02/2019

place, date (dd-mm-yyyy) — for company/organization signed and stamped

# TABLE OF CONTENTS

# LIST OF FIGURES

# LIST OF TABLES

# LIST OF SYMBOLS

| | |
|---|---|
| $A_{front}$ | Frontal area of 18-meter bus, m$^2$ |
| $a_{max}$ | Maximum acceleration for the bus to convert power from regenerative breaking, m/s$^2$ |
| $a_t$ | Acceleration of bus at time $t$, m/s$^2$ |
| $C_{drag}$ | Drag coefficient on bus |
| $E_{batt}$ | Battery capacity of the bus, kWh |
| $e_{c(i-1,i)}$ | Consumed energy by the bus when driving from bus stop $i$ to the next stop $i+1$, kWh |
| $E_{end}$ | Energy in battery at bus stop $n$ without any charging operation along route $k$, kWh |
| $E_{end,w}$ | Energy in battery at the end of route with considering charging stations, kWh |
| $E_{end,wo}$ | Energy in battery at the end of route without considering charging stations, kWh |
| $E_i$ | Energy in battery at a selected bus stop $i$, kWh |
| $e_{init}$ | Initial energy in the battery before the bus leaves the first bus stop, kWh |
| $E_{placed,i}$ | Energy in battery at those stops where a charging station is placed at stop $i$, kWh |
| $E_{rc}$ | Total recharged energy along bus route $k$, kWh |
| $E_{rc}$ | Total energy recharged along route $k$, kWh |
| $E_{req}$ | Total minimum energy required along route $k$, kWh |
| $E_{req}$ | Total required energy along bus route $k$, kWh |
| $E_t$ | Energy in battery at time $t$, kWh |
| $F_{air,t}$ | Air resistance force on bus at time $t$, N |
| $F_{grad,t}$ | Gradient resistance force on bus at time $t$, N |
| $F_{roll,t}$ | Rolling resistance force on bus at time $t$, N |
| $g$ | Gravitational acceleration on earth, m/s$^2$ |
| $h_t$ | Altitude at time $t$, m |
| $i$ | A specific bus stop in the route |
| $i+1$ | The bus stop next to bus stop $i$ |
| $i-1$ | The bus stop previously to bus stop $i$ |
| $I_{chg,i}$ | Charging current in charging station at bus stop $i$, A |
| $i$ | Current in battery according to time $t$, A |
| $ll$ | The battery's minimum preferable energy level, % |
| $l_t$ | Traveled distance at time $t$, m |
| $m$ | Total weight of the bus including passenger load and battery, kg |
| $m_{batt}$ | Battery weight, kg |

| | |
|---|---|
| $n$ | Number of stops in the route |
| $nC$ | Discharging or charging rate (C-rate) of battery, C |
| $n_{cell}$ | Number of parallel connected battery cells in a battery |
| $P_{acc}$ | Power required related to accessories in the bus, kWh |
| $P_{batt,t}$ | Battery power required to operate the bus at time $t$, kW |
| $P_{chg,i}$ | Charging power at bus stop $i$, kW |
| $P_{chg,max,i}$ | Maximum charging power at bus stop $i$, kW |
| $P_{chg,tot}$ | Total charging power for the chargers along the bus route, kW |
| $P_s$ | Battery energy density, wh/kg |
| $P_t$ | Power income or outcome of battery at time $t$, kW |
| $P_{tract,t}$ | Tractive power on bus at time $t$, kW |
| $Q_{cell}$ | Total battery capacity, Ah |
| $Q_{stored,t}$ | Energy stored at time $t$, Ah |
| $r$ | Regulation time at end stops, min |
| $r_{internal}$ | Internal resistance in battery, Ω |
| $soc_{end}$ | State-of-charge in battery at the end of the optimized bus route |
| $SOC_{init}$ | Initial energy in the battery before the bus leaves the first bus stop $i$ at time $t$, % |
| $SOC_t$ | State of charge in battery at time $t$, % |
| $t$ | At a specific time in the driving route, sec |
| $T_i$ | Stopping time at bus stop $i$, h |
| $ul$ | The battery's maximum preferable energy level, % |
| $U_{terminal(pack)}$ | Terminal energy in battery pack, V |
| $U_{terminal,t}$ | Terminal voltage in battery at time $t$, V |
| $V_{max(cell)}$ | Maximum voltage of one single battery cell, V |
| $V_{max(pack)}$ | Maximum voltage in battery pack, V |
| $v_{min}$ | Minimum velocity for the bus to covert power from regenerative breaking, m/s |
| $v_{oc}$ | Open circuit voltage in battery according to time $t$, V |
| $v_t$ | Velocity of bus at time $t$, m/s |
| $v_{w,t}$ | Wind speed at the location of the bus at time $t$, m/s$^2$ |
| $x_i$ | Placement of charging stations at bus stop $i$ |
| $\eta_{batt}$ | Battery efficiency factor |
| $\eta_{chg}$ | Charger efficiency factor |

| $\eta_{fd}$ | Final drive efficiency factor |
|---|---|
| $\eta_{mot}$ | Motor efficiency factor |
| $\eta_{re}$ | Regenerated efficiency factor |
| $\eta_{tot}$ | Total efficiency factor of the drivetrain and electric components of the bus |
| $\eta_{wh}$ | Wheel drive efficiency factor |
| $\theta_t$ | Road angle at time $t$, rad |
| $\mu$ | Rolling friction coefficient of bus |
| $\rho$ | Air density of Earth's surface, kg/m$^3$ |

# 1   INTRODUCTION

The Paris Agreement states that the globally greenhouse gas (GHG) emissions should be at a net zero level by 2050 [1, p. 10]. As a result, conscious actions towards decarbonization and a sustainable energy transition are to be prioritized in the coming years. Today, more than half of the population lives in cities and the share is being predicted to grow [2]. Also, the main energy source worldwide is fossil fuels; whenever this is for transportation use, electricity supply or industry [3]. Consequently, the GHG emissions in cities, which already stand for up to 70 % of the total GHG emissions [3, p. 51], will increase if no climate actions are made. Therefore, cities will be an important participator in achieving the climate goal.

The transit bus system in cities typically consist of diesel powered vehicles which does not only contribute to air pollution but also cause related airborne health issues [4]. One promising mobility alternative is the use of electric driven buses which currently are the most common net-zero bus system [5]. Electric buses are supplied with electricity by an on-board battery which is periodically charged from an energy source [6]. By ensuring the energy source is renewable, adopting a 100 % electric transportation service can reduce up to 23 % of the GHG emissions in a city [7]. An electric bus do also contribute to lower noise and vibration level than a conventional diesel bus, and gives better local air quality due to no harmful emissions when in operation [6]. These advantages makes electric buses an attractive alternative, and cities in especially Europe, China and North-America has started to procure them [4, 5].

Planning and implementation of an electric bus system is a complex work that differ from a conventional bus system [8]. Several factors and actors need to be considered such as establishing a dedicated charging infrastructure, as well make sure that the bus configuration is suitable for the routes and schedules. Modeling and simulating the system may provide valuable information about the bus and charging requirements for a specific route and can make the planning of such a system more accurate and effective.

## 1.1   MOTIVATION

The motivation for doing a study regarding electric buses was based on a preliminary project completed in the previous semester. From the preliminary work it came forward that optimization of electric bus charging stations are a more advanced task than assumed and that further studies may be done. Therefore, it was desirable to continue working on this subject. The preliminary project will be further described in the next section.

The interest of the electric bus technology started when writing the bachelor's thesis in 2016. In the bachelor, a pilot project on electric buses were considered and evaluated for a bus route in Hamar city, Norway. Based on this work it was desirable to continue the learning and get a more complex understanding of the challenges and considerations related to electric buses. In the beginning of 2016 when writhing the bachelor's thesis, for instance in Norway, two fully electric buses (excluding trolley buses) was in ordinary operation in Stavanger. Three years later, now finishing the master's thesis, electric buses are operating in many of the largest cities in Norway, and within a short period there are expected to be large scale fleets in Oslo, Trondheim and Bergen. Because of this development electric

buses are not only relevant to investigate but also important so that challenges can be noted, and the technology can be evolved in the most optimal way.

COWI, a consulting group with competence within engineering, economics and environmental science, was contacted to hear if a cooperation was possible. This was done because a cooperation with an external company seemed beneficial. Having a cooperation gave the opportunity to get insight in the electric bus marked through a company perspective. In addition, get a contact network that can be advantage for the master's thesis. It turned out that COWI was interested in doing a collaboration. They provided ideas, input and contacts regarding this study.

## 1.2 PRELIMINARY STUDY

This study is somewhat based on a preliminary work [9] done in the second semester of 2018 and will therefore briefly be described before the problem of this study. The preliminary study was an optimization problem considering placement of electric bus charging stations. The goal was to determine the number of charging stations required along a fictive bus route and place them so that the total installation cost would be minimized. A next-generation opportunity charging strategy was considered. This alternative is characterized by operating with high charging power for some seconds while the passengers are embarking and disembarking on the bus stops along the route. Linear programming was used to solve the optimization problem.

The learning outcome of the preliminary study was that this type of bus alternative may best suite bus routes with a 24/7-hour operation. It was found that the number of charging stations depends highly on the initial energy in the battery. A fully charged battery gives a longer range, and then consequently, fewer charging stations are required. However, to complete more than one trip the bus is dependent on having a charging station in the end to fully charge the battery. This is because the energy charged along the route would not be enough to operate on the next trip. The installation costs were found to be highly location specific depending on factors such as topography, available electrical subsection and the distance between the subsection and the charging station.

One recommendation for this study was to evolve and advance the system modeled including return trip and make it suitable for several buses along the route. Optimization of an actual route would be interesting to do as every route is unique making a general optimization not applicable for this type of problem. As this is put forward, the energy consumption and the actual conditions in the grid may be estimated.

## 1.3 PROBLEM DESCRIPTION

The main goal of this study is formulated as follows:

- Optimize the placement of electric charging stations for a public electric bus system with the purpose of minimizing the charging power.

This work intends to determine the required number of charging stations for one bus route and place them so that the charging power at each station will be minimized. By minimizing the charging power, power peaks in the distribution network may be kept at a minimized level. The main goal applies to

fully electric buses with opportunity charging strategy; Charging stations which are placed at bus stops charging the bus when in operation.

The developed strategies are proposed for an existing bus route in Oslo city, Norway. The selected route is currently operated by diesel buses and it will therefore be interesting to investigate the possibilities of integrating electric buses. In order to complete the problem of this study some sub goals were formulated:

- Determine the battery and charging specifications such as battery size.
- Determine the energy needs for an electric bus by performing measurements.
- Develop and verify a suitable mathematical optimization model.
- Optimize four cases based on the determined energy needs.

The first goal considers the input selection from a technical perspective. The second sub goal includes measurements regarding velocity of the bus and altitude of the selected route. The third sub goal intends to develop a mathematical model in terms of an objective function subject to constraint functions. The objective function is to return the minimized charging power of the charging stations which are restricted by the following constraints:

- The operating battery range aims to optimize the battery life.
- A battery energy level above the maximum preferable level will not permit a charging station.
- Maximum charging power is restricted by battery characteristics and maybe grid tolerance.
- The buses are to have the possibility of having a 24/7-hour operation.
- The total energy in the buses is limited by the battery size.

The last sub goal was to optimize four different cases. The cases consist of changes regarding battery capacities, desired battery energy levels in the end of the route (including one forward trip and one return trip), maximum charging powers and end stop regulation times.


## 1.4  LIMITATIONS AND ASSUMTIONS

In order to complete the problem of this study several limitations and assumptions needs to be considered. The optimization will be performed on one bus route with actual route characteristics and driving cycles. The electric buses intendent for the current bus route, are assumed to be identical. This to make all the buses compatible with the charging stations. The buses are also assumed to only operate on the current route to make the bus battery energy level predictable.

To determine the energy consumption of an electric bus some general values regarding electric bus characteristics are assumed. The velocity and altitude measurements for the current route is performed on a diesel bus. These measurements will be assumed equal for an electric bus.

The battery behavior in the electric buses are to be simulated. This model will include equations which are to determine the voltage and currents in the bus battery. Further restrictions regarding this model will be presented in the method section.

The inputs in the optimization model are based on a worst-case scenario. However, one of the inputs being the velocity measurements, may not reflect a scenario like this as only three recordings will be considered. Further, inputs like battery and charging specifications are not based on an economical

perspective but may be specified whenever this could be an aspect to consider. Other restrictions and assumptions regarding this study will be stated throughout the report.

## 1.5 STRUCTURE OF THE REPORT

The structure of this report is organized as follow. Firstly, theory that supports the method will be presented. In this thesis, some of the theory is based on the theory in the preliminary work. This applies for the first section in subsection 2.1, the first section in subsection 2.3 and the two first sections in subsection 2.3.1. The theory presents a brief introduction of the electric bus and charging infrastructures. Then a literature review will be presented starting with impacts on the distribution network due to charging station electric vehicles (EVs). Further, measures to minimize this impact followed by previous studies regarding optimization of electric charging placement. Last in the theory section, battery and charging characteristics are presented.

Secondly, the method will be presented. This section includes how data was collected and the values of them together with calculation operations used to complete the optimization model. Further, a description of the model's specifications, operation and verification process will be presented. Last, an explanation of how the optimization results will be reviewed.

Further, the results together with a discussion will be presented. First, the mathematical solver used for this study will be discussed followed by a discussion on the data selection. Sub results will then be presented including velocity and altitude measurements in addition to calculated battery power and battery behavior. Last, the optimization of the four cases were presented, compared and discussed.

In the end, a conclusion summing up the findings will be reviewed followed by recommendations on further studies.

## 2 THEORY

The trend of procuring electric buses are increasing [5]. The number of battery buses ordered in 2017 in Europe was more than doubled compared to 2016 reaching about 1 000 vehicles. The development continues and within the end of 2019, it is estimated to be more than 1 600 new electric buses in ordinary operation only in Europe. This evolvement stimulates the marked making the offers of electric bus and infrastructure designs wide and variated [10].

The different electric buses are defined at the size of the battery in the bus. An electric bus can typically operate with a battery capacity of 38 – 548 kWh [4]. The different capacities provide different ranges and charging times [6]. A battery of 250 kWh may provide a range of 200 km depending on the driving conditions and driving cycle, while a battery of 50 kWh may provide a range of only 20 – 30 km. Depending on the charging power, the charging time from 20 % to 80 % battery capacity may take 2 – 4 hours for the largest batteries while the smaller batteries may only take 5 – 10 minutes.

The charging time does not only depend on the battery capacity but also on the power the charging station operates with. A typical power range for electric bus charging stations extends from 40 kW to 600 kW [4, 11]. For each battery capacity the charging time will decrease as the charging power increase. The charging strategies for electric buses may be called opportunity, in motion or depot charging [12]. Opportunity charging operates with a typical power of 400 – 600 kW, in motion with a range of 40 – 400 kW and depot charging with 100 kW and below [4].

For the energy transfer there are used different interfaces depending on the charging concept [12]. Opportunity charging are typically stationary systems located along the route. This strategy may use conductive systems such as a pantograph seen in Figure 1. The pantograph is being mounted on the roof of the bus or on the wayside pole (inverted pantograph). There also exist inductive opportunity systems that enable wireless energy transfer. This system can also be used while the bus is in motion. Other in motion charging systems are trolleybus current collectors. Depot charging takes place at a selected area when the bus is not in operation. This is typically done with a manual IEC 62196 based plug (combined charging system) and can be seen in Figure 2.



*Figure 1. Pantograph (150 kW)*



*Figure 2. Conventional plug-in (43 kW)*

## 2.1 OPPORTUNITY CHARGING STRATEGY

In Norway, 2019 is considered as the great breakthrough year for carrying out zero-emission free buses for use in ordinary operation [13]. Fully electric buses are one of the technologies that seems to come in large scale in several regions. Within 2020, about 230 electric buses in Oslo are expected. Electric bus systems are also planned in Hamar, Nord Rogaland, Haugalandet, Bodø, Bergen centrum and Ryfylke Sør. Norway's first larger bus electric fleet has been put into operation in Drammen [14]. Currently six electric buses are operating at some bus lines charged by opportunity strategy using pantograph stations. The plan is to make seven more bus lines fully electric with the help of financial support from the state-owned enterprise Enova.

Opportunity charging has proven to be a convenient technology. Zhiming Gao et al. [4] simulated and evaluated the energy consumption and battery performance for electric buses in real routes and existing bus driving cycles. Different chargers and batteries were analyzed to investigate the ability to maintain reliability like the conventional buses. The results showed that frequent short-time on-board opportunity charging can eliminate schedule delays. The study concluded that the battery degradation of using high charging powers appears not more significant than normal repeated charging over time. Charging powers used for charging electric buses have an efficiency of about 97 %. This is due to the high voltages required for these kinds of charging stations. A bus charging station may operate with 600 V – 750 V, which is high compared to voltages used for charging passenger cars which is 120 V – 240 V. A high voltage gives lower electrical energy losses which gives higher efficiency. As what is for the energy consumption, the study found that an electric bus (12 - 18 meter) with a standardized bus driving cycle has an energy consumption of 1.24 kWh/km – 2.48 kWh/km. This is lower compared to a conventional bus which has an energy consumption of 1.7 – 3.3 kWh/km.

ABB, a delivery company of charging stations, writes that opportunity charging gives the buses possibility of having a 24/7-hour operation time [15]. Being able to have this operation, may eliminate the need of extra buses as buses with large batteries give longer charging time and therefore may affect the bus schedule. To prevent the charging time from affecting the bus schedule, extra buses may step in. Smaller batteries, which are typically for opportunity charging, also relives space in the bus which gives the possibility of managing a higher passenger capacity [11]. Smaller batteries also reduce weight which further lower the energy consumption of the bus. Figure 3 shows an electric bus being charged using opportunity charging strategy.

*Figure 3. An electric bus in action of being charged by a pantograph station*

## 2.2 IMPACTS ON THE NETWORK DUE TO ELECTRIC VEHICLE CHARGING

Electric buses are depended on the possibility of being connected to the distribution network to charge their batteries. Depending on the local grid capacity and charging power, the charging stations may be connected to the low-voltage grid of 230 V or 400 V [12]. Alternating current (AC) in the distribution network is transformed to direct current (DC) by an AC-DC converter so that the power can be used in electric charging stations. Depending on the desired output voltage from the charging station there might be a converter boosting the grid voltage or stepping down the grid voltage. A diagram of a proposed charging station is illustrated in Figure 4.
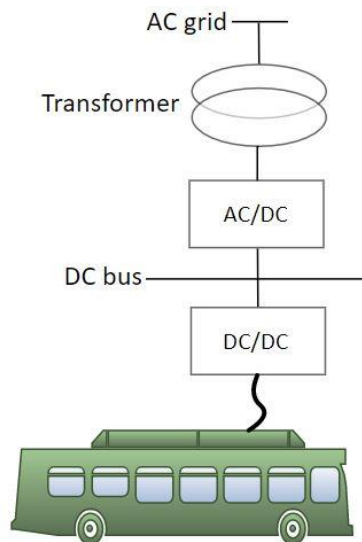


*Figure 4. Diagram of proposed charging station*

A study published by David Steen and Le Anh Tuan [16] investigated the impacts on the local distributed grid at the Chalmers University Technology in Gothenburg, Sweden. The results showed that the impact on the grid is limited due to a strong grid and that it would not be affected for charging powers up to 800 kW. It is significant to notice that these simulations were done with only one bus route, having several routes the impact may not be neglectable anymore. However, even though the

distribution network seemed to be strong, it was recommended to use smart management in the charging stations to reduce the power peak demands caused by using them.

Van-Linh Nguyen et al. [17] investigated the possibilities for power peak shaving during the charging process. Management algorithms were formulated to reduce peak consumption and make a charging plan for passenger vehicles in a parking lot. This was done by linear programming combined with bisection scheme and the strategy was to divide the daytime in many intervals. The results showed that the peak shaving could be reduced by 40 % of the original peak consumption without charging management. Figure 5 shows the different cases where the electric vehicle (EV) charging is managed and not.
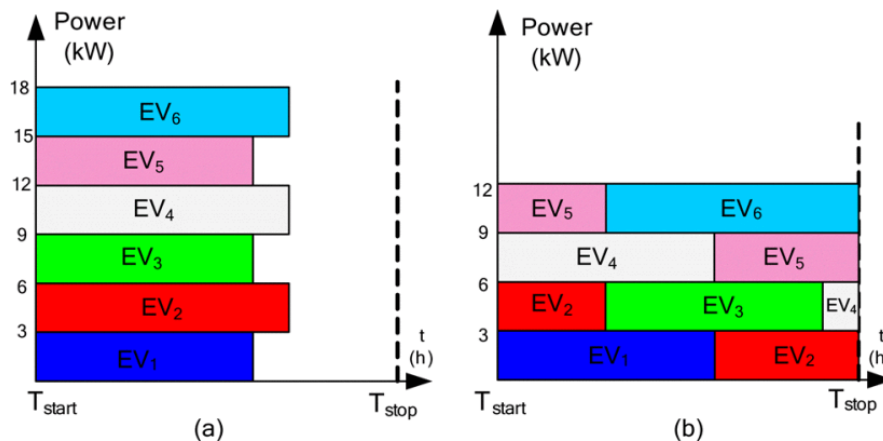


*Figure 5. Charging six EVs without management (a) and with management (b)*
*© 2015 IEEE [17]*

The EV charging effects depend on charging patterns, numbers of EV chargings, coordination, location, charging rate, time, duration and unbalance [18]. When it comes to implementation of EV charging stations in an already existing distribution network, the effect from the load will vary with network and each case requires an independent investigation to evaluate the limits and issues of the EV charging load. Studies on this problem has been investigated in several countries and from their results it shows that the distribution networks are robust enough to handle between 10 and 40 % of the distribution net capacity. This means implementation of charging stations with 10 - 40 % of the network capacity can be done without affecting the grid.

One strategy to reduce the peak load caused by EV charging stations may be to use energy storage systems connected to the charging station [12].  By doing so, some of the energy will be supplied from the network and some from the battery resulting in a lower power load on the network. The battery may be supplied with energy from the distribution network when the charging stations is not used. This would cause reduced power peak, since the charged energy is distributed over a longer time period. Another technique is to connect photovoltaic (PV) panels to the battery as considered in the studies by Charles C. Castello [19], Malin Andersson [20] and Wajahat Khan et al. [21].

Malin Andersson [20] investegated the economic advantage of implementing a li-ion battery at an bus charging station with opportunity charging strategy. The size of the battery was optimized based on minimizing the total annual cost of the connection. The study found that if the charging station was connected to the low-voltage grid with batteries, the battery have the possibility to decrease the

annual cost. However, batteries are not effective to decrease grid owner investments in new electrical substations, but may decrease the fees. The crucial characteristic whenever a battery will be benefitial is determined by the charging frequency of the bus. Longer time between buses charging on the station and the higher the charging power, the more advantageous was the battery option. The study investegated a case where 20 % of energy required is drawn from the battery while 70 % is drawn from the grid. Results showed that the required battery capacity would be a 215 kWh (lithium-titanat) and a 830 kWh (lithium iron phosphate) battery for a low-voltage connection with a power demand of 695 kW.

## 2.3 OPTIMIZATION OF ELECTRIC VEHICLE CHARGING STATIONS

The selection of placement of electric bus charging stations are based on the factor that the bus is to complete the route without the run out of fuel (electricity) [22]. In order to ensure this, charging stations may be installed along the route to provide the battery with additional energy. The simplest way to make sure the bus is to complete its route is to place a charging station at every bus stop along the route. However, for an electric bus system with multiple bus stops in a crowded city, it would be impractical and costly to have a charging station at every bus stop. The difficulty is to decide the placement of the stations at a few selected bus stops, which would give a more optimal solution.

One environmental factor to consider when planning EV charging stations is to meet the requirements of the traffic network design regarding the siting of each charging station [23]. Another perspective to consider is the power system; the location of the stations should be compatible with both a short-term and a long-term distribution system. An optimal solution for the placement of charging stations should be close to load centers to maintain power quality, load balance and power-supply reliability. Other factors such as connection fee related to the charging stations installation, the charging duration, the performance of the battery as well as charging demand and energy supply are essential to consider when planning EV charging station placement.

### 2.3.1 Previous studies

Several studies bring up the electric charging station matter. A study published by Maria Xylia et al. [24] used mixed integer linear programming in the GAMS software to optimize the distribution of charging infrastructure for electric buses and tested the model for the bus network in Stockholm, Sweden. The study considered two cases, one optimizing the energy and one the total cost. The study was based on an input of 143 bus routes and 403 existing bus stops where almost 70 % of the bus stops served more than one bus route. The routes and bus stops were selected based on their location. The authors hypothesis was that the placement of the charging stations was best suited at the major public transport hubs and at start and end stops of the bus routes. This was stated because the hubs were somewhat fixed in the long term because of the already existing railway system. Moreover, these locations already had a high-voltage grid system to provide electricity to trains. Both inductive and conductive charging opportunities were considered along with other alternative solutions. The study evaluated how many of the routes were optimal to be considered electric driven routes and which type of charging infrastructure that were to be selected. The results showed that only 10 – 25 % of the bus stops required charging infrastructure. The study found that introducing charging infrastructure requires high investment costs. Because of this, locating most of the bus stops in the major hubs will

make the investment cost justified. This will require thorough planning and logistics management. Depot charging was not included in this study due to lack of data, but the study stated that a placement of charging stations at a depot can be an optimal solution. The study concluded that determining the charging demands will be a critical and important study to do. This because the electricity grid might not be adapted for such demands.

A study performed by Xiumin Wang et al. [22] used integer linear programming (ILP) to consider charging station placement. The intention was to minimize the charging station cost. The study considered a guarantee of that the bus had enough energy to complete its route including return trip. The study investigated two cases, one where the battery size was considered and one where it was not considered. By taking the battery size into account it meant that it could contain a certain amount of energy and could therefore not exceed this. The study used the Meter-Kilogram-Second system of units in the simulation, meaning that 1-unit energy corresponds to 1 kWh. They considered a battery size of 20 units of energy, with a recharging rate varying from 4 to 10 units of energy. The energy consumption was set to be varying randomly between 1- and 2-units energy and the number of bus stops should vary between 15 and 25 stops. A multiple backtracking algorithm and greedy algorithm was designed and compared with the ILP results obtained in a program called NEOS server. The results showed that the greedy algorithm gave the highest cost, the multiple backtracking algorithm gave a lower cost, while the ILP provided the lowest investment costs. The difference in the algorithms was due to the complexity of the algorithms. A backtracking algorithm is more complex than the greedy algorithm resulting in values closer to the ILP which gave the most accurate results.

Inês Frade et al. [25] proposed a mixed-integer optimization model to determine the placement of EV charging stations in a neighborhood in Lisbon, Portugal. The model was to determine the location of the stations so that the estimated refueling demand could be met in the best possible way through a maximum covering model. The main challenge in the study was the estimation of the energy demand. The data used was somewhat outdated. The results showed that the model used can be suitable for planning electric mobility systems.

Sara Mehar et al. [26] composed an optimization model to determine the placement of EV charging stations. The algorithm resolved the required number of charging stations and the location of them regarding different factors and limitations for a real case study. The model was to optimize the placement based on two objectives; minimize the investment cost and minimize the transportation cost. The model was to ensure that the car only was connected to one charging station and ensure that the energy demand was lower than the charging station capacity. The proposed genetic algorithm named OLoCs (Optimization Scheme for Locating Electric Vehicles' Charging Stations) showed efficiency in terms of optimality and time.

Zhipeng Liu [23] optimized the placement of charging stations for passenger cars in an urban area. A mathematical model was developed to determine the size of the electric charging stations with the objective function to be solved by a modified primal-dual interior point algorithm. The study concluded that the optimization model gave a reasonable planning scheme for EV charging stations as well improved the voltage profile and reduced the network loss. The charging demand pattern, traffic situation and fleet distribution were considered important factors.

## 2.4 BATTERY AND CHARGING CHARACTERISTICS IN ELECTRIC VEHICLES

In order to plan and implement an electric bus system, several parameters need to be determined such as battery and bus type, size and weight of them, the driving and route(s) characteristics and the power of the charging station. To select these parameters, characteristics of batteries and charging procedures are essential to be aware of to make the planning accurate and effective.

A battery is an electrochemical power source that converts chemical energy into electrical energy when being discharged [27]. The electrical energy is electric current at a defined time and voltage. A battery consists of many electrochemical cells connected in series and parallel. Cells connected in series will increase the battery voltage while cells connected in parallel will increase the battery current. The so-called secondary cells have the possibility of being (re)charged which is an essential quality for batteries used in electric vehicles. When in recharge mode electrical energy is converted to chemical energy [28].

For portable applications, the energy storage system should have low volume and weight along with high specific energy density and large storage capacity [27]. Other desired features are long battery life, handling high and low temperatures, low cost, safety and minimum environmental impact. The wide criteria of demands result in that there is no type of battery which meets all the requirements and the battery selection is therefore often a compromise.

The most common battery used in modern electric buses are lithium-ion based batteries (li-ion) [12]. Compared to other rechargeable batteries li-ion batteries have higher power densities, higher energy densities and higher terminal voltages [28]. The chemical structure of a li-ion battery is presented in Figure 6.
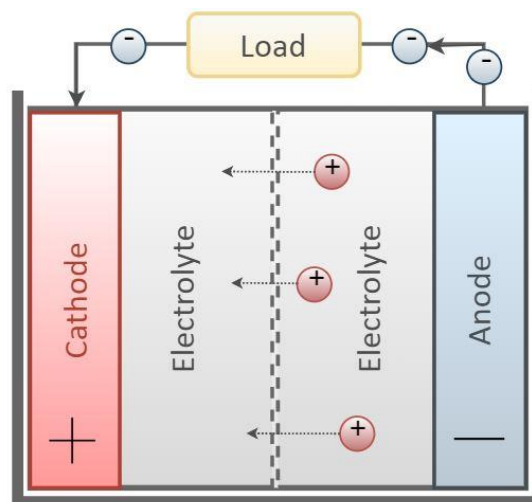


*Figure 6. Representation of a li-ion battery in discharge mode*

A battery consist of two electrodes separated by an electrolyte and connected with each other by an external circuit [27]. One electrode is positive while the other is negative for the chemical reactions to occur and thus produce electrical energy. The positive electrode is a transition-metal oxide while the negative electrode is carbon. When a load is connected to an external circuit (load in Figure 6) between the two electrodes, discharging happens and the li-ion protons (red circles in Figure 6) move from the negative electrode through the electrolyte while the electrons (blue circles in Figure 6) move through

the external circuit providing electrical energy. Battery recharging occurs when electrical energy is supplied to the cell which moves the li-ion protons and the electrons in the opposite direction giving the cell the opportunity to be discharged ones more.

The cell chemistry in li-ion batteries may vary and thus give different characteristics regarding charge rate, energy density and life time [12]. There are three typical cell structures used in electric buses; lithium titanium oxide (LTO), lithium iron phosphate (LFP) and lithium nickel manganese cobalt oxide (NMC). Their cell characteristics are presented in Table 1 and their capacity and charging power for a 3 400 kg battery are presented in Figure 7.

*Table 1. Specification of three different li-ion batteries*
*© 2018 Cambridge University Press [12, p. 8]*

| Parameter | LFP | LTO | NMC | Unit |
|---|---|---|---|---|
| Terminal voltage | ≈3.2 | ≈2.3 | ≈3.6 | V |
| Cell capacity | 14-45 | 20-65 | 37-53 | Ah |
| Energy density | 115-146 | 76-77 | 165-175 | Wh/kg |
| Maximum charge rate (C-rate) | 1 | $4-10$ | $2-3$ | C |
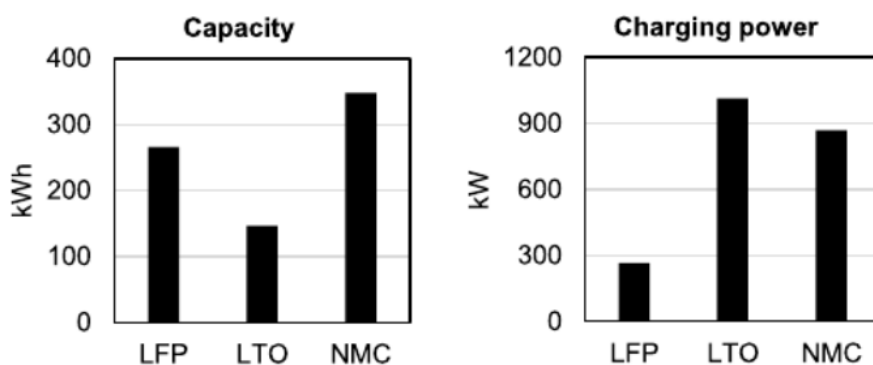


*Figure 7. Battery capacity and charging power for a 3 400 kg battery*
*© 2018 Cambridge University Press [12, p. 8]*

As seen in Figure 7 LTO batteries has the possibility of being charged at high powers but are restricted by the battery capacity due to the low energy density (see Table 1), making it only suitable for opportunity charging systems [12]. LFP batteries has higher power density than LTO batteries but can only be charged with low powered plug-in applications. NMC batteries permits high power in addition to having the highest battery capacity of the three types.

The charging power of a battery is restricted by the battery capacity and the charging rate presented in the following equation [12]:

$$P_{chg,max} = E_{batt} \cdot nC_{max} \qquad\qquad 2.1$$

where $E_{batt}$ (kWh) is the battery capacity and $nC_{max}$ (C) is the charging/discharging rate defined as [29]:

12

$$nC = \frac{I}{Q_{cell}}$$

2.2

where $I$ (A) is the charge/discharge current and $Q_{cell}$ (Ah) is the capacity of the battery cell. The C-rate vary with type of li-ion battery as seen in Table 1. Charging at a higher current, which means higher C-rate, will impact the battery capacity and eventually be decreased due to increasing polarization effects and internal resistance losses [27].

The battery capacity may be determined by the following equation [12, p. 8]:

$$E_{batt} = P_s \cdot m_{batt} \cdot 0.6$$

2.3

where $P_s$ (wh/kg) is the energy density of a battery cell and $m_{batt}$ (kg) is the battery weight. It can be assumed that the energy density in the battery system, including cooling equipment and electronics, is 0.6 times the energy density at cell level [12]. The weight of a battery affects the gross vehicle weight (GVW) of the bus which are permitted by EU regulations. Weight characteristic of two different buses are presented in Table 2.

*Table 2. Weight characteristic of alternatively fueled buses [12, p. 5, 30, p. 12]*

| Length (m) | GVW (ton) | Typical empty weight (ton) | Maximum payload (ton) | Maximum number of passengers |
|---|---|---|---|---|
| 12 | 19.5 | 11.6 | 7.9 | 115 |
| 18 | 29 | 17.3 | 10.7 | 156 |

The maximum payload (passenger load) presented in Table 2 is not considered realistic because of the floors limit in the bus [12]. A passenger capacity restricted by the floor limit relives weigh that can be used to include a battery in the bus. Different battery weights of a 12-meter bus in relation with the passenger capacity by GVW is illustrated by Figure 8.
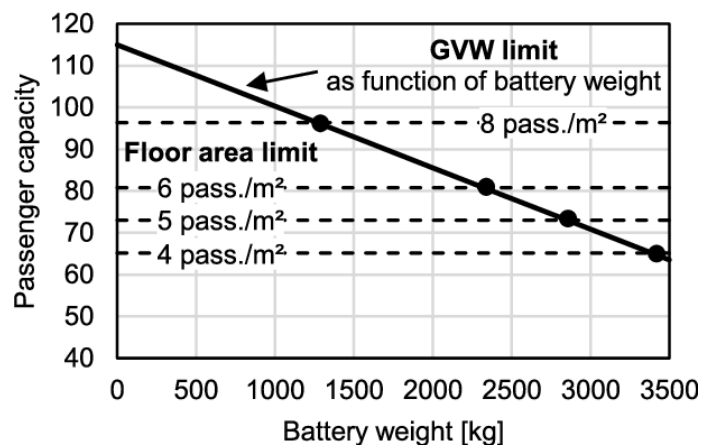


*Figure 8. The relation between passenger capacity and battery weight of a 12 m bus by GVW*
*© 2018 Cambridge University Press [12, p. 6]*

13

As seen in Figure 8 the number of passengers is restricted by the floor area limit which is at approximately 8 passengers/m$^2$. The battery weight can therefore be up to about 1 300 kg without affecting the passenger capacity [12, p. 6]. A battery heavier than 1 300 kg will provide a lower possible passenger load. A battery of 1 300 kg corresponds to about 84 % of the number of passengers stated in Table 2.

### 2.4.1 Charging and discharging a battery

Charging and discharging characteristics for a battery are determined by several parameters. One important feature of a secondary battery is the voltage-current characteristic which states that the electric power obtained/delivered by the battery at any time is defined as [27]:

$$P = I \cdot U_{terminal}$$
<div align="right">2.4</div>

where *I* (A) is the charge/discharge current and $U_{terminal}$ (V) is the accompanying terminal voltage measured across the poles of an electrochemical cell. The cell is connected to a load with a specific current under equilibrium conditions. When connected to a load the terminal voltage can be defined as [31]:

$$U_{terminal} = V_{oc} - I \cdot r_{internal}$$
<div align="right">2.5</div>

where $V_{oc}$ (V) is the open circuit voltage of the cell with no load and $r_{internal}$ (Ω) is the internal resistance of the battery when connected to a load. $V_{oc}$ may also be referred to as the electromotive force (*emf*) due to their equal operating conditions [32, p. 517].

The $V_{oc}$ is determined by the potential differences between the two electrode materials in the cell and when this potential is corrected by the internal resistance it presents the terminal voltage [27]. A large difference in the potential at each terminal gives a higher terminal voltage which is preferable. Therefore, alkaline metals such as lithium, which have a strong negative potential and low density, is attractive to use as the negative electrode. A high specific energy is obtained by including a positive electrode. The terminal voltage may be measured by a voltmeter or calculated from the thermodynamic data of the cell reaction by using equation 2.5. The same equation was also used by Ivan Baboselac et al. [33] and Antti Lajunen [8] when determining the terminal voltage having a dc motor. The measured and calculated terminal voltage often differ slightly from each other due to side reactions or inhibited equilibrium state.

The internal resistance is usually provided by the manufacture on the battery datasheet or it can be measured [34]. Francesco Marra et at. [34] used impedance spectroscopy to measure the internal resistance in a li-ion battery to be about 0.01 Ω. In real, the internal resistance is dynamic and depends on the state-of-charge (SOC), temperature, state-of-health (SOH) and current [28, 35] of the battery at a specific time. A study by Tarun Huria et al. [36] measured the internal resistance of a li-ion battery as a function of SOC and temperature and is presented in Figure 9.
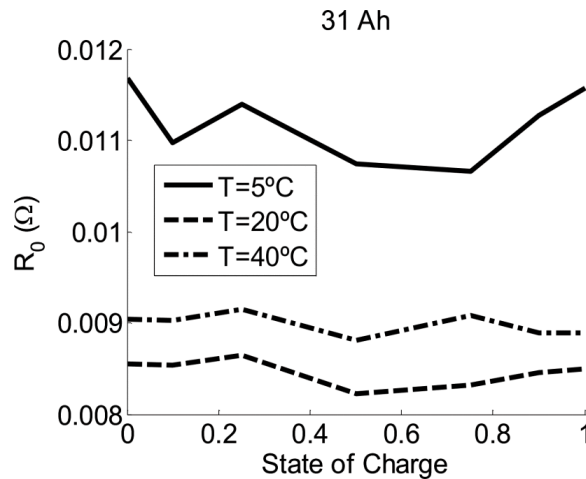
*Figure 9. Internal resistance ($R_0$) based on SOC and temperature*
*© 2011 IEEE [36]*

The study concluded that the internal resistance decreased as the temperature increase while the resistance is more stable for the variation in SOC as seen in Figure 9. Oliver Tremblay and Louis-A. Dessaint [35] developed a battery model. The model assumed a constant internal resistance for a li-ion battery of 0.01 Ω during charge and discharge modes. Two other studies published by Low When Yao et al. [28] and Ala Al-Haj Hussein et al. [37] used interpolation to determine the internal resistance.

Calculation of the open circuit voltage has been done in several studies. Ahmad Rahmoun and Helmuth Biechl [38] determined the $V_{oc}$ by a nonlinear least square algorithm to search the best fitted value between given measurements and a nonlinear function. Several studies [31, 34, 35] used Shepard relation or a modified one to determine the $V_{oc}$ in a li-ion battery cell. The equation is a function of different parameters that can be obtained by the battery manufactures discharge curve. The parameters include constant battery voltage, polarization constant, battery capacity, discharged capacity, dynamic current and time.

Caiping Zhang et al. [39] proposed a generalized SOC-VOC model for li-ion batteries. The model is developed by analyzing electrochemical possesses of li-ion batteries which resulted in a logarithmic, an exponential and a linear function with seven parameters:

$$V_{OC} = a + b \cdot (-ln \cdot SOC)^m + c \cdot SOC + d \cdot e^{n(SOC-1)} \quad (0 \leq SOC \leq 1) \qquad 2.6$$

where *a, b, c, d, m* and *n* are the coefficients resolve by a nonlinear estimation algorithm. The coefficients correspond to li-ion batteries having a charging rate of 1C, in ambient temperature of 25 °C and a degradation of 0 %. The coefficients for different types of li-ion batteries are presented in Table 3.

*Table 3. Parameters for equation 2.6 for various li-ion batteries at 25 °C and a degradation of 0 % [39]*

| Battery type | $a$ | $b$ | $c$ | $d$ | $m$ | $n$ |
|:---:|:---:|:---:|:---:|:---:|:---:|:---:|
| NMC | 3.5 | -0.0334 | -0.106 | 0.7399 | 1.403 | 2 |
| LFP | 3.135 | -0.685 | -1.342 | 1.734 | 0.478 | 0.4 |
| LTO | 2.235 | -0.00132 | -0.3503 | 0.6851 | 2.964 | 1.6 |

The results from the NMC battery model estimation and experimental measurements are presented in Figure 10.
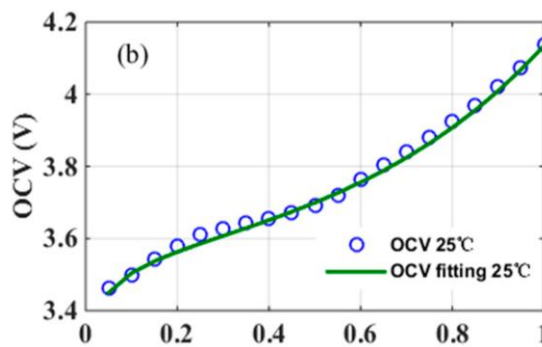


*Figure 10. (b) The VOC(OCV)-SOC relation measured (blue circle) and proposed model (green curve)*
*© 2016 MDPI [39, p. 10]*

As seen in Figure 10 the open circuit voltage increases as the SOC in the battery increases. It was found that the proposed model of this study had fitting errors within 0.5 % of measured values for different SOC which demonstrate an accurate and flexible model suitable for different types of li-ion batteries.

The charging procedure of a battery depends on parameters such as charging time, number of cycles and terminal voltage which influence the capacity of a battery cell [27]. The number of cycles or the lifetime of a battery is preferred to be high for ecological and economic reasons. The key to achieving long life cycle of a battery is to control the current to near full charge. However, the typical operating rang for batteries are between 20 % and 80 % of the battery's capacity. Charging outside these ranges degrades battery life faster and may cause to potentially dangerous situations [40].

One of the main barrier for EVs to be widely accepted are the charging time [21]. One solution to meet this problem can be to apply fast charging. By doing so the amount of energy recharged is the same as with other types of charging strategies but the time will be shortened. There is no clear definition of the term *fast charging*, but the most common fast charging time is 10 minutes (6C) [29]. In such cases a cooling system is required to maintain a safe level of battery temperature and to maintain a long lifetime. The delivered power of an electric charging station is defined by [29]:

$$P_{chg} = I_{chg} \cdot V_{\max(pack)} \qquad 2.7$$

where $V_{max(pack)}$ *(V)* is the maximum voltage in the battery pack and $I_{chg}$ (A) is the current provided by the charger to the battery.

The standard charging profile for a li-ion battery is linear in correlation with the SOC and the charging duration [34]. The charging profile is mathematically described by [17]:

$$T_{charge} = (1 - SOC_0)\frac{E_{batt}}{P_{chg}} \qquad (0 \leq SOC \leq 1) \qquad \text{2.8}$$

where $T_{charge}$ (h) is the time needed to fully charge the battery, $SOC_0$ is the initial SOC, $E_{batt}$ is the battery capacity (kW) and $P_{chg}$ (kW) is the charging power. The SOC is defined as the stored amount of energy in relation with the actual battery capacity [41, p. A1873]:

$$SOC = \frac{Q_{stored}}{E_{batt}} \cdot 100\ \% \qquad \text{2.9}$$

where $Q_{stored}$ (kWh) is the amount of stored energy in the battery at a given time.

A characteristic linear charging profile for an li-ion battery is due to the two distinct operational regions. The battery is either charged with a constant current (CC) or by a constant voltage (CV). The operational mode depends on the SOC. Most of the time the charging happens in a CC mode while the transition from CC to CV mode appares around 89 % SOC. At this point the upper voltage limit is reached. The operational modes for a 100 Ah, 48 V battery with 100 A charging current (C-rate=1C) is presented Figure 11 and Figure 12.

**Constant Current Mode:**

**Constant Voltage Mode:**
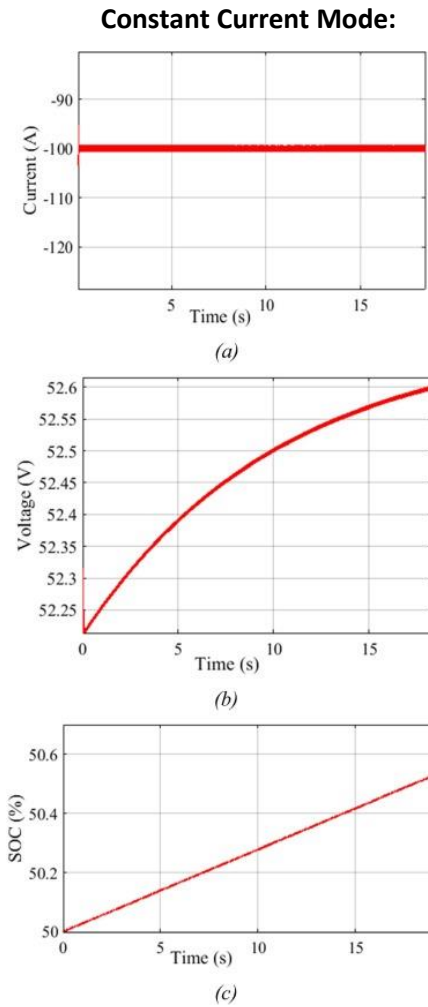


*Figure 11. Characteristics of an EV battery; (a) current, (b) voltage and (c) SOC*
*© 2018 Elsevier B.V. [21, p.148]*
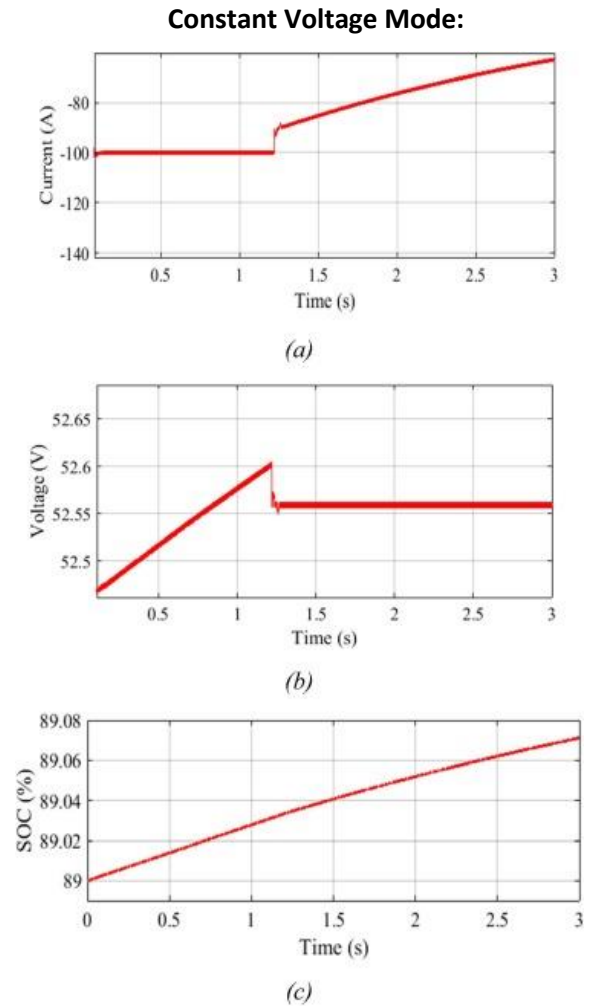
*Figure 12. Characteristics of an EV battery; (a) current, (b) voltage and (c) SOC*
*© 2018 Elsevier B.V. [21, p.148]*

As seen in Figure 11, when in the CC mode, the current is constant while the terminal voltage drops as the SOC decrease and rise if the SOC is increased. As seen in Figure 12, when in CV mode, the terminal voltage is constant (after about 1.2 s) while the current is dropping or rising propotionally according to the SOC.

## 2.5  BATTERY MODEL FOR ELECTRIC VEHICLES

When simulating an electric vehicle, energy consumption which reflects the SOC, voltage and current in the battery are some of the main battery characteristics to investigate.

There are a wide range of battery model approaches, including empirical model, electrochemical, experimental and electric circuit models [31]. Electric circuit models are simple yet effective and suitable for both steady-state and dynamic battery behavior. Figure 13 illustrates an electric circuit model for a battery.
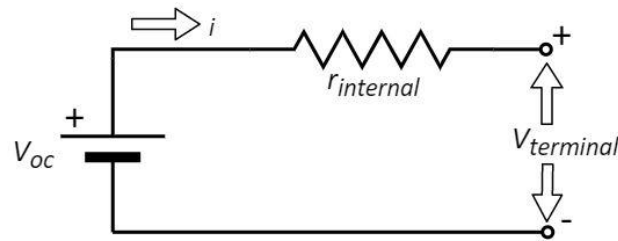
*Figure 13. Electric circuit model for a battery*

The model in Figure 13 is a common equivalent circuit model which has a constant voltage in series with a resistor representing the internal resistance in the battery [31]. This model makes it easy to understand the electrical characteristic of a battery [42]. The model was mathematically presented in the theory subsection 2.4.1, by equation 2.5. In this equation the SOC was not represented directly but can be determined as a function of the open circuit voltage as presented in equation 2.6 subsection 2.4.1.

A study performed by Emma Raszmann et al. [31] used the electric circuit model (Figure 13) to analyze the SOC effects on the internal resistance and capacity fading in EV batteries. The model was validated by comparing the manufactures discharge, voltage, current and SOC curve with the results by the proposed model.

An EV makes the battery discharge according to the movement of the bus which will affect the SOC in the battery. Ivan Baboselac [33] modeled a li-ion battery to power an Mitsubishi electric passenger vehicle (i-MiEV). The model was made in Simulink by using parameters of the battery provided by the manufacture and two standardized driving cycles. The battery voltage was determined by the Shepard model. The driving cycles represented the load of the battery which consisted of velocity measurements of the bus throughout the driving route. The movement of the vehicle was used to determine the SOC, current and voltage of the battery. The SOC calculation was determined by the total forces on the bus consisting of the air resistance, rolling resistance and gradient resistance. The model was verified by making sure the EV could provide driving distance, default motor speed and power according to the driving cycle.

Another study published by Zhiming Gao et al. [4] simulated and compared the energy consumption of a conventional bus and an electric bus using data from four standardized driving cycles. For this study similar calculation methods as the one by Ivan Baboselac et al. [33] were used to determine the SOC.

Antti Lajunen [8] proposed an electric bus model to investigate the energy requirements for different operating routes. The model validation was done by comparing measured results obtained from a prototype bus test. The input values were driving speed, road angle and charging power. The energy requirements for the bus were calculated based on forces the bus provided on the road. In addition, the current in the battery was calculated based on the SOC and the battery capacity while the terminal voltage in the battery was calculated by using equation 2.5 in subsection 2.4.1. An accessory load of 15 kW corresponding to cold or hot ambient conditions was considered. It was found that the energy consumption depends on weather conditions, weight of the bus and operating route. A lifecycle cost analysis was also performed, and it was found that a main factor affecting the EV life cost, was the

battery capacity. Therefore, to reduce this cost it will be attractive to reduce the capacity of the battery.

When making a battery model the type of motor load may be included. EVs have the characteristic of operating under variated speed conditions making the dc motor widely used for these systems due to their exceptional driving performance and ease torque control [43]. Ac motors on the other hand, are widely used in constant-speed applications because of their rugged construction and low cost.

# 3  METHOD

The objective of this study was to optimize the placement of electric charging stations for a specific route in Oslo city, Norway. In the following sections the method used to address this problem is presented. Figure 14 gives an overview of the approach used for this study consisting of five steps; data collection, develop different cases to optimize, develop and verify the optimization model and obtain results from the optimization.
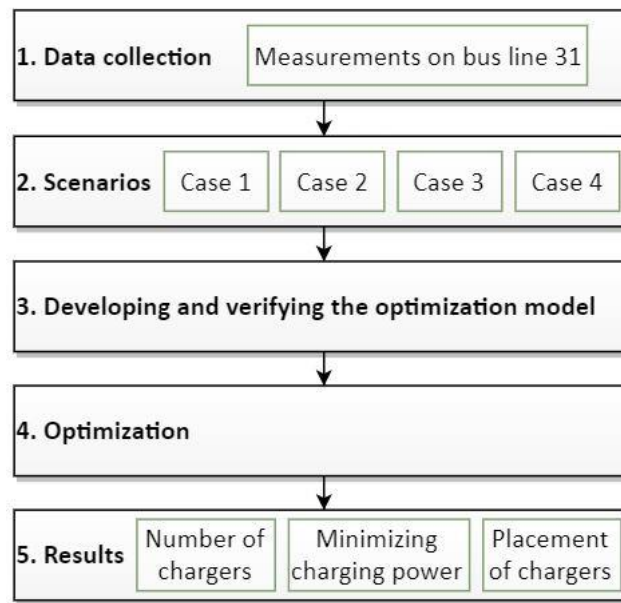


*Figure 14. Flowchart of the approach for this study*

As seen in Figure 14 the first step in this study was to collect data to use in the optimization model. Most of the data collected were based on literature research using google scholar, IEEE, science direct and the library at UiA. The following keywords were used in the search: Ev battery modeling, demand profile ev, dynamic mode of li-ion battery, optimizing electric bus, placement of electric bus charging stations, optimization of electric bus charging stations and tractive forces on bus. The literature research did also provide background theory regarding optimization, battery and charging characteristics so that the problem of this study could be solved.

Based on the literature research four different cases were developed shown as the second step in the approach. The different cases included changes in desired battery energy level in the end of the route (including one forward trip and one return trip), battery capacity, maximum charging power and regulation time.

The third step was to develop the optimization model including an objective function subject to a set of constraints. To make sure the model worked as intended, it was verified with simple input values and then extended as the model worked properly.

The fourth step was to optimize the cases and get results regarding the total number of charging stations required, the placement of them and the charging power of the charging stations. The steps (Figure 14) will be described in detail in the following sections.

## 3.1 DATA COLLECTION

The data collection is shown in Figure 14 as the first step in the approach for this study. The collection consisted of gathering input data for use in the optimization model. The data was obtained from a literature research and by doing measurements on the selected route. As the model was developed it came clear which input data that were required, and the main parameters are presented in Table 4.

*Table 4. Key parameters required for the optimization*

| Parameter | Description | Unit |
|-----------|-------------|------|
| $E_{batt}$ | Installed battery capacity in the bus | kWh |
| $e_{c(i-1,i)}$ | Consumed energy by the bus when driving from bus stop *i-1* to the next bus stop *i* | kWh |
| $e_{init}$ | Initial energy in the battery before the bus leaves the first bus stop | kWh |
| $i$ | The sequence of stops for the bus along the route | # |
| $ll$ | The battery's minimum preferable energy level | % |
| $P_{chg,max,i}$ | The maximum allowable charging power at stop *i* | kW |
| $T_i$ | The stopping time at bus stop *i* | h |
| $ul$ | The battery's maximum preferable energy level | % |
| $\eta_{chg}$ | Charging efficiency factor | - |

The parameters presented in Table 4 were used directly in the optimization model or in calculation procedures which indirect was connected to the optimization inputs. Some of the parameters may also be the result of sub calculations which were based on other parameters. These other parameters will be presented as they are reviewed in the next subsections.

### 3.1.1 Battery model assumptions

A battery model was developed to provide optimization inputs regarding energy consumption. In addition, the current and voltage were simulated to investigate the battery characteristics in the bus for the selected route. In the following sections the battery model developed, in addition to the battery assumptions, will be presented. Further, how the specifications of the bus system were collected and determined and how calculations on SOC, current, voltage was performed.

Some assumptions and limitations for the battery model were set to complete this study:

- Temperature effects due to battery operation was not considered which means that temperature does not affect battery behavior.
- The determination of open circuit voltage is based on 1C charging rate. The charging rate in this study may differ from this value but effects due to this variation were not considered.
- The battery did not consider hysteresis feature of the voltage curve.
- Battery capacity does not change in relation to current changes.

- The maximum battery capacity is constant and does not change due to memory effects.
- Self-discharge of the battery is neglected.
- The internal resistance in the battery is considered constant throughout the charge and discharge cycle.

### 3.1.2 Specifications of the electric bus and charging stations

The specification of the bus used in this study is based on different research works like the studies done by Dietmar Göhlich et al. [12], by Zhiming Gao et al. [4] and by Ivan Baboselac et al. [33]. Some of the inputs used from these studies were compared with technical data sheets for two electric buses; Irizar, a Spanish company [44] and BYD, a Dutch company [45].

The bus used in the optimization model was assumed to have a length of 18 meters, operating with a dc motor powered by an NMC li-ion battery. To calculate the maximum battery capacity, equation 2.3 in the theory subsection 2.4 was used. The weight of the battery was assumed to not affect the passenger load and the maximum battery capacity was thus determined based on the gross vehicle weight (GVW). For a 12-meter bus, the practical maximum passenger load will be 84 % of the theoretical load due to the floor area limit (see Figure 8 subsection 2.4). For an 18-meter bus it was assumed the same percentage passenger load as for a 12-meter bus. This gave a released passenger weight of 16 %, consequently reliving weight to be used on a battery in the bus. In addition, for an 18-meter bus driving on alternative fuel like electricity, an extra weight of 1 000 kg is allowed. The passenger capacity for an 18-meter bus assumed in this study was equal to the passenger capacity stated for the 18-meter bus provided by the Irizar company [44].

The maximum charging power was assumed to not exceed the preferable C-rate presented in Table 1 subsection 2.4 to prevent unnecessarily degradation. This assumption gave restriction for the maximum charging power calculated by using equation 2.1 in subsection 2.4. The maximum charging power turned out to be calculated to be above 688.5 kW. Bus charging stations may operate with up to 600 kW as stated in the theory. Therefore, the maximum charging power was reduced with 88.5 kW to reflect actual marked offers.

Another parameter determined was the operational SOC which was assumed to be in between the range of 40 % - 80 % to obtain a longer battery life. In addition, the range functions as a driving range in case of traffic or other unexpected happenings. The initial energy in the battery was set to be 80 % at the highest to reflect a worst case-scenario. In the beginning of the day the battery might be fully charged but as the bus is operated for several trips the initial energy level may end up being 80 % or below.

The voltage and current in the battery were simulated to investigate the characteristics of them when the bus was being charged and discharged along the route. The maximum voltage for the battery pack was assumed to be 600 V which corresponds to about 154 parallel connected cells with a maximum cell voltage of 4.1 V. The number of cells were determined by dividing the maximum battery pack voltage with the maximum battery cell voltage. The maximum cell voltage is the open circuit voltage when the SOC is 100 % obtained from equation 2.6 in subsection 2.4.1 by using the coefficients for the NMC li-ion battery listed in Table 1.

By knowing the maximum voltage and the required power, the current in the battery was determined by using equation 2.7 in subsection 2.4.1. This equation is originally for determining the current in the

charging station of the battery but do also reflect the current in the battery for SOC between 0 and 89 % (CC mode). For this study the SOC in the battery was assumed to be within these ranges. A negative current indicates charging mode while a positive current corresponds to a discharging mode.

Equation 2.4 in subsection 2.4.1 was used to determine the voltage in the battery at a given time adjusted by multiplying the number of parallel connected cells with the open circuit voltage:

$$U_{terminal(pack)_t} = v_{oc} \cdot n_{cell} - r_{internal} \cdot i \qquad\qquad 3.1$$

where $r_{internal}$ is the internal resistance of one battery cell set constant to 0.01 Ω and $n_{cell}$ is the number of battery cells that make up the whole battery assembly. $v_{oc}$ (V) is the open circuit voltage at time $t$ (s) and $i$ (A) is the current at time $t$. The open circuit voltage was calculated based on equation 2.6 in subsection 2.4.1 by using the coefficients for the NMC li-ion battery listed in Table 1:

$$v_{oc} = 3.5 - 0.0334 \cdot (-ln \cdot SOC_t)^{1.403} - 0.106 \cdot SOC_t + 0.7399 \cdot e^{2(SOC_t - 1)} \qquad 3.2$$

The SOC was calculated based on the energy needs which was determined by the drive cycle parameters of the bus. The SOC and the drive cycle parameters will be reviewed in the next two subsections.

The parameters assumed for the 18-meter bus are summarized in Table 5. The values in the table represent case 1 in this study. Three other cases regarding different battery size, maximum charging power and regulation time were formed to compare the outcomes. Case 2, 3 and 4 has the same input variables as case 1 but with some adjustments which are presented in Table 6.

*Table 5. Parameters assumed for an 18-meter bus and used in the battery and optimization model*

| Case 1 | | | |
|---|---|---|---|
| **Parameter** | **Value** | **Unit** | **Notation** |
| Battery density, $P_s$ | 170 | Wh/kg | From Table 1 (mean of NMC) |
| Battery size, $E_{batt}$ | 275.4 | kW | Equation 2.3 |
| Desired end SOC, $soc_{end}$ | 80 | % | - |
| Empty bus weight | 17 300 | kg | From Table 2 |
| Internal resistance, $r_{internal}$ | 0.01 | Ω | [34, 35] |
| Battery weight, $m_{batt}$ | 2 700 | kg | - |
| Maximum cell voltage, $V_{max(cell)}$ | 4.1 | V | Equation 3.2 (SOC=1) |
| Maximum charging power, $P_{chg,max}$ | 600 | kW | Equation 2.1 |
| Maximum C-rate, $nC_{max}$ | 2.5 | C | From Table 1 (mean of NMC) |
| Maximum payload | 9 000 | kg | 85 % of load from Table 2 |
| Maximum preferable energy level, $ul$ | 80 | % | - |
| Maximum battery voltage, $V_{max(pack)}$ | 600 | V | [4, p.594] |
| Minimum preferable energy level, $ll$ | 40 | % | - |
| Number of parallel linked cells, $n_{cell}$ | 154 | # | $V_{max(pack)}/V_{max(cell)}$ |
| Regulation time at both end stops, $r$ | 10 | min | - |
| Total maximum bus weight, $m$ | 29 000 | kg | Including passengers |

*Table 6. Adjusted input parameter(s) for case 2, 3 and 4*

| | **Adjusted parameter(s)** | **From value** | **To value** | **Unit** |
|---|---|---|---|---|
| **Case 2** | Regulation time at both end stops, $r$ | 10 | 7 | min |
| **Case 3** | Desired end SOC, $soc_{end}$ | 80 | 70 | % |
| **Case 4** | Battery size, $E_{batt}$ | 275.4 | 200 | kWh |
| | Maximum charging power, $P_{chg,max}$ | 600 | 500 | kW |
| | Desired end SOC, $soc_{end}$ | 80 | 70 | % |

As seen in Table 6 one to three parameters for each case was adjusted, the other parameters remain the same as for what is for case 1 in Table 5. It is important to note that when charging battery size, the maximum charging power will change. The maximum charging power for a battery of 200 kWh for case 4 will therefore be 500 kW.

### 3.1.3    Specifications of the selected bus route

For this study drive cycle measurements of an existing bus route were used to determine the energy needs for an electric bus. Further, the energy needs were used to determine the state-of-charge (SOC) in the battery. The SOC was then used in the optimization. The measurements included velocity and altitude profiles as a function of time and distance. The measured parameters were recorded using a mobile with an application named *Speed Tracker*. Speed Tracker is a GPS speedometer that logs the characteristics of driving routes [46]. The route is located in Oslo city, Norway, driving between the end stops Grorud T and Snarøya, crossing Oslo centrum halfway [47, p.8-13]. The route is called line 31 and the buses driving on it are operated by Nobina Norge AS on contract by the bus company Ruter AS [48]. The route is operated by 18-meter diesel buses (see Figure 15) driving a 24/7-hour operation with different time intervals depending on the time of the day and night [47, p.8-13]. The shortest scheduled regulation time at the end stops throughout the day and night is 12 minutes.



*Figure 15. An 18-meter diesel bus operating on bus line 31*

For this study it was assumed that the same buses operate on the route and have to manage a regulation time of 10 minutes, giving a buffer time of 2 minutes at both end stops. It was assumed that the driving cycle measured for an 18-meter diesel bus would be equivalent to a driving pattern of an 18-meter electric bus on the same bus line. The route specifications for bus line 31 are presented in Table 7 and a sketch of where the route is located is showed in Figure 16.

*Table 7. Key parameters of bus line 31 [47, p.8-13]*

| Parameter | Grorud T → Snarøya | Snarøya → Grorud T | Total | Unit |
|---|---|---|---|---|
| Estimated time | 01:06:00 | 01:06:00 | 02:12:00 | hh:mm:ss |
| Estimated time at end stop | 00:12:00 | 00:12:00 | 00:24:00 | hh:mm:ss |
| Distance | 22 | 22 | 44 | km |
| Total number of bus stops | 43 | 43 | 86 | # |
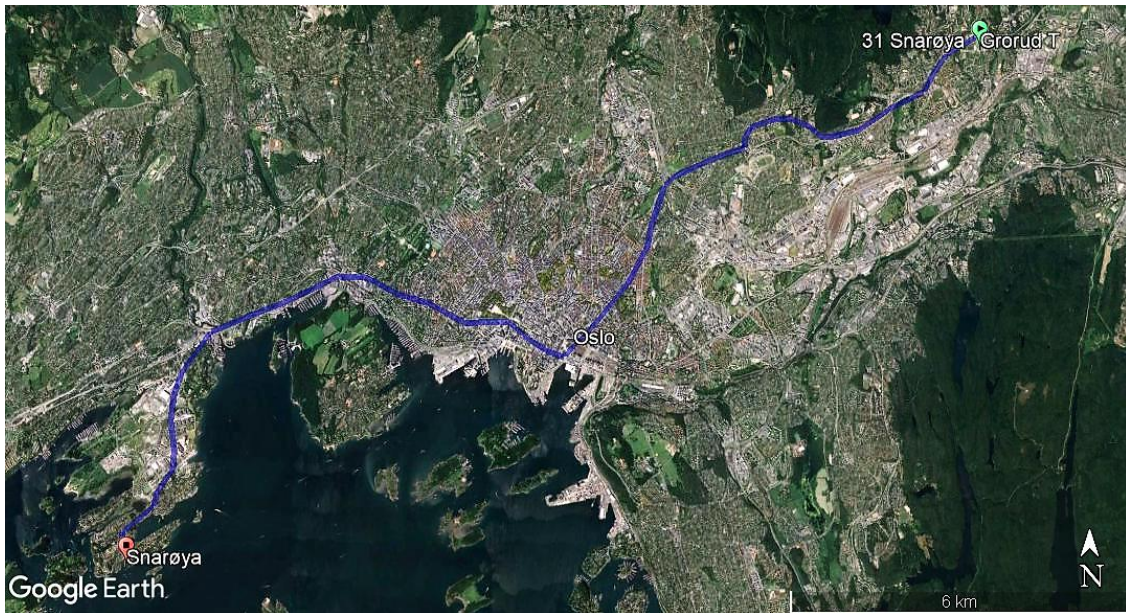
*Figure 16. Sketch of bus line 31 between Grorud T and Snarøya*
*Kartdata © 2019 Google*

The measurements of velocity and altitude were performed three times on three different days at the same time of the day (at 18:37). Further, the measured data were exported to the MATLAB software so it could be used in the calculation of energy consumption (energy needs). A maximum acceleration of 5.4 m/s$^2$ [4] was set to remove data that might be wrong due to bad GPS signals causing some missing values.

The Speed Tracker recorded each time the bus stopped but did not mark if the stop was caused by traffic lights, a bus stop or for some other reason. The model would therefore not be able to separate the stops and sort out what kind of stop it was. Therefore, the model could not know whenever a stop would be suitable for a charging station or not. This matter was neglected and thus assuming that a charging station may be placed at any stops along the route.

It was expected that the measurements taken may vary in driving time and number of stops. Therefore, to compare and validate the measurements a moving average calculation was performed so data points over a longer time interval than 1 second could be obtained. The moving average was calculated over a time interval equal to the average time delay of the measurements. The function called *movmean* in MATLAB was used for this operation. The moving mean calculation was done in MATLAB and the script can be found in appendix A. The moving mean will be presented as a plot in the result and discussion section.

### 3.1.4    Determination of the state-of-charge

The measured drive cycle data were used to determine the drive parameters who affects the dynamics of the battery. The driving parameters determine the tractive power the vehicle exerts on the surface. The tractive power was then used to calculate the SOC in the battery. Using the tractive power to determine the energy requirements for a battery is a common approach, as reported by Zhiming Gao et al. [4], Ivan Baboselac et al. [33] and by Dietmar Göhlich et al. [12]. The forces on a driving bus is illustrated in Figure 17.

27
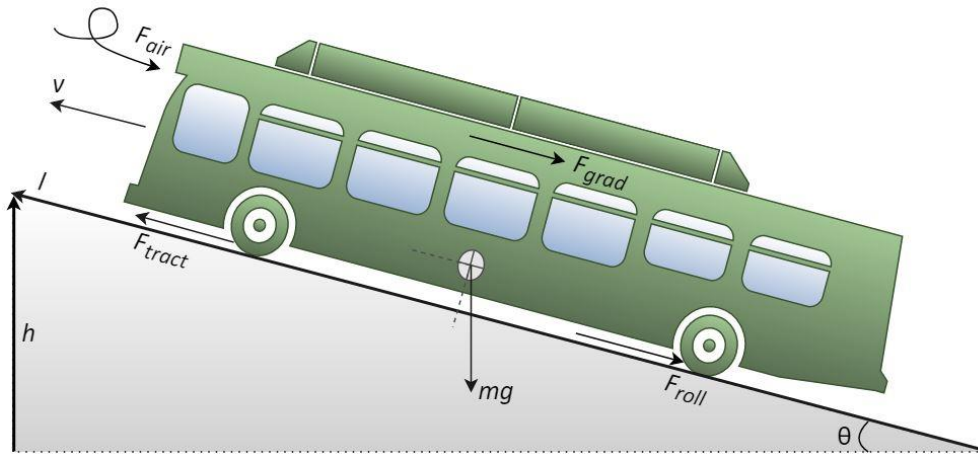
*Figure 17. Forces acting on the bus*

The tractive power caused by the speed and movement of the bus according to time *t* (sec), is defined by Newtons first and second law [33]:

$$P_{tract_t} = (F_{grad_t} + F_{air_t} + F_{roll_t} + m \cdot a_t) \cdot v_t \qquad 3.3$$

where $F_{grad,t}$ (N) is the gradient resistance force, $F_{air,t}$ (N) is the air resistance force and $F_{roll,t}$ (N) is the rolling resistance force. *m* (kg) is the mass of the bus including passenger load, $a_t$ (m/s²) is the acceleration of the bus determined by the derivative of the bus velocity $v_t$ (m/s). The velocity was determined by the driving cycle recorded by the Speed Tracker application. The gradient resistance force is given by [33]:

$$F_{grad_t} = m \cdot g \cdot \sin(\theta_t) \qquad 3.4$$

$$where: \theta_t = sin^{-1}\left(\frac{l_t - l_{t+1}}{h_t - h_{t+1}}\right) \qquad 3.5$$

where $\theta_t$ (rad) is the road angle calculated by the trigonometric functions using the elevation profile $h_t$ (m) and the distance profile $l_t$ (m) obtained with the Speed Tracker application. The air resistance force is given by [33, 49]:

$$F_{air_t} = \frac{1}{2} \cdot C_{drag} \cdot A_{front} \cdot \rho \cdot (v_t + v_{w_t})^2 \qquad 3.6$$

where $C_{drag}$ is the drag coefficient, $A_{front}$ (m²) is the frontal area of the vehicle, $\rho$ (kg/m³) is the air density and $v_{w,t}$ (m/s²) is the wind speed which is neglected in this study due to no recorded data. The rolling resistance force is given by [49]:

$$F_{roll_t} = \mu \cdot m \cdot g \cdot \cos(\theta_t) \qquad 3.7$$

where $\mu$ is the rolling friction coefficient and *g* (m/s²) is the gravitational speed.

The load on the battery is not only defined by the tractive power but also power caused by using accessories in the bus such as air conditioning, air compressor, power steering and other electricity demanding components. Another aspect considered is the energy losses caused by the electric components and the related drivetrain components, illustrated in Figure 18.
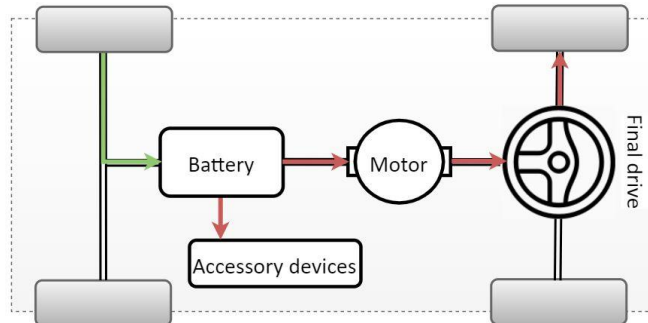


*Figure 18. Proposed block diagram of the powertrain for an electric bus*

As seen in Figure 18, the battery supplies the devices marked by a red arrow. The supplied energy to the battery is marked with a green arrow which is obtained from regenerative breaking or by a charging station. Considering the energy losses from these components and the power required from the accessories, the total battery power load required to make the bus operate according to time is determined [33] and presented by a flow diagram in Figure 19.
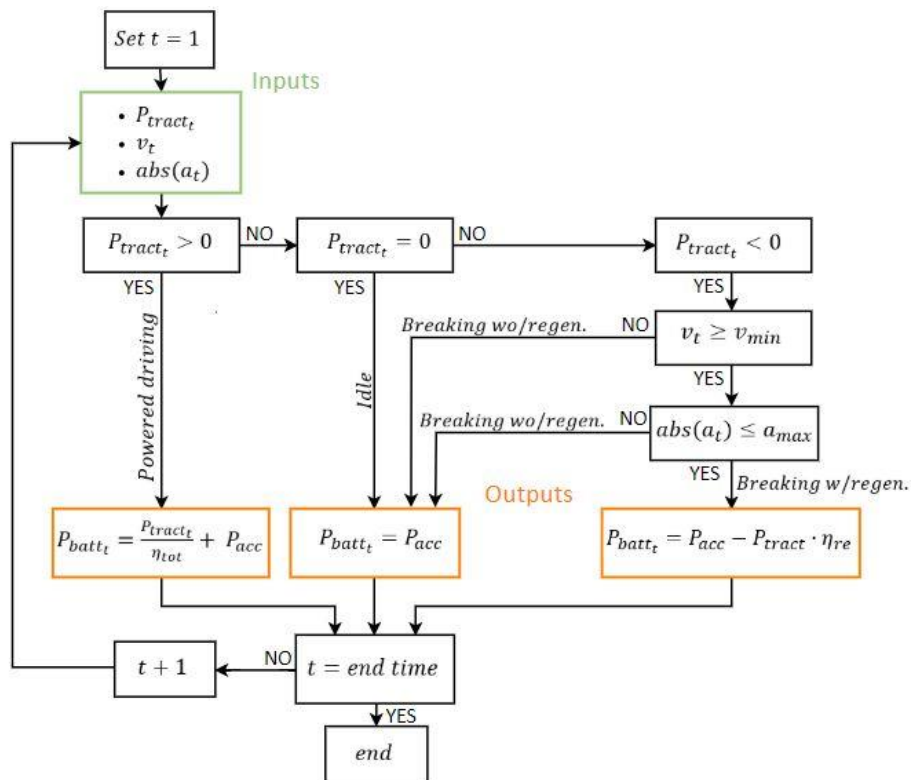


*Figure 19. Flow diagram of how the battery power was determined*

$$where: \qquad \eta_{tot} = \eta_{wh} \cdot \eta_{fd} \cdot \eta_{mot} \cdot \eta_{batt} \qquad\qquad 3.8$$

where $P_{acc}$ (kW) is the power consumed by using the accessories in the bus. $v_{min}$ (m/s) is the minimum speed for which kinetic energy can be converted into electric energy while $a_{max}$ (m/s$^2$) is the maximum acceleration the regenerative braking system can convert kinetic energy into electric energy. $\eta_{re}$ is the efficiency of converting regenerated energy into useful energy, $\eta_{tot}$ is the efficiency of the electric components and the related drivetrain components; battery efficiency ($\eta_{batt}$), motor efficiency ($\eta_{mot}$) final drive efficiency ($\eta_{fd}$) and wheel drive efficiency ($\eta_{wh}$). Negative power is considered regenerated or charged while positive power is considered consumed.

As seen in Figure 19 the battery power load was determined by different conditionally statements regarding tractive power ($P_{tract,t}$), velocity ($v_t$) and acceleration ($a_t$) of the bus. The battery power was determined for every second along the entire bus route with an initial time of 1 sec (*set t=1*). A tractive power greater than zero gave a battery power equal to the tractive power corrected by the total efficiency and added by the accessory load. This is characterized by a powered driving mode. A tractive power equal to zero indicated that the vehicle has stopped. For this case, the battery power is equal to the load caused by the accessories. This is characterized by an idling mode. Further, a tractive power below zero gives a battery power is defined by whenever it causes regenerative breaking or not. If the velocity is high enough and the breaking acceleration below its maximum value, it would cause battery energy regeneration.

The values assumed for the parameters in equations 3.3 to 3.8 are presented in Table 8.

*Table 8. Parameters used for simulating the power load of an 18-meter bus*

| Parameter | Value | Unit | Notation |
|---|---|---|---|
| Frontal area, $A_{front}$ | 8.5 | m$^2$ | [4] |
| Drag coefficient, $C_{drag}$ | 0.8 | - | Square frontal area [50] |
| Gravitational speed, $g$ | 9.81 | m/s$^2$ | Standard, earth's atm |
| Accessory load, $P_{acc}$ | 15 | kW | [51] |
| Air density, $\rho$ | 1.2 | kg/m$^2$ | Standard, earth's surface |
| Rolling friction coefficient, $\mu$ | 0.02 | - | [50] |
| Minimum velocity, $v_{min}$ | 5 | m/s | [33] |
| Maximum deceleration, $a_{max}$ | 3 | m/s$^2$ | [33] |
| Wheel drive efficiency, $\eta_{wh}$ | 0.99 | - | [4] |
| Final drive efficiency, $\eta_{fd}$ | 0.98 | - | [4] |
| Motor efficiency, $\eta_{mot}$ | 0.88 | - | [4] |
| Battery efficiency, $\eta_{batt}$ | 0.98 | - | [4] |
| Regenerated efficiency, $\eta_{re}$ | 0.65 | - | [52, p. 8] |

The frontal area in the bus presented in Table 8 have the same area of the 18-meter bus provided by the Irizar company [44]. The drag coefficient is based on a square frontal area and the value used is similar to the one applied in the study by Zhiming Gao et al. [4]. The rolling friction coefficient is based on worn asphalt and is a bit higher than the one used in the study by Gao. This may be due to assuming

a newer asphalt causing less friction. The energy consumption related to accessories in the bus is assumed based on a 12-meter bus in ambient temperature of -25°C. The efficiencies for the different parts of the electric and drivetrain components are based on an electric bus. Type and size of the different components may cause different efficiencies but is neglected.

When knowing the power load of the battery, the SOC at a given time can be calculated by [4]:

$$SOC_t = \begin{cases} SOC_{init} & if\ t = 1 \\ SOC_{t-1} - \dfrac{P_{batt_{t-1}} \cdot \dfrac{1\ s}{3600\ s/h}}{E_{batt}} & otherwise \end{cases} \qquad 3.9$$

where $SOC_t$ is a factor between 0 and 1 but converted to percentage when multiplied by 100. $SOC_{init}$ is the initial energy in the battery before the bus leaves the first bus stop at time 1 s. $E_{batt}$ (kWh) is the energy storage capacity of the battery, $P_{batt}$ (kW) is the power in the battery multiplied by the time between each measurement which is 1 sec. The 1 sec time frame is converted to hours by dividing with 3 600 sec to get the correct index. The *SOC* is expressed in kWh by [4]:

$$E_t = SOC_t \cdot E_{batt} \qquad 3.10$$

The SOC calculation together with the force and power calculations was performed in MATLAB and the script can be found in appendix B. The SOC and other related calculations will be presented graphically in the result and discussion section.

When implementing electric charging stations, the capacity of the electrical substation would be essential to investigate, especially for bus charging stations due to their high charging power. Some charging stations may be connected to existing substations while other need to have a new substation suited for their required charging power. The capacity for the substations at Snarøya and Grorud T were inspected by contacting Hafslund Nett AS which provided data on their substations (see appendix C). At Grorud T the highest capacity offered was one substation with 550 kVA operating at 400 V. At Snarøya the highest offer of capacity was 325 kVA operating with 230 V.

## 3.2 OPTIMIZATION MODEL

Further the optimization model will be explained, which is shown in Figure 14 as the third and fourth step in the approach for this study. A description of the system and how the optimization model are to be operating will be reviewed. For this optimization, numerical approximation was used to solve the problem mathematically by means of algorithms. A numerical method provides approximate but accurate solutions to a problem where the exact solutions may be impossible or prohibitively expensive to calculate [53]. The mathematically solver used, will be presented along with the objective function and constraints for the system. Last, a review of how the model was developed, adapted and verified.

### 3.2.1    Specification of the optimization model

An electric bus is dependent on electricity in order to operate and is typically provided by electricity from an on-board battery. As the bus is driving, the energy in the battery is drained meaning it eventually needs to be charged to prevent the bus from stopping. Charging along the route applies especially for small batteries containing less energy leading to an empty battery sooner. Placing a charging station at every stop along the route were assumed to be possible, however, not more than one at each stop.

The energy stored in the battery is restricted by its capacity, meaning that if the bus is charged when the battery is nearly full the charging may not be fully distributed. This limitation was considered for the optimization model. It was desirable to consider the placement of the electric charging stations to be in those areas where the bus stopped for the longest time. However, due to the limited amount of energy in the battery the bus may run out of electricity before it reaches this stop. Therefore, the placement of the charging station may be at a previous stop to make sure the battery is charged before the running out of electricity.

Lastly only one route was considered in the optimization including both the forward and return trip. The time and distance traveled, number of stops and driving pattern were given by measurements preformed on the bus line 31 at specific time of the day.

### 3.2.2    The operation of the optimization model

A simplified description of how the model was to operate are shown in Figure 20.
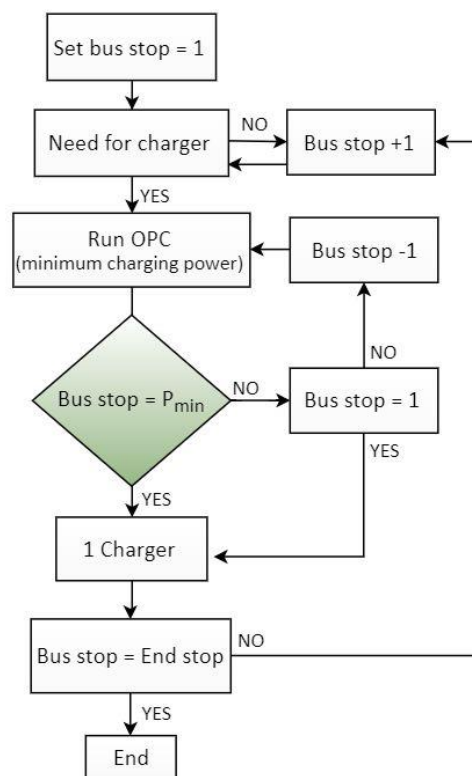


*Figure 20. Overview of how the operation of the optimization model*

As seen in Figure 20 the optimization model was to start investigating the battery in the bus at the first bus stop (*Set bus stop =1).* The bus was evaluated for whenever a charging station was needed or not based on the available energy in battery versus the energy needed to reach the next stop. If the energy in the battery was higher than required to reach the next stop, there was no need for a charger and vice versa. If there was no need for a charger the model was to proceed onto investigating the need of a bus charging station at the next stop (*bus stop +1*). If the bus required a charging station at the current bus stop, the optimization model was to examine whenever that bus stop was the optimal location of placing a charging station (*OPC*). The placement was based on achieving a minimized charging power ($P_{min}$). If the current bus stop was not the optimal one, the model went on to examine the previous stops (*bus stop − 1)* until the optimal placement was discovered. If the bus required a charger and the current bus stop happened to be the first, the model was to select a charger at the first stop regardless if the placement was the optimal. Further on, in the flowchart, if a charger was required and the current bus stop happened to be the optimal placement, the model was to place a charger at that current stop. When a charger was placed in the system, the model investigated if this was the last bus stop or not. Did the bus stop happened to not be the end stop, the model went onto investigating the next bus stop (*bus stop + 1*) until it reached the end stop and the simulation was complete.

### 3.2.3 Framework and the formulation of the optimization problem

The study by Wang Xiumin et al. [22] which is presented in the theory section was used as a base and guide of how to address a problem related to electric vehicle charging station placement. In addition, the preliminary work described in the introduction, was used for basic knowledge about optimization problems.

The optimization of this study was a linear programming problem solved numerically in the MATLAB software by a solver called *fmincon*. The *fmincon* solver optimizes parameters subject to constraints to find the minimized or maximized objectives [54]. The model can generally be described mathematically as:

$$min\ f(x)\ such\ that \begin{cases} lb \le x \ge ub & upper\ and\ lower\ bounds \\ c(x) \le 0 & (non)linear\ inequality \\ ceq(x) = 0 & (non)linear\ equality \\ A \cdot x \le b & linear\ inequality \\ Aeq \cdot x = beq & linear\ equality \end{cases} \quad 3.11$$

where *f(x)* is the objective function including the optimization parameter *x*. *f(x)* is to satisfy the constraints listed at the right side of the equation. *x*, *lb* and *ub* can be stated as vectors or matrices, *c(x)* and *ceq(x)* are functions that return vectors, *A* and *Aeq* are matrices while *b* and *beq* are vectors.

For the *fmincon* solver there are five algorithm options depending on the type of functions, the complexity and scale of the problem [54]. The *active set* was selected as the algorithm option based on recommendations from the provider of the MATLAB software [55]. *Active set* is considered a medium scale algorithm and are one of the more efficient algorithms within mathematically optimization [56]. The algorithm makes it possible to operate with inequality constraints which were necessary for the problem of this study.

The *fmincon* solver allows to define self-made functions and matrices such that a unique and costume made optimization model can be programmed. For this optimization, it was desirable to make one objective function that returned a minimized scalar subject to bound constraints, linear inequality and equality constraints. The linear inequality and equality constraints were coded as functions (*ceq* and *c*, see equation 3.11) while the optimization parameter (*x* in equation 3.11), upper and lower bound (*ub* and *lb* in equation 3.11) was coded as vectors.

A solver called *ga* (genetic algorithm) was tested in addition to the *fmincon* solver. As mentioned in the literature review in the theory, several studies used this numerical method when optimizing placement of electric charging stations.

Another linear programming solver called *linprog* may have worked as well as the *fmincon* solver. The difference between the two solvers is the way the objective function and the constraint functions are typed. However, this solver was not tested.

The programming code made in MATLAB consists of a main script, including the programming solver *fmincon* and two separate subscripts, one containing the constraints while the other containing the objective function. The scrips work together in such way that the objective function and the constraint functions are imported to the main script were *fmincon* solves the optimization parameters and return the objective function to a minimized scalar. The scripts are found in appendix D.

Further in this section, the objective function and constraint functions used in the optimization model will mathematically be described.

The objective of the optimization problem was to minimize the charging power. The minimized total charging power is mathematically described as an objective function containing a set of unknown optimization variables ($P_{chg,i}$):

$$P_{chg,tot}(P_{chg,i}) = min \sum_{i=1}^{n} P_{chg_i} \qquad 3.12$$

subject to a set of constraints:

$$c_1 \geq E_{batt} \cdot \frac{ll}{100} - E_i \qquad 3.13$$

$$if: E_i \geq E_{batt} \cdot \frac{ul}{100} \qquad ceq_1 = -P_{chg_i} \qquad 3.14$$

$$else: E_i < E_{batt} \cdot \frac{ul}{100} \qquad 0 \geq P_{chg_i} \leq P_{chg_{max}} \qquad 3.15$$

$$c_2 \geq E_i - E_{batt} \cdot \frac{ul}{100} \qquad 3.16$$

$$c_3 \geq E_{batt} \cdot \frac{soc_{end}}{100} - E_{end,w} \qquad 3.17$$

where $n$ is the total number of bus stops in the current bus route investigated, $i$ is the number of bus stop where $i=1$ is the first stop and $i=n$ is the last stop. The location of each $i$ is determined by the driving cycle of the bus according to time and distance. $T_{stop,i}$ (h) is the stopping time at bus stop $i$ and $P_{chg,i}$ (kW) is the required power in the charging station at bus stop $i$. $P_{chg,i}$ are the unknown variables which are to be solved by the optimization ($P_{chg,i}$ is considered as $x$ in equation 3.11).

$E_{batt}$ (kWh) is the battery capacity, $ll$ (%) is the minimum preferable energy level in the battery, $E_i$ (kWh) is the energy in the battery at stop $i$, $ul$ (%) is the maximum preferable energy level in the battery for the possibility of placing a charging station at stop $i$ and $P_{chg,max}$ (kWh) is the maximum possible charging power one charging station can operate with. $soc_{end}$ (%) is the minimum preferable energy at the end of the bus route and $E_{end,w}$ (kWh) is the energy in the battery at the last bus stop when charging stations are considered. The parameter values explained are presented in Table 5 and Table 6 in subsection 3.1.2.

By investigating each optimized $P_{chg,i}$, the placement of the charging stations are obtained by the following statement:

$$
\begin{aligned}
&if: P_{chg,i} > 0 && a\ charger\ is\ placed\ at\ stop\ \boldsymbol{i} \\
&else: P_{chg,i} = 0 && no\ charger\ is\ placed\ at\ stop\ \boldsymbol{i}
\end{aligned}
\qquad 3.18
$$

Meaning that a value of $P_{chg,i}$ greater than zero express that a charging station is placed at stop $i$ with its corresponding charging power, while if $P_{chg,i}$ is zero a station is not placed at stop $i$.

The constraints are mathematically described as bounds ($ub$ and $ll$), linear equalities ($ceq$) and inequalities ($c$), some of them working under different conditionally statements (if- and else-sentences). Equation 3.13 states that the energy in the battery at any stop along the route is to be equal or greater than the minimum preferable energy level. Equation 3.14 states that if the energy level in the battery at any stop is greater than the maximum preferable energy level, $P_{chg,i}$ is to be zero indicating that no charging station is placed at those stops. Equation 3.15 states that if the energy in the battery are below the maximum preferable energy level, a charging station may be placed with a charging power equal or between zero and the maximum possible charging power. Equation 3.16 states that the optimized charging power shall never cause energy level in the battery to be above the maximum preferable energy limit. Equation 3.17 states that the energy in the battery at the end stop is to be equal or above the minimum preferable energy level set for the system.

The energy stored in the battery is restricted by the battery capacity which is included in the following equation defining the energy in the battery:

$$
E_i = \begin{cases} e_{init} & if\ i = 1 \\ \min\{E_{i-1} + (P_{chg_{i-1}} \cdot \eta_{chg} - P_{acc}) \cdot T_{i-1}, E_{batt}\} - e_{c_{i-1,i}} & otherwise \end{cases}
\qquad 3.19
$$

where $e_{init}$ (kWh) is the initial energy in the battery, $T_{i-1}$ (h) is the stopping time at stop $i$, $P_{acc}$ (kW) is the power drawn by the heating and ventilation system in the bus and $e_{c,i-1,i}$ (kWh) is the consumed energy from stop $i-1$ to $i$. $e_{c,i-1,i}$ is the sum of battery power between each stop $i$. The equation states that at the first stop ($i=1$) the energy in the battery is equal to the initial energy in the battery. For the remaining stops the energy in the battery is equal to the energy in the battery at the previous stop ($i$-

*1*) summarized with the charged energy. Further, this is corrected by the power drawn from the accessories in the bus and then subtracted by the energy consumed caused by driving from stop *i-1* to *i*. The *min* statement ensures that the energy in the battery is limited by the battery capacity $E_{batt}$.

Other constraints which are automatically set by using a counting variable like *i*, is that a charging station cannot be placed at any location where the bus is in motion. Moreover, that each charging station charges with a constant charging power for a given amount of time. Another constraint is the driving time and stopping time which is given by the measured driving cycle of the bus.

### 3.2.4 Verification of optimization model

The process of developing the model included trying out several coding options in the MATLAB software. A build-in help database named MathWorks was used as support to make the coding functional. The model was developed to consider the constraints and the conditionally statements set for the system. The model was verified by manually investigating the results obtained by the optimization model:

- The energy required for the bus to complete its route was calculated and then compared with the optimized charged energy. To determine if the model was providing correct solution the two values should meet the following statement:

$$E_{rc} \geq E_{req} \tag{3.20}$$

where $E_{rc}$ (kWh) is the charged energy along the route determined based on the outcome of the optimization and $E_{req}$ (kWh) is the calculated minimum required energy to make the bus complete its route. The two parameters are determined as follow:

$$E_{rc} = \sum_{i=1}^{n} P_{chg_i} \cdot T_i \tag{3.21}$$

$$E_{req} = E_{batt} \cdot ll - E_{end,wo} \tag{3.22}$$

where $P_{chg,i}$ (kW) is the optimization parameter and $T_i$ (h) is the stopping time given by the driving cycle measurements. The product of $E_{batt}$ and $ll$ indicates the lower allowable energy level in the battery and $E_{end,wo}$ (kWh) is the energy in the battery at the end of the route without any charging operation along the route.

- The energy in the bus at the end of the route including charging stations was confirmed equal to or above the minimum allowable energy in the battery:

$$E_{end,w} \geq E_{batt} \cdot ll \tag{3.23}$$

This statement was investigated to make sure constraint in equation 3.13 was considered.

- The charging power at each stop was confirmed did not exceed the maximum charging power set by the system:

$$P_{chg_i} \leq P_{chg_{max}} \qquad\qquad 3.24$$

This statement was investigated to make sure constraint in equation 3.15 was considered.

- The placement of the charging stations was investigated to be in the location were the bus had the longest possible charging time.
- The energy in the battery at those locations where the charging stations were placed (*E*<sub>placed,i</sub>) were investigated to make sure it was equal or below the upper energy level of the battery:

$$E_{placed_i} \leq E_{batt} \cdot ul \qquad\qquad 3.25$$

This statement was investigated to confirm that the constraint in equation 3.14 was considered.

The first step in developing and verifying the optimization model was to use simplified inputs. This was done for convenient reasons to make sure the model worked properly before evolving and expanding it with measurements from bus line 31. The simplified inputs contained velocity data which were obtained from an already measured bus route in Braunschweig city, Germany [57]. This cycle was obtained by an online database named Drive Cat. The characteristics of the driving pattern and route specifications are presented in appendix E. The simplified inputs did not consider altitude data. When the model worked as intended, real inputs which were used in the optimization, were included. A verification of the final input data was also done.

Multiple changes in parameter inputs were performed to make sure the model provided accurate results regardless of scenario. When the model did not work as desired, errors were fixed by improving the programming code and then the simulations were run once more.

## 3.3 RESULTS EXPLANATION

The results are showed in Figure 14 as the last step in the approach for this study. Three results were obtained from the simulation; The total number of charging stations, the placement of them and charging power of each charging station. Figure 21 shows an example of how the optimization results will be presented in the result and discussion section.
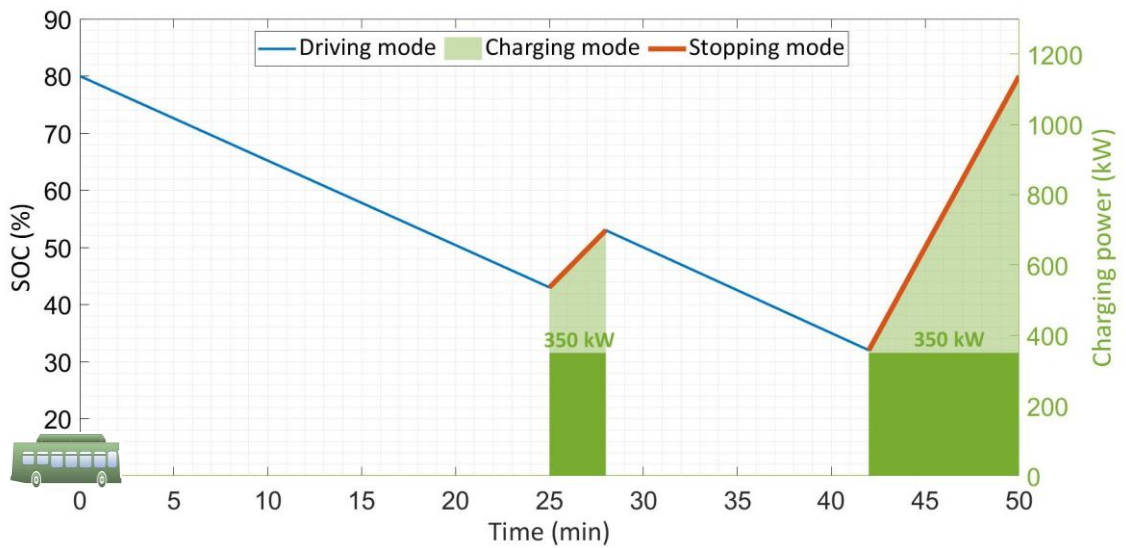
*Figure 21. Presentation of optimized cases*

The x-axis in Figure 21 represent the time traveled for the bus, where the driving is starting at time = 0 min and the end time is in the end of the figure to the right. The left y-axis represents the energy in the battery also stated as the state-of-charge (SOC). The blue curve shows the SOC at a given time. A decreasing curve indicates energy consummation while an increasing curve indicates energy charged. The red marks on the blue curve represent a stop in the route. The longer the mark is, the longer time the stop lasts. The right y-axis represents the charging power for the charging stations that are determined by the optimization model. The charging power for each station is illustrated by the dark green bars with its corresponding power presented at the top of the bar. As for this case, two charging stations are placed along the route with 350 kW charging power each. The lighter green represent that the bus is in charging mode. The horizontal length of the lighter green indicates for how long time the charging is lasting.

# 4   RESULTS AND DISCUSSION

Numerical approximation was used to solve the optimization problem of this study. The MATLAB software was used as the solver by including one object function and five constraints for different conditionally statements. In this section the results and a discussion of the optimized cases will be presented. But first, a discussion of the mathematical solver used, and the data collection will be reviewed together with results on SOC, current and voltage in the battery.

## 4.1   THE MATHEMATICAL SOLVER

The objective of this study was to minimize a power function by using the linear programming solver *fmincon* in the MATLAB software. The *fmincon* solver considered all the constraints and conditionally statements fast but accurate for various input data. The problem may be calculated manually, however, this would be time consuming and using a calculation tool like MATLAB was more efficient.

The *fmincon* solver was selected based on the experience of using it in the optimization in the preliminary work presented in the introduction section. As stated in the method section a solver called *ga* was tested in addition to the *fmincon* solver. However, it turned out that the solver did not get out accurate results as it could not include the equality constraints.

Linear programming has been proven to be a convenient approach in similar optimization problems. By using this experienced method, it strengthens that this method is suitable for its purpose. It was desirable to use a functional and accurate approach to solve an optimization problem and not discover and compare numerical alternatives. Therefore, no other solvers than *ga* were tested. However, the optimization may work with other algorithms like greedy or backtracking which were used in the study by Wang Xiumin et al. presented in subsection 2.3.1.

## 4.2   DATA COLLECTION

### 4.2.1   Specification of the electric bus and charging station

A Li-ion battery was selected as the on-board power supplier for the electric bus as this is currently the most common and suitable rechargeable battery for EVs. As described in the theory, there are different kinds of li-ion batteries based on their different cell chemistry. These differences give variations in battery characteristics such as energy density and possible operating charging power. The NMC li-ion battery was selected as this battery had the highest energy density and the possibility of being charged with high powers. As described in the theory, opportunity charging often operates with higher charging powers than depot charging. As for this case, LTO batteries may have the possibility of being charged with higher charging powers than NMC batteries. A higher charging power will provide energy to the battery at a faster rate which is time effective. However, LTO batteries have lower energy densities than NMC batteries. This means that an LTO battery contain less energy per weight than an NMC battery. Therefore, an LTO battery will weigh more than an NMC if the capacity is considered equal. Further, this additional weight may affect the passenger capacity or driving range. The battery selection may also be determined based on an economical perspective which could be a further study to investigate.

The battery size selection was based on the desire to not make the weight and size of the battery affect the passenger capacity of the bus negatively. An 18-meter bus was selected because it was reasonable to choose a similar bus size of what is the case on the route today. A dc motor was selected as this is the most common motor used in EVs as described in the theory section.

For the battery a maximum preferable energy level of 80 % was set to prevent the battery from being overcharged. The battery may be charged to nearly 100 % in the end of the day by a lower charging power to minimize the effect on the battery. The optimization model also had a minimized preferable energy level to prevent the bus from deep discharging and thus obtain a longer battery life. The 40 % energy limit may also give a longer range of security and the possibility of operating even though the bus might miss one charging operation. Missed charging operations may occur due to power outage or during rush hours making the bus delayed so that the regulation time at the end stops shortens.

### 4.2.2    Velocity and altitude measurements

Three measurements were performed regarding velocity and altitude to get inputs for calculating the energy needs of the bus. These energy calculations were done to determine the state-of charge (SOC) at any given time along the bus route. Further, the SOC was used as input to the optimization model to determine the number of charging stations, their placement and charging powers.

Taking measurements was a time-consuming process where each measurement took more than 2 hours. Therefore, only three measurements were performed. To get more accurate results additional measurements should be done to make sure a worst-case scenario is covered.

By doing more than one measurement, they could be compared and validated. The measurements were performed on the same time of the day to make the traffic conditions similar. The weather was sunny or clouded so the roads were dry. Doing on-site measurements reflected characteristics close to reality. A disadvantage of this approach is that the velocity profile will vary with each measurement, and it may take many measurements to validate the data properly and also difficult to illustrate different scenarios.

Another approach than measuring the velocity can be to calculate the mean velocity between each bus stop based on the route schedule. By doing so more general data on the velocity would be obtained. However, the drawback of this would be the incorrect determination of whenever the bus is regenerating any energy due to breaking. Moreover, the driving time in the schedule is given in minutes. If the bus is using under 1 min between two stops, the schedule shows 0 min. This driving time is therefore needed to be assumed. Another assumption required is the stopping time at each bus stop.

Bus line 31 was selected based on the route's characteristics of being suitable for opportunity charging with longer stops at some bus stops and having a 24/7-hour operation. In addition, it was interesting to select a longer route to investigate how an electric bus with limited battery capacity would manage. The key measurements that was recorded for bus line 31 are presented in Table 9.

*Table 9. Key measurements of the driving cycle performed on bus line 31*

| Parameter | Measurement 1 08.04.2019 | Measurement 2 17.04.2019 | Measurement 3 22.04.2019 | Unit |
|---|---|---|---|---|
| Total time tracked | 02:01:26 | 00:36:25 | 02:06:17 | hh:mm:ss |
| Total stopping time at the end stops | 00:24:08 | 00:11:12 | 00:27:12 | hh:mm:ss |
| Total distance | 45.16 | 21.72 | 44.95 | km |
| Max speed | 75.3 | 65 | 72.3 | km/h |
| Average speed (including stops) | 18.54 | 18.01 | 16.95 | km/h |
| Average driving speed | 28.73 | 28.45 | 26.37 | km/h |
| Number of stops (bus stops + traffic stops) | 70 | 12 | 71 | # |

From Table 9 it can be seen that measurment 1 and 3 are similar to each other having approximately the same driving time, stopping time, distance and number of stops. Small differences can be seen on the average speed of the two measurements, and this may be due to different drivers of the bus. The smiliar characteristics of the two measurments indicate resonable data for the spesific time of day and weather conditions. However, variations will occure due to different drivers, GPS signals, traffic, weather and climate. Additional measurments will therefore be advantageous to cover different scenarios. The two measurments also correspond well with the distance, scheduled driving time and end time at destination presented in Table 7 in the method subesction 3.1.3.

Measurment 2 presentes a much shorter time and distance recorded. This was due to lack of GPS signals and a tracker that did not record for the entire bus route. Measurement 2 was therefore excluded from further use in the optimization, but the velocity and altitude profiles can be found in appendix F. Measurement 1 and 3 of the forward trip is showed in Figure 22 while the return tirp is showed in Figure 23, both according to time. The two measurements according to distance can be found in appendix F.
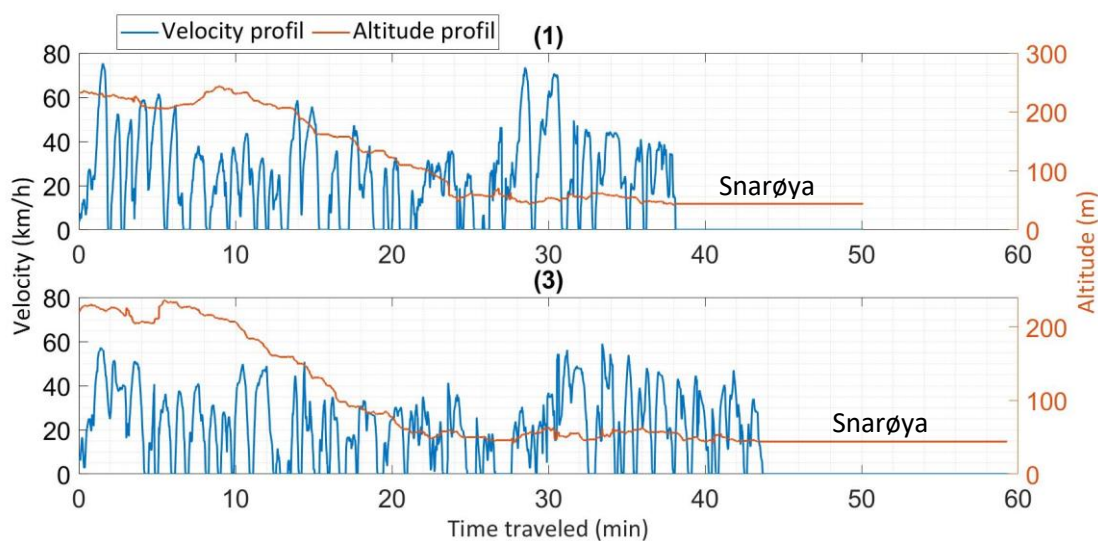
*Figure 22. Driving cycle of measurement 1 and 3 for bus line 31 on forward trip*
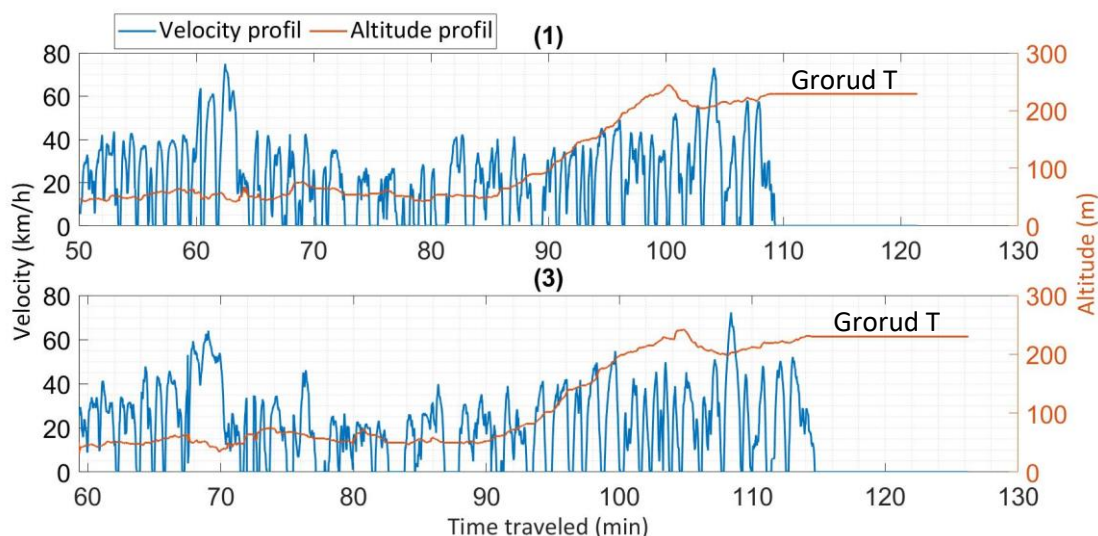


*Figure 23. Driving cycle of measurement 1 and 3 for bus line 31 on return trip*

By doing a visual inspection on the two measurements on both the velocity and the altitude in Figure 22, it seems like the graphs have the same trends. By trends meaning that the graphs have similar behavior. The bus in measurement 1 reaches the end bus stop at Snarøya some minutes before the bus in measurement 3. This may be because the bus in measurement 1 has a slightly higher average driving speed (see Table 9) resulting in that the bus reaches the end stop sooner. As for the return trip in Figure 23 the graphs have the same trends as the forward trip. Theoretically, the velocity measurements on the return trip would have been the forward trip mirrored. However, due to slightly different driving style and traffic occurrences the profiles are not identical. As for the altitude, the measurements on the forward and return trip seem to be more equal which is expected due to the fixed ground elevation. When recording the measurements, it was discovered that the tracker

42

application had some difficulty in logging all the measurements due to missing GPS signals. This happened when driving through a tunnel but did not last for more than some seconds. However, missing GPS signals other places along the route may be a fact that makes the measurements differ from actual conditions.

A throughout inspection of the two measurements were done by calculating the moving average over a time interval of 4.83 minutes which was the time difference between the two measurements. A moving average calculation gave an easier basis of comparation. This because the fluctuations due to frequent stops were removed and thus giving an improved visual inspection. The results from a combined forward and return trip is presented in Figure 24. The forward trip for both measurements starts at 0 min while the return trip starts at about 50 min for measurement 1, and at about 60 min for measurement 3.
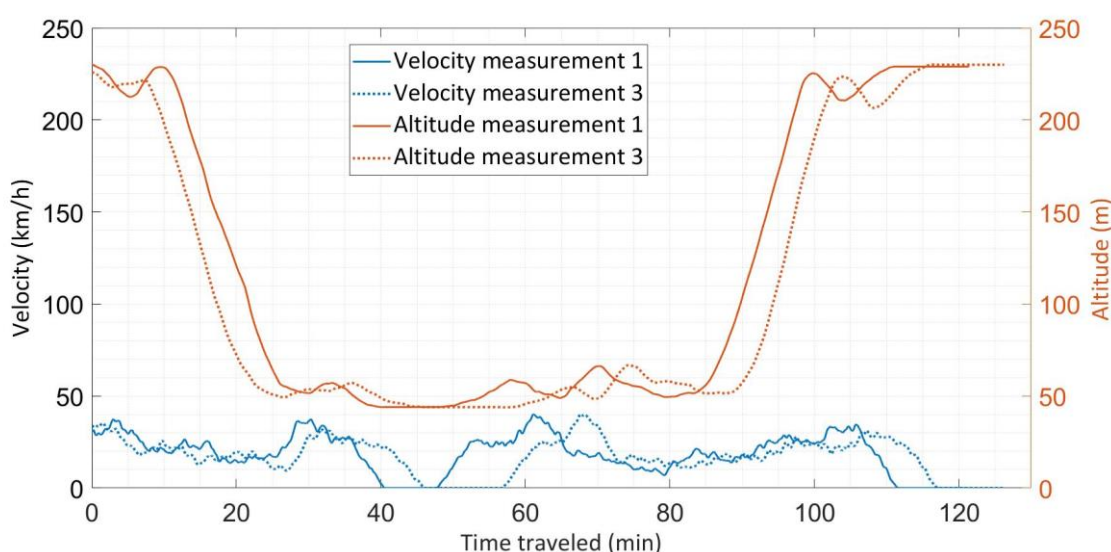


*Figure 24. Moving average of forward and return trip for measurement 1 and 3*

By inspecting Figure 24 the trends of both the velocity and the altitude graphs corresponds quite well with each other. However, the graphs are time shifted due to a slightly difference in the driving time.

### 4.2.3 State-of-charge determinations

The velocity and altitude measurements were used to calculate the tractive force which further determined the battery energy level (SOC). The SOC was then used as input to the optimization model. When determining the SOC, a lot of input values in addition to the velocity and altitude were required. The input values included tractive force, drivetrain efficiencies and accessory load. The values of the accessory load, friction coefficient and passenger load were selected to reflect a worst-case scenario. Further, the SOC for case 1 will be presented for measurement 1 and 3 in Figure 29. The input values used is presented in Figure 5 subsection 3.1.2 and in Table 8 subsection 3.1.3. In order to determine the SOC, different sub calculations were done and will therefore be presented before the SOC curves. The sub calculations are presented for measurement 3. The sub calculations for measurement 1 can be in appendix G. The sub calculations include acceleration, road angle, tractive power and the battery power load. First, the acceleration is presented in Figure 25.
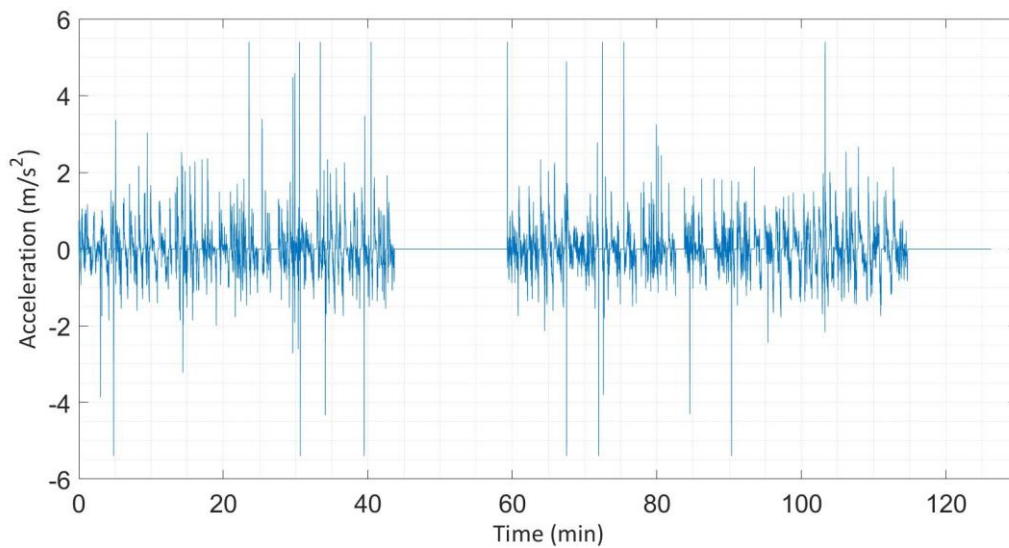
*Figure 25. Acceleration of forward and return trip for measurement 3*

As seen in Figure 25 the acceleration is highly fluctuating often between the range of 2 and -2 m/s². The values seem reasonable for a bus driving in an urban area with frequent stops. Positive value is considered as acceleration while negative is considered as deceleration. The maximum acceleration was set to be 5.4 m/s² as mentioned in the method. This restricted some few measurements. The acceleration without the limits can be found in appendix G. Further, the road angle is presented in Figure 26.
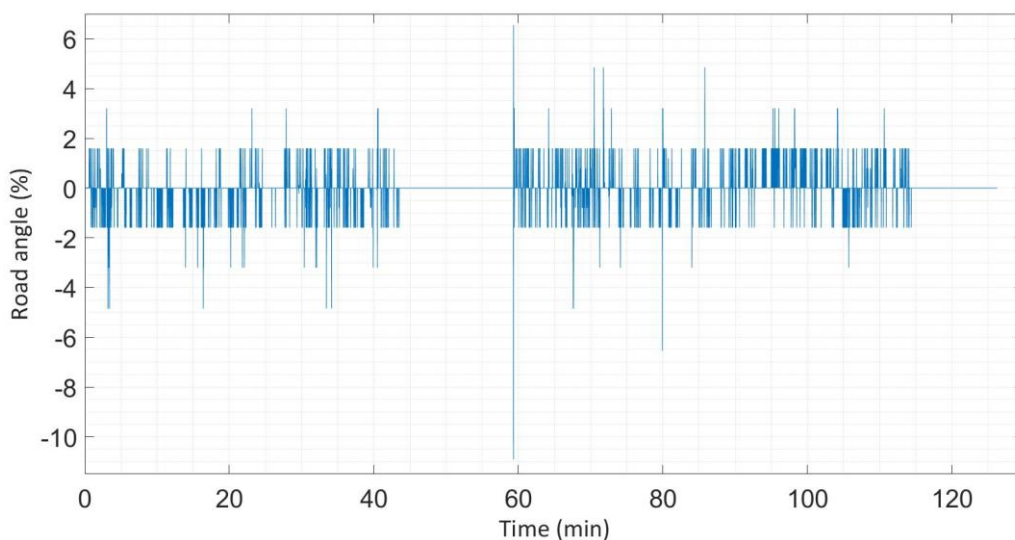


*Figure 26. Road angle of forward and return trip for measurement 3*

As seen in Figure 26 the road angle is typically kept between -2 and 2 % which seems reasonable by comparing the length driven and height climbed for one second. However, right before the bus is starting at its returning trip (time=60 min), an abnormality occurs. This seems to be incorrect because if so, these peaks would have occurred at right after 40 min because the bus is driving the same route

on the forwarding trip as the return trip. The peaks might be due to some missing GPS signals making the angle incorrect. Positive road angle reflects uphill while negative illustrate downhill. Further, the tractive power is presented in Figure 27.
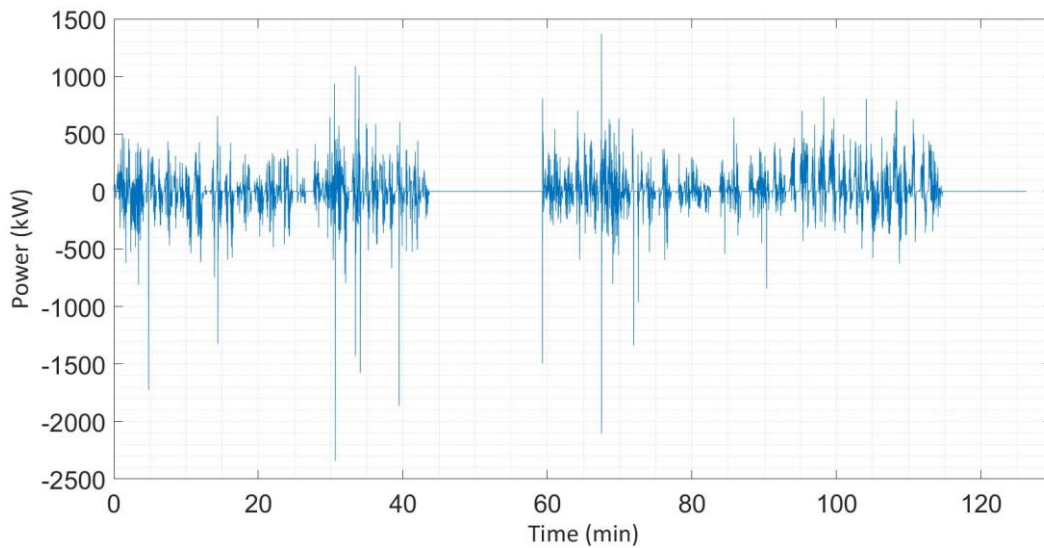


*Figure 27. Tractive power for measurement 3*

As seen in Figure 27 the tractive power is typically between 500 and -500 kW. The power peaks are due to the higher road angle and higher deceleration at those specific times. A comparation of the tractive power was done with the study published by Ivan Baboselac et al. [33] presented in the theory section. The study by Baboselac investigated a passenger car so naturally the tractive power would be less than it is for this study. However, it gave an idea of how the power would behave when calculating it based on a measured driving cycle. The power trends seem to be similar, however, the power is some ten times higher in this study which may not be unlikely as this study has a higher vehicle weight. Further, the battery power is presented in Figure 28.



*Figure 28. Required battery power for measurement 3*

As seen in Figure 28 the power in the battery is almost similar to the tractive power in the previous Figure 27. The difference is that the battery power is corrected for the efficiency in the drive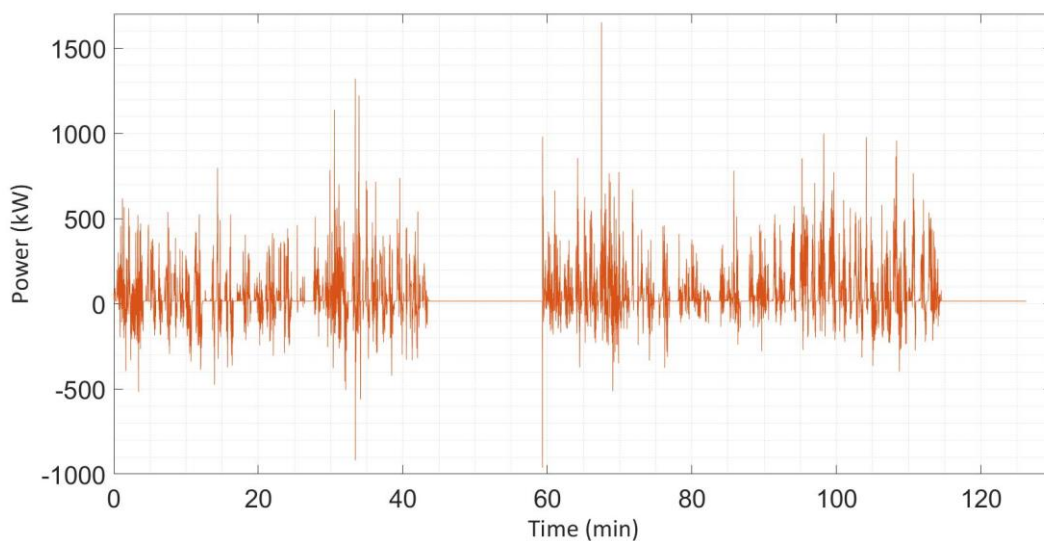train components and accessory load. The negative power is considered as regenerated power corrected by an efficiency of 60 % and the precondition of having a deceleration below 3 m/s$^2$ and a greater velocity than 5 m/s. As seen, most of the theoretically regenerated energy can be used to reduce some of the required power to drive. Further, the SOC is presented in Figure 29.
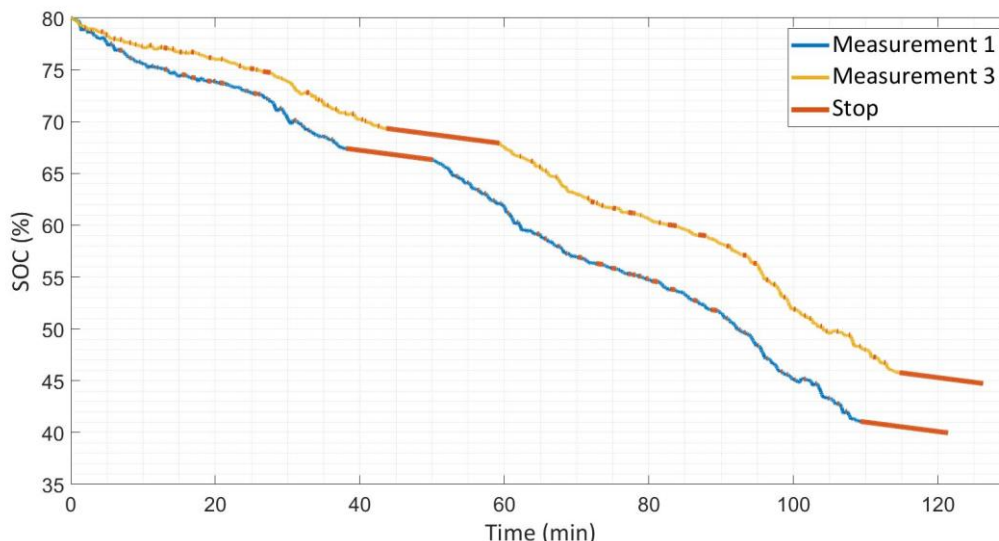


*Figure 29. SOC for 275.4 kWh battery starting at 80 % SOC without any charging mode*

As seen in Figure 29 the SOC in the battery are dropping with time due to the consumption of energy because the bus is driving. The bus is stopping for about 12 min after driving for about 40 min which is the end stop at Snarøya. At about 110 min the second longer stop occurs which is at the end stop at Grorud T. Here it stops for about 12 minutes before it travels to Snarøya again. The remaining red marks indicate small frequent stops along the route for the passengers to disembark and embark. Even though measurement 3 (yellow curve) takes longer time, measurement 1 (blue curve) is the one that consumes the most energy illustrated by being below measurement 3. The energy consumptions for the measurements are presented in Table 10.

*Table 10. Consumed energy for driving one forward trip and one return tip*

| Parameter | Measurement 1 | Measurement 3 |
|---|---|---|
| Energy consumed | 110.1 kWh | 96.6 kWh |

Looking at Table 9 in subsection 4.2.2, the average driving speed is higher for measurement 1 than for 3 which can explain the different energy consumptions. This might indicate that the driving style has an impact on the energy consumption of the bus.

### 4.2.4   Voltage and current without charging stations

The voltage and current in the battery were simulated to investigate how the battery characteristics might behave. When developing a battery model there are a lot of parameters that might affect the operation of the battery which may be challenging to anticipate. Therefore, a simplified battery model

was made to investigate the battery behavior. Temperature due to the battery's operation may affect the behavior but was not included in this battery model. In real, if the temperature is decreased to low temperatures, the internal resistance may increase causing a lower open circuit voltage. Other excluded features such as variation in charging rate may also cause a different outcome in the voltage and current. The expectation of the battery to degrade over time made it necessary to include some range security to make sure the energy in the battery would be enough for the bus to operate. The security range makes the lifetime of the battery extended because the battery was set to not be deeply discharged. The internal resistance was set to a common constant value used in different studies presented in the theory section. However, for actual conditions this may vary. One more factor not considered was the variety of temperatures which affects the operation of the battery regarding different charging rates.

Degradation of a battery such as decreased battery capacity is highly depended on several factors. These factors may not be possible to estimate in a simulation, especially for simulations over a longer time period. The terminal voltage in this study was calculated based on having a degradation of 0 %. An older battery might give a lower voltage. The proposed estimations of current and voltage may therefore vary from actual conditions.

Further, the current in Figure 30 along with the voltage in Figure 31 and Figure 32 are presented. The voltage and current were determined based on the SOC curves for the two measurements shown in Figure 29. Later, when the optimization results are presented, the operation of the voltage and current will be presented once more to investigate the characteristics including charging caused by the installed charging stations.
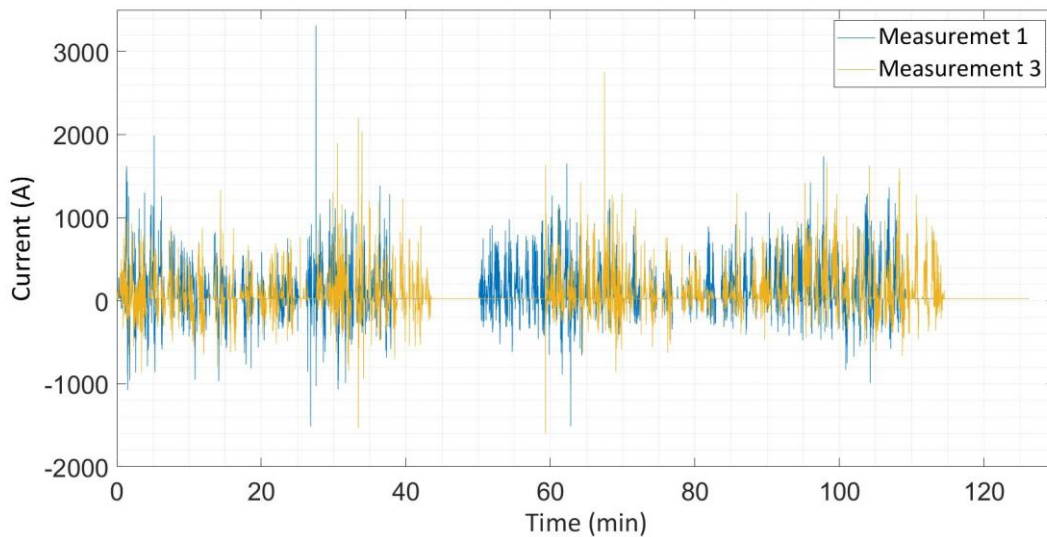


*Figure 30. Current in battery according to operated time without charging stations*

A positive current in Figure 30 indicates a dicharigng mode while a negative current indicates a charging mode. The discharging current is highly fluctive typically between 0 A and $\pm\,500-1000$ A. This is due to the frequent stops. Some breaking is regenerated and creates current which is seen as negative current. Further, the terminal voltage is presented in Figure 31.
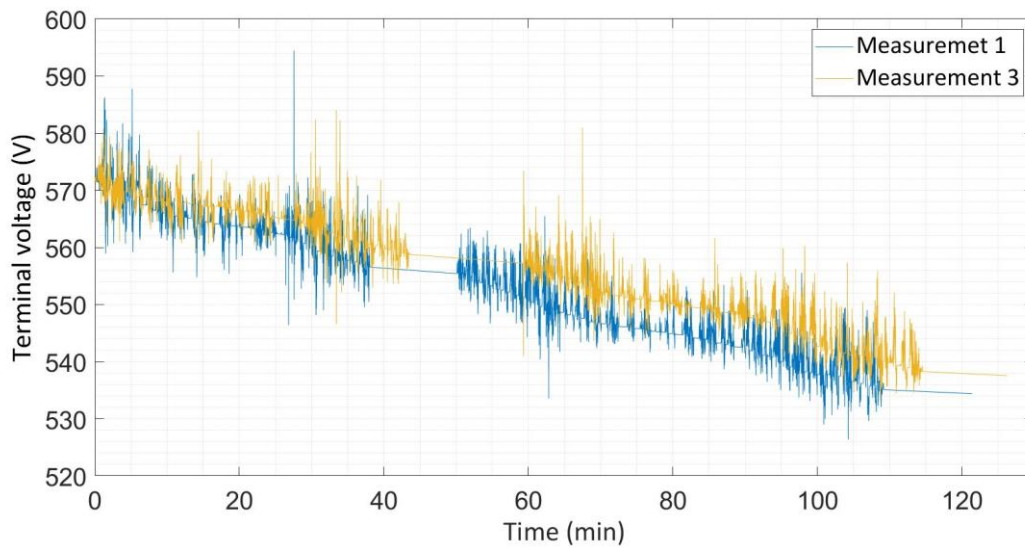
*Figure 31. Terminal voltage of battery pack according to operated time without charging stations*

As seen in Figure 31 the terminal voltage for both measurements decreases with time, this is due to a decreasing in the SOC. The terminal voltage never exceeds the maximum battery voltage of 600 V. The positive peaks in the voltage occurs due to regenerative breaking. If the voltage was exceeding the maximum voltage due to breaking it may be a control system in the vehicle converting it to a suitable voltage. The terminal voltage may also be presented according to the SOC as in Figure 32.
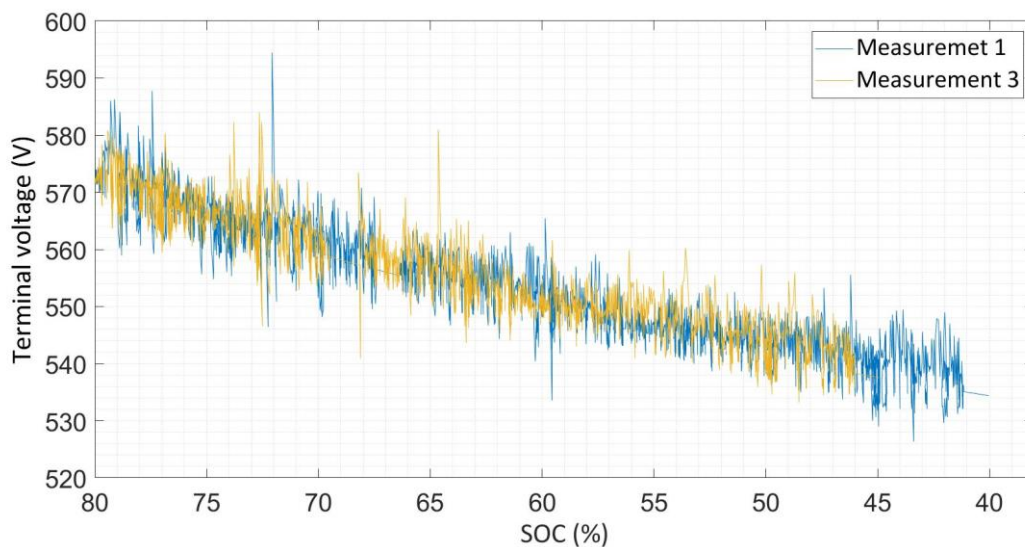


*Figure 32. Terminal voltage of battery pack according to SOC without charging stations*

As seen in Figure 32 the terminal voltage almost drops linearly with the SOC in the battery. This trend seems reasonable for how a battery is operating. However, to validate the simulated results the open circuit voltage for one single cell were simulated and compared with Figure 10 in the theory subsection 2.4.1. The comparation indicated reasonable open circuit voltages and can be found in appendix H.

## 4.3 DEVELOPING AND ADAPTING THE OPTIMIZATION MODEL

The most time-consuming process of this study was creating and verifying an accurate and reliable optimization model. To make the model work, mathematical expressions were coded in the correct form in the MATLAB software.

A built-in help database was used to make the modeling more effective and understandable. When developing the model, understanding how the solver worked and how to connect the different scripts was essential. Having primary knowledge about how to use the optimization tool and basic program features in MATLAB made the modeling easier. In the preliminary study, an optimization model was developed in MATLAB. By having this experience an improved and evolved model could be made in this study.

The model in this study considered a lot more bus stops and included a return trip than the model developed in the preliminary study. The model in this study operated with an actual route and based the energy consumption on measured data. The preliminary study had an objective function that was to minimize the installation cost for the charging stations while this study was to minimize the charging power for the charging stations.

One main difference between the two models was the consideration of limited energy storage in the battery of the bus. The optimization model in the preliminary work calculated the number of electric charging stations based on the total consumption of the bus. Further, placed the stations at the least costly bus stops regardless of the energy in the battery. Because of this, the placement did not reflect the constraint of the battery having a maximum possible energy storage. In the optimization model in this study another approach was applied to include the limit of the battery not containing more energy than its maximum capacity. Therefore, instead of making its placement after the total energy consumption was calculated, the selection was decided after the energy consumption was calculated for every stop along the way. By this making it possible to consider whenever the energy level in the battery exceeded the battery capacity.

Another difference was the possible charged energy at each stop. The model in this study had different stop time intervals at each bus stop making the possible charged energy vary with each stop. The model in the preliminary work had a constant charging time at every stop making the possible energy charged equal at every bus stop.

Comparing the two optimization models, the one in this study is more complex and is better suited for actual routes. However, further and improved modeling can be done and are required if it is to be used in an electric bus system containing more than one bus route. Further, investigations on the inputs such as accessory load and worst-case driving cycle are necessary to cover actual energy consumption. However, the model gives an indication of how electric buses with opportunity charging strategy might be and in what range the battery size and charging power is needed. The placement might also be an indication of where it would be optimal to locate them. However, economic considerations might be a factor to include when considering placement and number of charging stations.

## 4.4 VERIFYING THE OPTIMIZATION MODEL

To make sure of correctly simulations, that the objective function worked properly with the constraints and the conditionally statements, a verification was performed. Firstly, the model was made simple, with input data on the driving cycle from an online database as mentioned in the method section. The verification process was done for both the simplified model and for the optimization model with inputs from bus line 31. The verification of the manually investigations will now be presented for case 1, measurement 1, taking base in the bullet points in the method subsection 3.2.4:

- Equation 3.20 was fulfilled: $E_{rc}$ = 108.8 kWh $\geq E_{req}$ = 27.1 kWh.
- Equation 3.23 was fulfilled: $E_{end,wo}$ = 112.2 kWh $\geq E_{batt} \cdot ll$ = 27.5 kWh.
- Equation 3.23 was fulfilled: $P_{chg,i}$ = 0 – 443 kW $\leq P_{chg,max}$ = 600 kW.
- The placement of the charging stations had the longest possible charging time of 10 minutes.
- Equation 3.25 was fulfilled: $E_{placed,i}$ = 220.3 kWh $\leq E_{batt} \cdot ul$ = 220.3 kWh.

By following this verification approach, it indicated correct simulations and it would be clear where the errors could come from. The verification process was time-consuming and another approach than investigating the results manually would be to compare them with other similar optimizations. However, for the optimization done in this study, it was not possible to do so because it differed to much from the optimizations in the literature.

## 4.5 RESULTS FROM THE OPTIMIZATION

Optimization of electric charging stations are a complex task that will vary with the specific route(s) that is going to be considered. A large battery provides a long range, so the bus is not required to charge so often. However, a large battery may affect the passenger load and the weight of the bus negatively as well give a long charging time which may result in schedule delay. Having a smaller battery, the weight of the bus will be lower giving less energy consumption, on the other hand more charging stations will be required. The battery size and number of charging stations may therefore be a compromising matter. It can be considered that a large battery may only be used for one bus while charging stations may be used by more than one bus, and thus making charging stations more effective than large batteries. However, a more throughout investigation needs to be done.

Some of the considerations in the optimization includes estimating charging requirements, traffic situation in the area and distribution of the transportation fleets. Because there might be several solutions for one route, several cases were developed for this study. Four cases were optimized by having some of the parameters adjusted (see Table 6 in the method subsection 3.1.2). As for the optimization, measurement 1 was used as the main input for all the cases on consummation of energy. This was because measurement 1 had the highest energy consumption of the two measurements and thus illustrate a worst-case scenario. In addition, case 4 was optimized for measurement 3 in addition to measurement 1 so the different recordings could be compared. The optimization of measurement 3 for case 1, 2 and 3 can be found in appendix I.

### 4.5.1 Case 1

For case 1, a maximum battery capacity of 275.4 kWh was considered with a possible maximum charging power of 600 kW. As stated in the method section the bus had a regulation time of 12 minutes

at both end stops. In the measurements recorded, the end stop times were close to this schedule. However, events may occur, resulting in a lower regulation time at the end stop. Therefore, for the simulation, the possible time to charge at the end stop was set to 10 minutes such that a buffer was considered. This buffer may vary, and further investigation of this matter may be done.

The battery SOC operation was set to be between 40 % and 80 % with an initial and desired end energy level of 80 %. Having a minimum preferable energy level of 40 % gave the possibility of having a security range for rush hours or if unexpected events happens. This level may also cover up additional energy consumption that may differ from actual conditions and simulated conditions. One example of this may be the wind speed that was neglected when calculating the energy consumption. Another may be a higher accessory load than the one assumed for this study. The accessory load was based on a 12-meter bus and may differ for an 18-meter bus selected for this study. Having a 40 % minimum limit does also give the battery possibility of extending its lifetime which would be beneficial in an economic aspect.

The maximum preferable battery energy level of 80 % was selected based on the literature review. When operating at high energy level the battery operates under other characteristics such as lower maximum charging rates and charging powers. In addition, does the charging station have other current and voltage characteristics. One possibility may be to charge the buses fully at the end of their shift (at nighttime) with a lower charging power. However, this depends on the logistics of the bus route. Bus line 31 has a 24/7-hour operation, but the buses have a longer time interval between each other at the night giving the possibility of being charged for a longer time with a lower charging power. The optimization of case 1 was done for measurement 1 and is presented in Figure 33.
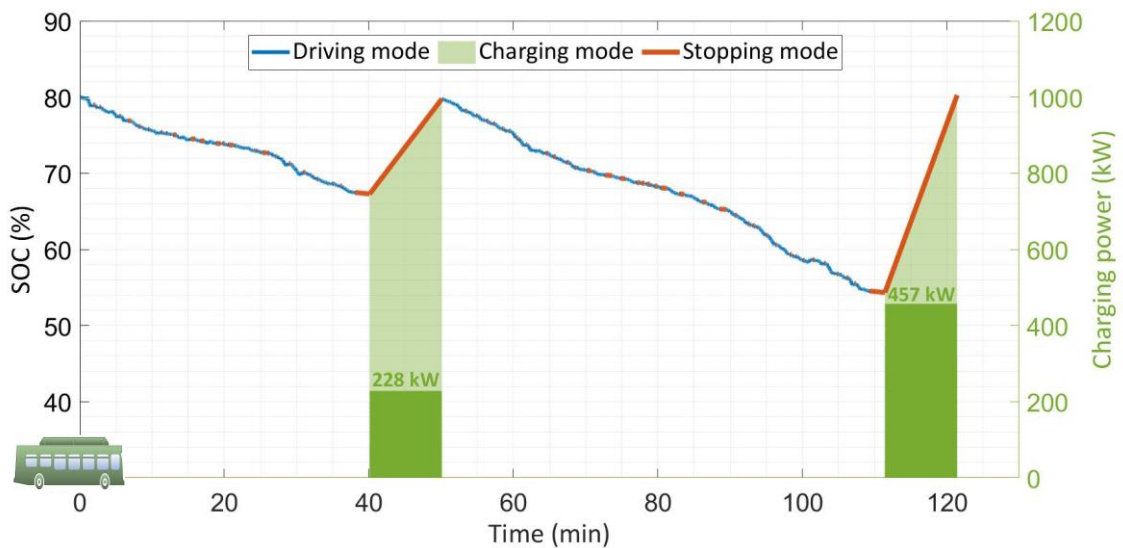


*Figure 33. Optimization of measurement 1, case 1*

As seen in Figure 33 the system is optimized to have two charging stations along the route; first at the end stop Snarøya (time = 40 min) in the forward trip, and then at the end stop at Grorud T (time = 110 min) in the return trip. The two locations for the charging stations were selected based on their potential of charging for a longer time compared to the other stops along the route stopping for some seconds.

If the constraint regarding maximum charging power would have been below 457 kW, the number of charging stations would have been higher. As seen in the green area where the two charging stations are placed, the charging mode starts about 2 minutes after the bus has stopped indicated by the red line starting some time before the green area. This is due to the regulation time of 10 minutes set instead of the scheduled regulation time of 12 minutes. As seen this event is considered at both end stops.

The two charging stations placed in case 1 are supposed to operate with the same charging power. This is because they have equal possibilities of charging the same amount of energy due to equal stopping time. However, the first charging station along the route is optimized with a charging power of 228 kW, while the other with a charging power of 457 kW. The one with the lowest power is restricted by the battery's characteristic of not wanting an operation mode above 80 % of the its capacity. The second charging station does have a bit higher power but does not exceed the maximum charging power level.

It may be an idea to only have one charging station at the end of the return trip if the maximum charging power is heighted, but still two charging stations must be installed. This is based on the assumptions set for the system regarding a minimum preferable battery energy level set to 40 %. If a charging station was not placed at the first end stop at Snarøya, the energy when reaching Grorud T would be below 40 %. It may be a possibility to have a larger battery but then it will be a passenger load problem. Another solution may be to have a higher operational battery level, above 80 %. If so, battery behavior needs to be investigated further. Another solution may be to have a lower preferable energy level. If so, an evaluation between the number of charging stations and charging power needs to be performed.

Before moving on to the next case the operation of the current and voltage in the battery were simulated to investigate the characteristics when including the two charging stations. This was only done for case 1 as the characteristics for the other cases will somewhat be the same. The current is presented in Figure 34 while the terminal voltage is presented in Figure 35.
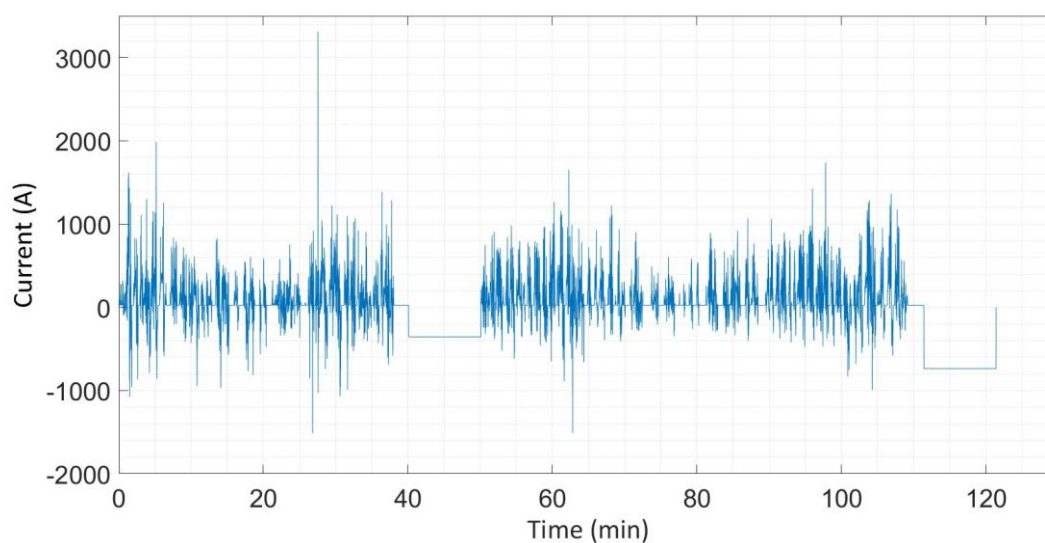


*Figure 34. Current in battery according to operation time with charging stations*

As seen in Figure 34 the current at about 40 min and 110 min indicates a charging mode in the battery. The charging current at 40 min is approximately 355 A which is lower than the current at 110 min being 737 A. This correlates with the power of the charging stations where the first charging station is charged with a lower power than the second station (see Figure 33). Both of the charging currents will have a C-rate below 2.5C which is acceptable for an NMC battery according to the literature review in the theory section. From the two charging modes it can clearly be seen that the charging stations charge in a CC mode as the current is constant. This characteristic is applicable for the charging type assumed and for the SOC simulated in this study. A SOC above 89 % may provide a CV mode.
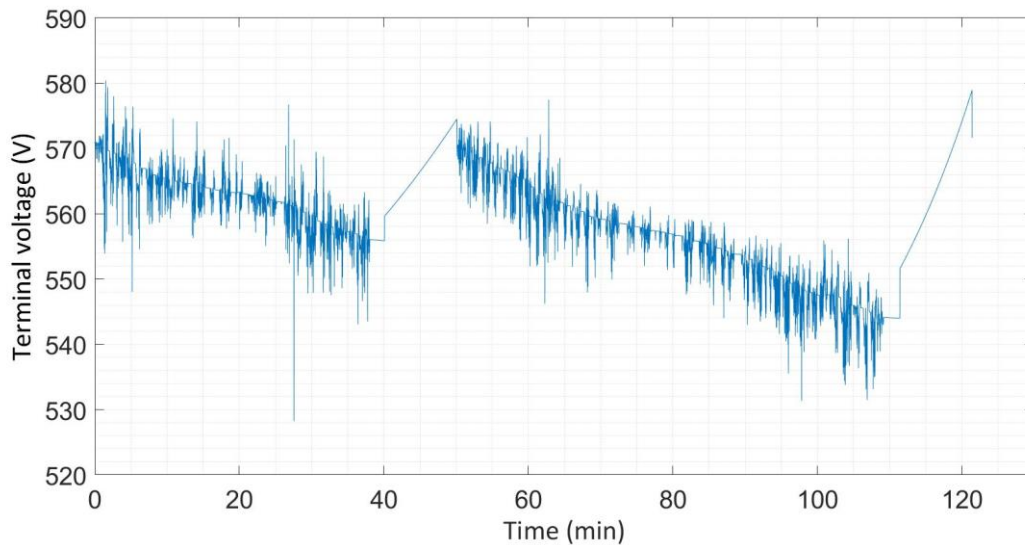


*Figure 35. Terminal voltage in battery according to operation time with charging stations*

As seen in Figure 35 the voltage at about 40 min and 110 min indicates a charging mode for the battery. As the battery is being charged the voltage in the battery increases linearly which it is supposed to do in a CC mode. Both the voltage curve and the current curve has the same characteristics when charging as what was presented in the study done by Ivan Baboselac et al. mentioned in the theory subsection 2.5.

### 4.5.2 Case 2

Further, the system was simulated on how much delay time the bus could operate with before one more extra charging stations would be necessary. The result showed that a delay higher than 4 min would result in needing one extra charging station. The result from considering a regulation time of 7 min is presented in Figure 36.

*Figure 36. Optimization of measurement 1, case 2*

As seen in Figure 36 the system is optimized to have three charging stations along the route; Two at the end stops and one along the return trip at about 70 min. The charging occurs after driving 70 min and last the entire stop time for about 1 min. If a charging station was to be placed there, furth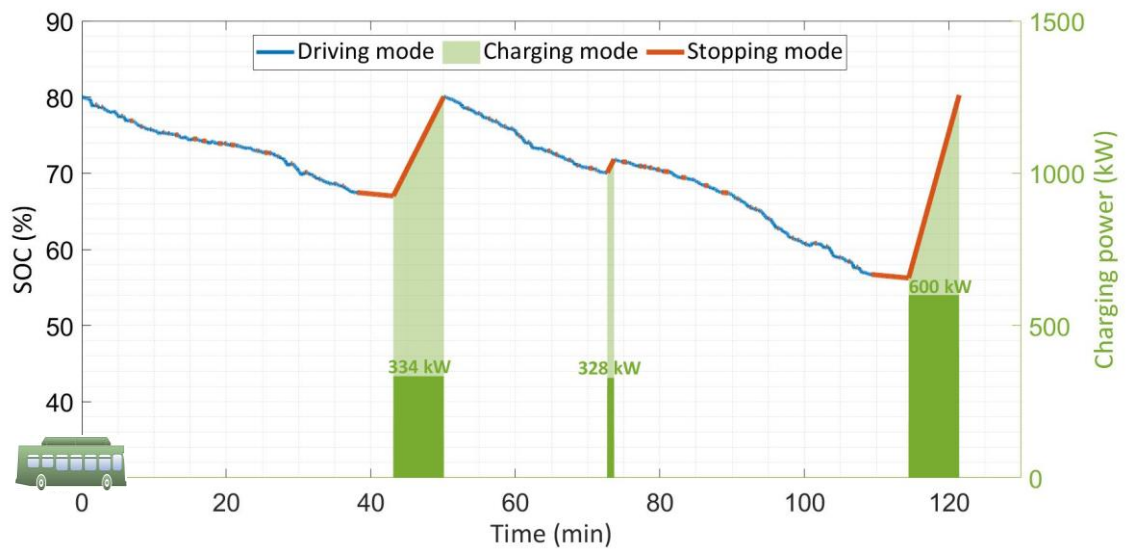er investigations needs to be done. This includes if the stopping time is a common happening and if it is a bus stop and not just a result of traffic. Another aspect is wherever the charging station could be used to charge the bus on the forward trip as well, or if it would already be occupied by a bus driving the return trip. The power of the first charging station along the route is restricted by the upper preferable level of 80 %. The second charging station is a result of that the maximum charging power is reached for the third station. The result from this optimization states that a regulation time of 7 min is possible but one extra charging station is needed to cover the energy needs. As seen at the end stops the charging stations exceed in required charging power compare to case 1 to cover the lost energy due to delay. However, the charging power does not exceed the upper maximum charging power. The outcome of this case is not comparable with the other cases as the regulation time is different. However, this case was interesting to simulate as it shows how much delay the bus can have before needing one extra charging station.

### 4.5.3 Case 3

For case 3 the desired energy level at the end of the route was set to 70 % battery capacity, leaving an initial energy at 70 %. The regulation time is 10 min like for case 1. The optimization is presented in Figure 37.

*Figure 37. Optimization of measurement 1, case 2*

As seen in Figure 37 the system is optimized to have two charging stations as for case 1. However, the difference between case 1 and this is that the charging power at the first stop is increased to 343 kW while the second charging station is reduced to 343 kW. This outcome is beneficial for the grid power load which is reduced by 114 kW compared to case 1. The reason for the changed charging power is due to the initial energy in the battery being lower. When stopping at Snarøya the bus can be charged with a higher power but still be kept below the upper operation level of 80 %.

### 4.5.4 Case 4

For case 4 several input values were changed to investigate the impact of reducing the battery capacity. By having a smaller battery, the bus would use less fuel and possibly reduce the battery cost. On the other hand, the bus would have a lower security range despite the lower energy level is kept at 40 %. The optimization for measurement 1 is presented in Figure 38.
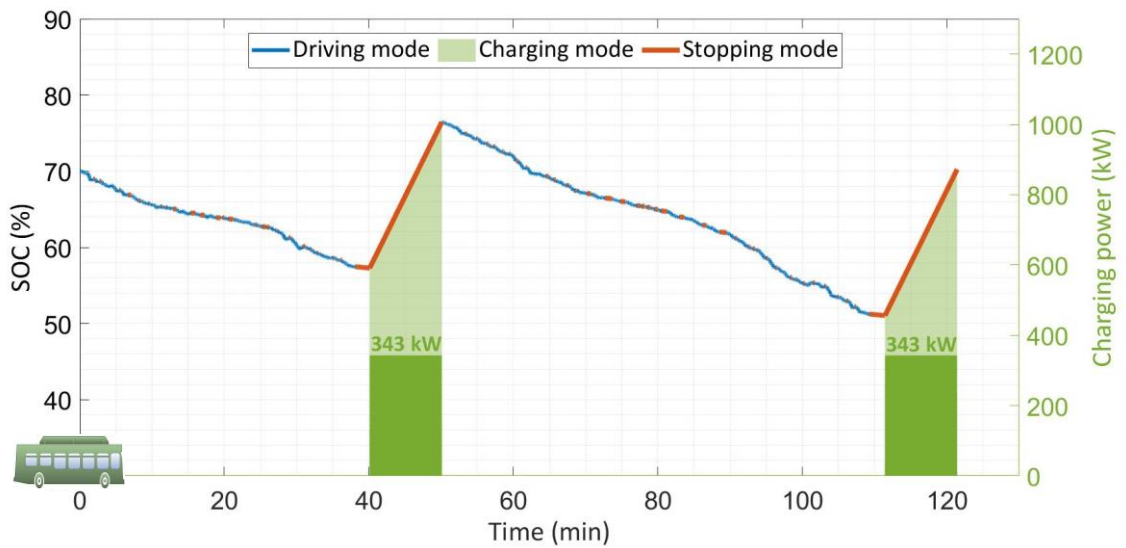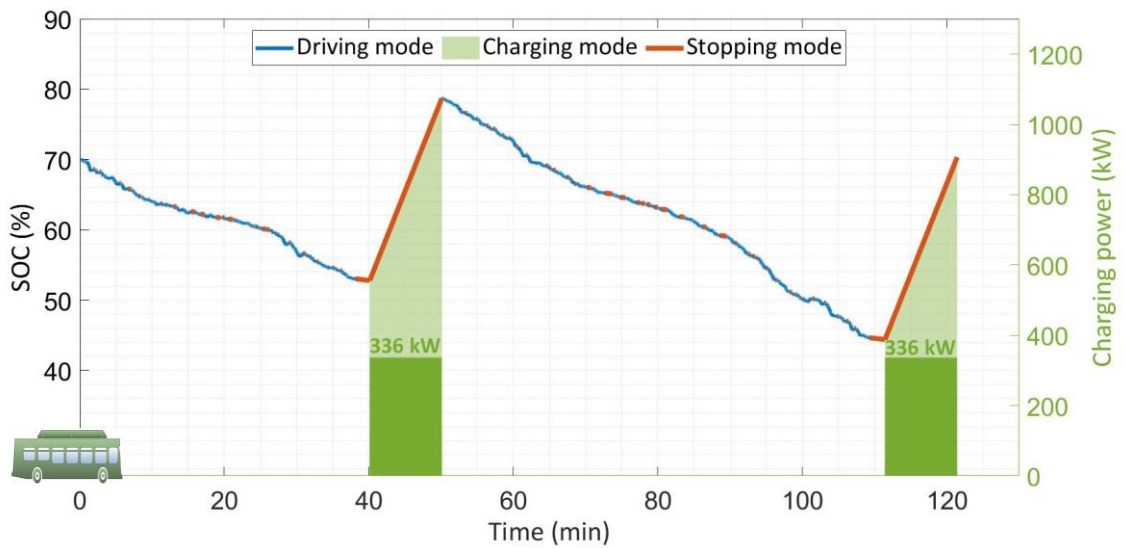
*Figure 38. Optimization of measurement 1, case 4*

As seen in Figure 38 the route is optimized to have two charging stations along the route. The solution also presents the lowest maximum charging power which is beneficial for the grid load. By reducing the battery capacity some security range will be lost and is therefore something that must be evaluated as a compromise whenever a smaller battery should be selected.

Further, for this case, there was performed an optimization for measurement 3 which had slightly different driving cycles than measurement 1 (see Figure 29 in subsection 4.2.3). These differences resulted in different required charging powers. Measurement 3 is presented in Figure 39.



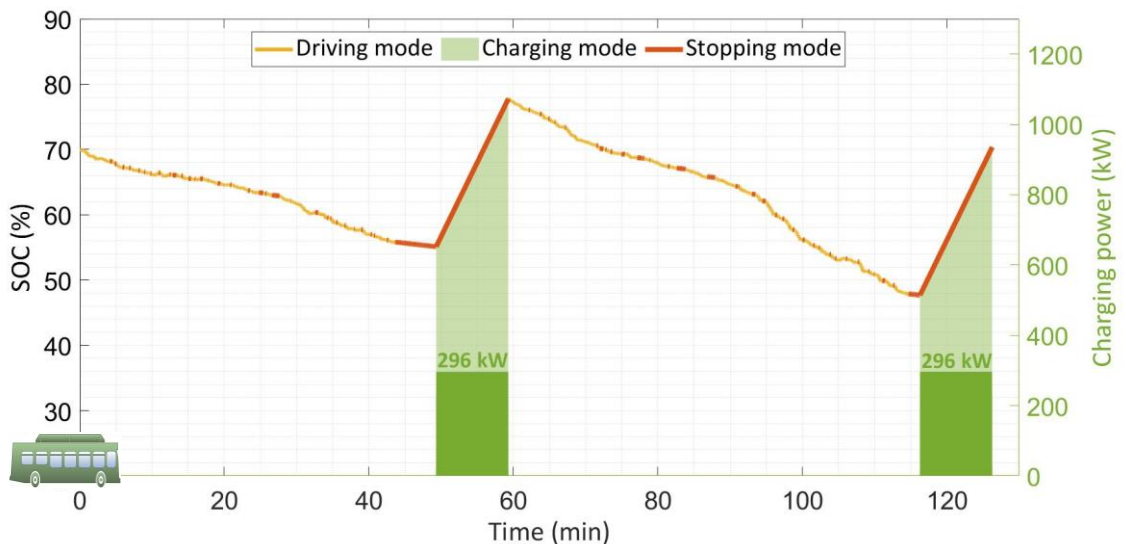*Figure 39. Optimization of measurement 3, case 4*

As seen from Figure 39, still two charging stations in both end stops will be required. However, the charging power is reduced at both stations with about 12 % compared to measurement 1 in case 4. This indicates that the charging power may be reduced by driving more effectively.

### 4.5.5 Summary of the cases

Factors such as bus route characteristics, driving cycles and available grid capacity are essential considerations to be aware of when planning an electric bus system. Because of these factors, the placement of bus charging stations is location specific and each bus route will have their own optimal solution.

As stated in the theory section bus charging stations are connected to the low voltage distribution network of 230 V or 400 V. As for the problem of this study only some few charging stations were planned and for one route. Connection to a 400 V grid may be a solution by using a converter that boost 400 V to the battery voltage of 600 V. One electrical substation at Grorud T may be suitable for a charging station having 500 kVA available. This applies for charging stations in case 1, 3 and 4. At Snarøya the highest available energy capacity in a substation was 325 kVA and a charging station connection to this only applies for case 1. However, this substation operates with 230 V.

In a larger perspective Oslo's plan is to invest in hundreds of new electric buses and naturally several charging stations may be placed in the same area. Therefore, in a future perspective this matter needs to be considered as it may change the outcome of the grid connection. Another factor is the grid robustness. As stated in the theory, countries have the capacity to handle some tens of percentage of increased load on the distribution network. So, by implementing one electric route with charging stations as what was done in this optimization problem, may not cause any affects. However, a larger electric bus fleet is expected, making the factor not to be neglectable.

Connecting charging stations to the grid may cause unwanted peaks in the grid and different techniques to reduce these peaks has been studied. By distributing the charging time over a longer period, charging power will be reduced as presented in Figure 5 in the theory subsection 2.2. As for the placement of bus charging stations along a route this measure should be considered. The theoretically solution would be to have a charging station at each stop along the route. By having this, the total charging time would have been maximized and charging power minimized. An inductive charging system may in this case be less space consuming than a pantograph system. However, having charging stations at each stop may be more costly than having some few stations. Finding the right balance between the number of charging stations and the load of charging power is a crucial factor when determining the optimal solution. As seen in the optimization of this study having charging stations at stops were the bus is standing for a longer period, is beneficial. This because it makes the station more effective than a station used for a shorter time.

As seen from the optimization results, the possible charging power for one charging station may be up to 600 kW. High charging powers may cause peaks in the distribution net. However, even though the battery is being charged with high powers the charging station may share their power output with other sources than the distribution net. A stationary battery connected to the charging station may be a solution to smooth some of the peaks in the distribution net. The battery may be connected to the distribution net and draw energy form it over a longer time when the station is not used. If this strategy is applied, the bus route is depended on being operated by buses driving with some time interval between each other. This to have time for the stationary battery to be charged when the station is not being used. As for the case with bus line 31, the time interval between the buses are frequent which may be impractical. Another possibility is to let the battery be charged with PV panels. As PV panels

are depended on weather conditions, the source might not be stable enough, especially for Norway with high season variations. This may be a further work to consider.

As stated in the theory, the placement of charging stations should be close to load centers due to stronger grids in these areas. As for bus line 31, the end stop at Grorud T is located closely to the tube network running on electricity. This may be an advantage as the area already has large power capacity to ensure sufficient power supply to the tube. Another advantage is that the area is a crossing center of buses on different routes. Therefore, having a charging station here may function as a reserve energy source for electric buses on other routes. It might even be used when buses at line 31 are not charged. A disadvantage of placing it at Grorud T may be the lack of space for a pantograph as the location is crowded with buses and passengers. Induction charging may therefore suite better as this interface is placed beneath the ground. Placing charging stations at the end stop may be a more optimal solution than placing them at stops along the route. The possibility of charging the battery along the route may be more unpredictable than at the end stop. The stopped time at each bus stop along the route will vary or even be nonexistent as there might not be passenger that are to embark or disembark.

# 5 CONCLUSION

This study considered placement of electric charging stations for a public electric bus system with the intention of minimizing the charging power. This was an optimization problem where fully electric buses with opportunity charging strategy were considered. This technology was selected because it is considered as a convenient bus system alternative. The developed strategies were proposed for an existing bus route in Oslo city, Norway.

Battery and charging specifications were determined based on the literature review presented in the theory section. Measurements regarding velocity and altitude on the route were performed. This data where further used to determine the energy needs for an electric bus. Four cases were formed regarding different battery capacities, desired end battery levels, maximum charging powers and end stop regulation times. Further, a mathematical model was developed and verified in order to solve the optimization. The model solved the cases by linear programming in the MATLAB software. The optimization model was developed in terms of one objective function with the intention of minimizing the charging power subject to constraints regarding battery operation ranges and charging power restrictions. The model was successfully developed and verified.

In general, it was found that the selection of battery size and number of charging stations are a compromising matter. Large batteries require fewer charging stations but is heavy while small batteries are lighter but require more charging stations. Further, it was found that by doing velocity measurements on the specific route, the regenerated energy would be included. Having the possibility of regeneration will give a smaller required battery capacity for the bus. It could be seen from the two measurements that driving for some longer time would not necessarily result in higher energy needs but may rather be determined by the driving style.

The results from the four optimized cases showed that having electric buses with opportunity charging strategy on bus line 31, is possible. For this route it might be enough with two charging stations, one at each end bus stop having a regulation time of 10 minutes. The required charging power would be reduced with longer stopping time and with equally sharing the total charging power on the charging stations along the route. When having a route with a regulation time of several minutes at the end stop, utilizing these locations for charging operations seems to be an optimal solution. Having a 24/7-hour operation, like bus line 31, it is suitable for an opportunity charging system. By comparing case 1, 2 and 4 having equal regulation time, case 4 provided the optimal solution. Case 4 does not only have the lowest charging power but also the lowest battery weight. Further, the case will give some less range security but is still within the limit of never decrease below 40 % of the battery capacity.

As for further works, it might be interesting to develop the optimization model to consider multiple routes, possibly entire bus systems for a specific urban area. Oslo are planning to adapt a large-scale electric bus fleet. Considering all the routes as an entirely, provides a wider perspective giving the opportunity to plan a more effective and accurate electric bus system.

Having well developed and effective programming tools will be crucial to keep up with the increasing digitization. As the population is moving towards a more electrified society, new optimization models are proposed. One proposed model with potential is the one developed in this study.

# 6 FURTHER WORK

For this study, there are several further works to consider. The optimization problem of this study only includes one bus route and may reflect a pilot project in real. However, the implementation of multiple electric buses and even entire electric bus systems are on the move towards being more common. The model developed for the optimization in this study may be evolved to a more complex one including multiple routes connected by each other having some of the same bus stops. When a bus stop is operated by more than one bus line logistics regarding schedules and charging, needs to be considered and available space for several buses to pass a charging bus needs to be made sure of. Optimization of multiple electric buses has been performed by using linear programming. Other software programs than MATLAB that are specifically made for optimization with in-built models may be used for problems of a larger scale.

The objective function in this study considered minimizing the charging power. Including multiple objective functions with different weightings will give a deeper insight. This including how the problem might become closer to an optimal solution meeting all the considerations. This may be objective functions considering costs and space availability for placing charging stations. The model may also include the possibility of some stops being restricted to not have the possibility of having charging stations. For example, at stops related to rush traffic or traffic lights.

Doing a further research on the route characteristics regarding driving cycle and regulation times can be interesting to get more accurate results. One solution may be to compare measurements done with the scheduled route and in that way maybe coming closer to obtain a worst-case scenario. As the use of electric charging for EVs are increasing, the power peaks in the distribution network is desired to be reduced. This may be done by using a stationary battery connected to a charging station. The battery may be connected to PV panels which can supply the battery with electricity and thus be a solution for reducing power peaks in the grid. Performance on how much this can reduce the peak, how large the battery must be and how the logistics should be performed, may be an interesting future study. Further works on energy consumption regarding different driving styles may also be performed. This to ensure that the bus can operate the entire route for all driving styles but also to develop the most environment and cost-effective driving pattern.

# LIST OF REFERENCES

[1]     UNFCCC, "Paris Agreement," presented at the United Nations Climate Change Conference, Paris, France, 30.11.15-12.12.15, 2015. Available: https://unfccc.int/sites/default/files/english_paris_agreement.pdf

[2]     United Nation, "World Urbanization Prospects: The 2018 Revision," 2018, Available: https://population.un.org/wup/Publications/Files/WUP2018-KeyFacts.pdf, Accessed on: 29.09.2018.

[3]     UN-HABITAT, "Cities and Climate Change: Global Report on Human Settlements 2011," Earthscan, London and Washington DC2011.

[4]     Z. Gao *et al.*, "Battery capacity and recharging needs for electric buses in city transit service," *Energy,* vol. 122, pp. 588-600, 2017/03/01/ 2017.

[5]     Transport and Environment, "Electric buses arrive on time," 2018.

[6]     M. Mahmoud, R. Garnett, M. Fergusonk, and P. Kanaroglou, "Electric buses: A review of alternative powertrains," *Renewable and Sustainable Energy Reviews,* vol. 62, pp. 673-684, 2016/09/01/ 2016.

[7]     K. Austin, M. Shield, S. Bouton, S. Hansen, S. Knupfer, and C. Shih, "Focused acceleration: A strategic approach to climate action in cities to 2030," McKinsey Center for Business and Environment, C40 Cities 2017, Available: https://www.c40.org/researches/mckinsey-center-for-business-and-environment, Accessed on: 29.09.2018.

[8]     A. Lajunen, "Lifecycle costs and charging requirements of electric buses with different charging methods," *Journal of Cleaner Production,* vol. 172, pp. 56-67, 2018/01/20/ 2018.

[9]     R. H. Bækken, "Optimization of electric vehicle charging station placement," A, Department of Engineering Sciences, University of Agder, 2018.

[10]    S. Jeong, Y. J. Jang, and D. Kum, "Economic Analysis of the Dynamic Charging Electric Vehicle," *IEEE Transactions on Power Electronics,* vol. 30, no. 11, pp. 6368-6377, 2015.

[11]    ABB, "TOSA – Enabling a new generation of electric buses," 2017.

[12]    D. Göhlich, T.-A. Fay, D. Jefferies, E. Lauth, A. Kunith, and X. Zhang, "Design of urban electric bus systems," *Design Science*, vol. 4*,* p. e15. doi: 10.1017/dsj.2018.10 Available: https://www.cambridge.org/core/article/design-of-urban-electric-bus-systems/1C0E4AA05F6E1FBF8A545E13F6A8D2DE under a CC-BY 4.0 license https://creativecommons.org/licenses/by/4.0/

[13]    Zero Emission Resource Organisation. (n.a.). *2019 – det store gjennombruddet for utslippsfrie busser i Norge!* Available: https://zero.no/nyheter-om-utslippsfri-og-fornybar-buss-og-kollektivtrafikk/

[14]    Naturpress. (2019). *Seks elektriske busser i Drammen og Nedre Eiker settes på veien, og det planlegges for mange flere*. Available: http://naturpress.no/2019/02/11/seks-elektriske-busser-i-drammen-og-nedre-eiker-settes-pa-veien-na-og-det-planlegges-for-mange-flere/

[15]    ABB, "Electric buses Solutions portfolio," 2017, Available: https://search-ext.abb.com/library/Download.aspx?DocumentID=9AKK107045A5045&LanguageCode=en&DocumentPartId=&Action=Launch, Accessed on: 09.10.2018.

[16]    D. Steen and L. A. Tuan, "Impacts of fast charging of electric buses on electrical distribution systems," *CIRED - Open Access Proceedings Journal,* vol. 2017, no. 1, pp. 2350-2353, 2017.

[17]    V.-L. Nguyen, T. Tran-Quoc, S. Bacha, and B. Nguyen, "Charging strategies to minimize the peak load for an electric vehicle fleet," in *IECON 2014 - 40th Annual Conference of the IEEE Industrial Electronics Society*, 2014, pp. 3522-3528.

[18]    M. A. Awadallah, B. N. Singh, and B. Venkatesh, *Impact of EV Charger Load on Distribution Network Capacity: A Case Study in Toronto*. 2017, pp. 268-273.

[19]    C. C. Castello, T. J. LaClair, and L. C. Maxey, "Control strategies for electric vehicle (EV) charging using renewables and local storage," in *2014 IEEE Transportation Electrification Conference and Expo (ITEC)*, 2014, pp. 1-7.

[20]    M. Andersson, "Energy storage solutions for electric bus fast charging stations ", Energy Systems Engineering, Uppsala University, Diva portal, 2017.

[21]    W. Khan, F. Ahmad, and M. S. Alam, "Fast EV charging station integration with grid ensuring optimal and quality power exchange," *Engineering Science and Technology, an International Journal,* vol. 22, no. 1, pp. 143-152, 2019/02/01/ 2018.

[22]    X. Wang, C. Yuen, N. Ul Hassan, N. An, and W. Wu, "Electric Vehicle Charging Station Placement for Urban Public Bus Systems," *IEEE Transactions on Intelligent Transportation Systems,* vol. 18, no. 1, pp. 128-139, 2017.

[23]    S. Liu, F. Wen, and G. Ledwich, "Optimal Planning of Electric-Vehicle Charging Stations in Distribution Systems," *IEEE Transactions on Power Delivery,* vol. 28, no. 1, pp. 102-110, 2013.

[24]    M. Xylia, S. Leduc, P. Patrizio, F. Kraxner, and S. Silveira, "Locating charging infrastructure for electric buses in Stockholm," *Transportation Research Part C: Emerging Technologies,* vol. 78, pp. 183-200, 2017/05/01/ 2017.

[25]    I. Frade, A. Ribeiro, G. Gonçalves, and A. Pais Antunes, *Optimal Location of Charging Stations for Electric Vehicles in a Neighborhood in Lisbon, Portugal*. 2011.

[26]    S. Mehar and S.-M. Senouci, *An optimization location scheme for electric charging stations*. 2013, pp. 1-5.

[27]    C. Daniel and J. O. Besenhard, *Handbook of Battery Materials*, 2. ed. Germany: Wiley-VCH, 2011.

[28]    L. Wen Yao, J. Aziz, P. Yee Kong, and N. R. N. Idris, "Modeling of lithium-ion battery using MATLAB/simulink," 2013.

[29]    G. Pistoia, *Lithium-Ion Batteries : Advances and Applications*. Oxford, NETHERLANDS: Elsevier, 2013.

[30]    The European Parliament and The Council of The European Union, "Directive (EU) 2015/719 of the European Parliament and of the Council " 2015.

[31]    E. Raszmann, K. Baker, Y. Shi, and D. Christensen, "Modeling stationary lithium-ion batteries for optimization and predictive control," in *2017 IEEE Power and Energy Conference at Illinois (PECI)*, 2017, pp. 1-7.

[32]    U. A. B. Bakshi, Varsha U., *Electrical circuits and mechines*, 5. ed. India: Technical publications pune, 2009.

[33]    I. Baboselac, Ž. Hederić, and T. Bensic, *Matlab simulation model for dynamic mode of the lithium-ion batteries to power the ev*. 2017, pp. 7-13.

[34]    F. Marra, G. Y. Yang, C. Træholt, E. Larsen, C. Nygaard Rasmussen, and S. You, "Demand profile study of battery electric vehicle under different charging options," in *2012 IEEE Power and Energy Society General Meeting*, 2012, pp. 1-7.

[35]    O. Tremblay and L.-A. Dessaint, "Experimental Validation of a Battery Dynamic Model for EV Applications," *World Electric Vehicle Journal,* vol. 3, pp. 289-298, 2009.

[36]    T. Huria, M. Ceraolo, J. Gazzarri, and R. Jackey, "High fidelity electrical model with thermal dependence for characterization and simulation of high power lithium battery cells," in *2012 IEEE International Electric Vehicle Conference*, 2012, pp. 1-8.

[37]    A. A.-H. Hussein, N. Kutkut, and I. Batarseh, "A hysteresis model for a Lithium battery cell with improved transient response," in *2011 Twenty-Sixth Annual IEEE Applied Power Electronics Conference and Exposition (APEC)*, 2011, pp. 1790-1794.

[38]    A. Rahmoun and H. Biechl, *Modelling of Li-ion batteries using equivalent circuit diagrams*. 2012, pp. 152-156.

[39]    C. Zhang, J. Jiang, L. Zhang, S. Liu, L. Wang, and P. Loh, A generalized SOC-OCV model for lithium-ion batteries and the SOC estimation for LNMCO battery, 2016, p. 900. [Online]. Available: https://www.mdpi.com/1996-1073/9/11/900 under a CC by 4.0 licence https://creativecommons.org/licenses/by/4.0/.

[40]    H. Rahimi-Eichi, U. Ojha, F. Baronti, and M.-Y. Chow, "Battery Management System: An Overview of Its Application in the Smart Grid and Electric Vehicles," *IEEE Industrial Electronics Magazine,* vol. 7, no. 2, pp. 4-16, 2013.

[41]    P. Keil *et al.*, *Calendar Aging of Lithium-Ion Batteries: I. Impact of the Graphite Anode on Capacity Fade*. 2016, pp. A1872-A1880.

[42]    J. Meng, G. Luo, M. Ricco, M. Swierczynski, D.-I. Stroe, and R. Teodorescu, "Overview of Lithium-Ion Battery Modeling Methods for State-of-Charge Estimation in Electrical Vehicles," vol. 8, p. 659, 2018.

[43]    K. Sang-Hoon, *Electric Motor Control: DC, AC and BLDC Motors*. Kangwon National University, India: Joe Hayton, 2017.

[44]    Irizar Sociedad Cooperativa. (n.a., 26.04.2019). *Technical data*. Available: https://www.irizar.com/en/autobuses-y-autocares/autobuses/irizar-i2e-18m/

[45]    BYD. (n.a., 26.04.2019). *18M BATTERY-ELECTRIC BUS*. Available: http://bydeurope.com/downloads/eubs_specification/BYD_18_Meters_Electric_bus.pdf

[46]    AppAnnex. (n.a., 27.04.2019). *Speed Tracker GPS Speedometer and Trip computer*. Available: http://www.appannex.com/speed-tracker-gps-speedometer-and-trip-computer/

[47]    Ruter AS. (2019, 27.04.2019). *Snarøya - Fornebu - Tonsenhagen - Grorud*. Available: https://ruter.no/globalassets/rutetabeller/buss-oslo/buss-30-37-rutetabell-03032019.pdf

[48]    Ruter AS. (n.a., 27.04.2019). *Selskapsinformasjon, Organisering*. Available: https://ruter.no/om-ruter/selskapsinformasjon/

[49]    C. He, H. Maurer, and G. Orosz, *Fuel Consumption Optimization of Heavy-Duty Vehicles with Grade, Wind, and Traffic Information*. 2016.

[50]    J. Carvill, "2 - Applied mechanics," in *Mechanical Engineer's Data Handbook*, J. Carvill, Ed. Oxford: Butterworth-Heinemann, 1993, pp. 57-101.

[51]    A. Lajunen and A. Kalttonen, "Investigation of thermal energy losses in the powertrain of an electric city bus," in *2015 IEEE Transportation Electrification Conference and Expo (ITEC)*, 2015, pp. 1-6.

[52]    S. Van Sterkenburg, E. Rietveld, F. Rieck, B. Veenhuizen, and H. Bosma, *Analysis of regenerative braking efficiency — A case study of two electric vehicles operating in the Rotterdam area*. 2011, pp. 1-6.

[53]    MathWorks. (n.a., 13.11.2018). *Numerical analysis with MATLAB*. Available: https://se.mathworks.com/discovery/numerical-analysis.html

[54]    MathWorks. (n.a., 18.04.2019). *fmincon*. Available: https://se.mathworks.com/help/optim/ug/fmincon.html

[55]    MathWorks. (n.a., 03.11.2018). *Choosing the algorithm*. Available: https://se.mathworks.com/help/optim/ug/choosing-the-algorithm.html#bsbwxm7

[56]    MathWorks. (n.a., 03.11.2018). *Constrained Nonlinear Optimization Algorithms*. Available: https://se.mathworks.com/help/optim/ug/constrained-nonlinear-optimization-algorithms.html

[57]    National Renewable Energy Laboratory. (2018, 28.03.2019). *NREL DriveCAT - Chassis Dynamometer Drive Cycle* [Online]. Available: https://www.nrel.gov/transportation/drive-cycle-tool/

# APPENDICES

## A. MATLAB SCRIPTS OF MESAUREMENTS ON VELOCITY, ALTITUDE AND DISTANCE

```matlab
close all;
clear;
clc;
% % % Script code by Rikke Helene Bækken, 24.05.2019

%Measurment 1 - 08.04.2019 (imported from app):
speedf1=importdata('Speedcorrf.mat')'; %Forward speed, km/h
speedr1=importdata('Speedcorrr.mat')'; %Return speed, km/h
altif1=importdata('altif.mat')'; %Forward altitude, m
altir1=importdata('altir.mat')'; %Return altitude, m
stoptf1=importdata('stoptf.mat')'; %Forward stop time, s
stoptr1=importdata('stoptr.mat')'; %Retrun stop time, s
disf1=importdata('disf.mat')'; %Forward distance, km
disr1=importdata('disr.mat')'; %REturn distance, km

jj1 = find(speedf1 == 0);
ii1 = find(speedr1 == 0);
vf1 = speedf1(sort([find(speedf1),jj1,repelem(jj1,stoptf1-1)]));
vr1 = speedr1(sort([find(speedr1),ii1,repelem(ii1,stoptr1-1)]));
v1 = [vf1 vr1];

hf1 = altif1(sort([find(speedf1),jj1,repelem(jj1,stoptf1-1)]));
hr1 = altir1(sort([find(speedr1),ii1,repelem(ii1,stoptr1-1)]));
h1 = [hf1 hr1];

lf1 = disf1(sort([find(speedf1),jj1,repelem(jj1,stoptf1-1)]));
lr1 = disr1(sort([find(speedr1),ii1,repelem(ii1,stoptr1-1)]));
l1 = [lf1 lr1+lf1(end)];

%Time driven:
t1=0:length(v1)-1; %s

%Plot with time axis:
figure;
fig1=plot(t1/60,v1);
ylabel('Velocity (km/h)', 'FontName', 'Calibri','FontSize',20);
set(gca,'fontsize',20);
set(fig1,'LineWidth', 1.5);
hold on
yyaxis right
fig2=plot(t1/60,h1);
grid minor;
set(fig2,'LineWidth', 1.5);
xlabel('Time traveled (min)', 'FontName', 'Calibri','FontSize',20);
ylabel('Altitude (m)', 'FontName', 'Calibri','FontSize',20);
legend('Velocity profil','Altitude profil');

%Plot with km axis:
```

```matlab
figure;
fig2=plot(l1,v1);
ylabel('Velocity (km/h)', 'FontName', 'Calibri','FontSize',20);
set(gca,'fontsize',20);
set(fig2,'LineWidth', 1.5);
hold on
yyaxis right
fig3=plot(l1,h1);
grid minor;
set(fig3,'LineWidth', 1.5);
xlabel('Distance traveled (km)', 'FontName', 'Calibri','FontSize',20);
ylabel('Altitude (m)', 'FontName', 'Calibri','FontSize',20);
legend('Velocity profil','Altitude profil');

%Measurment 2 - 17.04.2019 (imported from app):
speedf2=importdata('Speedcorrf2.mat')';
altif2=importdata('altif2.mat')';
stoptf2=importdata('stoptf2.mat')';
disf2=importdata('disf2.mat')';

jj2 = find(speedf2 == 0);
vf2 = speedf2(sort([find(speedf2),jj2,repelem(jj2,stoptf2-1)]));
v2 = [vf2];

hf2 = altif2(sort([find(speedf2),jj2,repelem(jj2,stoptf2-1)]));
h2 = [hf2];

lf2 = disf2(sort([find(speedf2),jj2,repelem(jj2,stoptf2-1)]));
l2 = [lf2];

%Time driven;
t2=0:length(v2)-1;

%Plot with time axis:
figure;
fig4=plot(t2/60,v2);
ylabel('Velocity (km/h)', 'FontName', 'Calibri', 'Color', [0.8500, 0.3250,
0.0980],'fontsize',20)
set(gca,'fontsize',20);
set(fig4,'LineWidth', 1.5);
hold on
yyaxis right
fig5=plot(t2/60,h2);
grid minor;
set(fig5,'LineWidth', 1.5);
xlabel('Time traveled (min)', 'FontName', 'Calibri','fontsize',20);
ylabel('Altitude (m)', 'FontName', 'Calibri', 'Color', [0.8500, 0.3250,
0.0980],'fontsize',20)
```

```matlab
legend('Velocity profil','Altitude profil','FontName', 'Calibri','Fontsize',20);
xlim([0 37]);

%Plot with km axis:
figure;
fig6=plot(l2,v2);
set(gca,'fontsize',20);
ylabel('Velocity (km/h)', 'FontName', 'Calibri','FontSize',20);
set(fig6,'LineWidth', 1.5);
hold on
yyaxis right
fig7=plot(l2,h2);
grid minor;
set(fig7,'LineWidth', 1.5);
xlabel('Distance traveled (km)', 'FontName', 'Calibri','FontSize',20);
ylabel('Altitude (m)', 'FontName', 'Calibri','FontSize',20);
legend('Velocity profil','Altitude profil');
xlim([0 22]);

%Measurment 3 - 22.04.2019 (imported from app):
speedf3=importdata('Speedcorrf3.mat')';
speedr3=importdata('Speedcorrr3.mat')';
altif3=importdata('altif3.mat')';
altir3=importdata('altir3.mat')';
stoptf3=importdata('stoptf3.mat')';
stoptr3=importdata('stoptr3.mat')';
disf3=importdata('disf3.mat')';
disr3=importdata('disr3.mat')';

jj3 = find(speedf3 == 0);
ii3 = find(speedr3 == 0);
vf3 = speedf3(sort([find(speedf3),jj3,repelem(jj3,stoptf3-1)]));
vr3 = speedr3(sort([find(speedr3),ii3,repelem(ii3,stoptr3-1)]));
v3 = [vf3 vr3];

hf3 = altif3(sort([find(speedf3),jj3,repelem(jj3,stoptf3-1)]));
hr3 = altir3(sort([find(speedr3),ii3,repelem(ii3,stoptr3-1)]));
h3 = [hf3 hr3];

lf3 = disf3(sort([find(speedf3),jj3,repelem(jj3,stoptf3-1)]));
lr3 = disr3(sort([find(speedr3),ii3,repelem(ii3,stoptr3-1)]));
l3 = [lf3 lr3+lf3(end)];

%Time driven:
t3=0:length(v3)-1;

%Plot with time axis both measurement 1 and 3:
%Measurement 1:
```

```matlab
figure;
subplot(2,1,1);
t1f=0:length(vf1)-1;
t1r=length(vf1):(length(vf1)+length(vr1)-1);
fig8=plot(t1f/60,vf1);
ylabel('Velocity (km/h)', 'FontName', 'Calibri','FontSize',20);
set(gca,'fontsize',20);
set(fig8,'LineWidth', 1.5);
ylim([0 80]);
hold on
yyaxis right
fig9=plot(t1f/60,hf1);
grid minor;
set(fig9,'LineWidth', 1.5);
xlabel('Time traveled (min)', 'FontName', 'Calibri','FontSize',20);
ylabel('Altitude (m)', 'FontName', 'Calibri','FontSize',20);
%legend('Velocity profil','Altitude profil');
title('(1)');
%xlim([50 130]);


%Measurement 3:
subplot(2,1,2);
t3f=0:length(vf3)-1;
%t3r=length(vf3):(length(vf3)+length(vr3)-1);
fig10=plot(t3f/60,vf3);
set(gca,'fontsize',20);
ylabel('Velocity (km/h)', 'FontName', 'Calibri','FontSize',20);
set(fig10,'LineWidth', 1.5);
hold on
ylim([0 80]);
yyaxis right
fig11=plot(t3f/60,hf3);
grid minor;
set(fig11,'LineWidth', 1.5);
xlabel('Time traveled (min)', 'FontName', 'Calibri','FontSize',20);
ylabel('Altitude (m)', 'FontName', 'Calibri','FontSize',20);
legend('Velocity profil','Altitude profil', 'FontName', 'Calibri','Fontsize',20);
title('(3)');
%xlim([length(vf3)/60 130]);


%Plot with km axis both measurement 1 and 3:
%Measurement 1:
figure;
subplot(2,1,1);
fig12=plot(l1,v1);
ylabel('Velocity (km/h)', 'FontName', 'Calibri','FontSize',20);
```

```matlab
set(gca,'fontsize',20);
set(fig12,'LineWidth', 1.5);
hold on
ylim([0 80]);
yyaxis right
fig3=plot(l1,h1);
grid minor;
set(fig3,'LineWidth', 1.5);
xlabel('Distance traveled (km)', 'FontName', 'Calibri','FontSize',20);
ylabel('Altitude (m)', 'FontName', 'Calibri','FontSize',20);
legend('Velocity profil','Altitude profil');
title('(1)');
xlim([0 45]);

%Measurement 3:
subplot(2,1,2);
fig13=plot(l3,v3);
ylabel('Velocity (km/h)', 'FontName', 'Calibri','FontSize',20);
set(gca,'fontsize',20);
set(fig13,'LineWidth', 1.5);
hold on
ylim([0 80]);
yyaxis right
fig2=plot(l3,h3);
grid minor;
set(fig2,'LineWidth', 1.5);
xlabel('Distance traveled (km)', 'FontName', 'Calibri','FontSize',20);
ylabel('Altitude (m)', 'FontName', 'Calibri','FontSize',20);
title('(3)');
xlim([0 45]);

%Plot moving average for measurement 1 and 3:
fig=figure;
set(fig,'defaultAxesColorOrder',[[0.8500, 0.3250, 0.0980]]);
grid minor;
set(gca,'LineWidth', 1.5);
M1h = movmean(h1,[145 145]);
M3h = movmean(h3,[145 145]);
M1v = movmean(v1,[145 145]);
M3v = movmean(v3,[145 145]);
fig14=plot(t1/60,M1v,'Color',[0, 0.4470, 0.7410]);
set(gca,'fontsize',20);
hold on
fig15=plot(t3/60,M3v,':', 'Color',[0, 0.4470, 0.7410]);
set(fig14,'LineWidth', 1.5);
set(fig15,'LineWidth', 1.5);
ylabel('Velocity (km/h)', 'FontName', 'Calibri', 'fontsize',20, 'Color',[0, 0.4470, 0.7410]);
```

## B. MATLAB SCRIPTS OF DETERMINING SOC, CURRENT AND VOLTAGE

```matlab
close all;
clear;
clc;
% % % Script code by Rikke Helene Bækken, 24.05.2019

%Input data for measurement 1:
h1=importdata('h1.mat'); % Altitude, m
speed1=importdata('v1.mat'); %Velocity, km/h
l1=importdata('l1.mat'); %Distance, km
v1=(speed1)*1000/3600; %Velocity, m/s
t1=0:length(speed1)-1; %Time taken to drive route, sec
a1=diff([v1 0])./diff([t1 t1(end)+1]); %Acceleration, m/s^2
a1(a1>5.4)=5.4;
a1(a1<-5.4)=-5.4;

%Air resistance force:
rho=1.2; %Air density (kg/m^3)
Cd=0.79; %Aerodynamic drag coefficient
Af=8.5; %Frontal area of bus (m^2)
Fair=((1/2)*rho*Cd*Af).*(v1.^2); %N
diffh1=diff([h1 h1(end)]); %m
diffl1=diff([l1 l1(end)]*1000); %m

%Gradient resistance force:
sintheta=(diffh1./diffl1); %rad
sintheta(isinf(sintheta))=0; %replace inf value
sintheta(isnan(sintheta))=0; %replace nan value
theta=asin(sintheta); %rad
theta=real(theta); %real values, rad
m=29000; %<-case 1,2 and case 3,4=28260.8; %mass of total bus including passernger
load
g=9.81; %gravitational acceleration, m/s^2
Fgrad=m*g*sin(theta); %N

%Rolling resistance force:
Crr=0.0098; %Rolling resistance coefficient
Froll=m*g*Crr*cos(theta); %N

%Total force and total tractive power on the bus:
Fsum=(Fair+Froll+Fgrad+m*a1); %N
Ptract=(Fsum.*v1)/1000; %kW

%Plot road angle:
figure;
fig1=plot(t1/60,theta*15.91549430919); %convert from rad to %
set(gca,'fontsize',20);
grid minor;
xlabel('Time (min)', 'FontName', 'Calibri','fontsize',20);
ylabel('Road angle (%)', 'FontName', 'Calibri','fontsize',20);
xlim([0 130]);
ylim([-11.5 7]);
```

```matlab
%Plot resistance force of bus:
figure;
fig2=plot(t1/60,Fsum/1000);
%figure;
%fig3=plot(t1/60,Ptract);
plot(t1/60,Fair/1000);
hold on
plot(t1/60,Froll/1000);
plot(t1/60,Fgrad/1000);
set(gca,'fontsize',20);
grid minor;
xlabel('Time (min)', 'FontName', 'Calibri','fontsize',20);
ylabel('F (kN)', 'FontName', 'Calibri','fontsize',20);
legend('F_{air}','F_{roll}','F_{grad}','Fontname','Calibri','Fontsize',20);
xlim([0 125]);
%ylim([-5200 2000]);

%Plot velocity of bus:
figure;
fig4=plot(t1/60,(v1*3600/1000)); %convert from m/s to km/h
set(gca,'fontsize',20);
grid minor;
xlabel('Time (min)', 'FontName', 'Calibri','FontSize',20);
ylabel('Speed (km/h)', 'FontName', 'Calibri','FontSize',20);

%Plot acceleration of bus:
figure;
fig5=plot(t1/60,a1);
hold on
set(gca,'fontsize',20);
grid minor;
xlabel('Time (min)','FontSize',20,'FontName','Calibri');
ylabel('Acceleration (m/s^{2})','FontSize',20,'FontName','Calibri');
xlim([0 130]);

%Powered driving:
Pacc=15; %Accessory load,kW
nwh=0.99; %Wheel efficiency
nfd=0.98; %total drive efficiency
nmot=0.88; %Motor efficiency
nbatt=0.98; %Battery efficiency
n=nwh*nfd*nmot*nbatt;
Pdis=Pacc+(abs(Ptract)/(n)); %kW

%Breaking w/regeneration:
nre=0.65;
Preg=(Pacc-(abs(Ptract)))*nre; %kW
amax=-3; %the maximum acceleration for when the regenerative braking system can
convert kinetic energy, m/s^2
vmin=5; %the minimum velocity for when the regenerative braking system can convert
kinetic energy into electric energy, m/s
```

```matlab
%Recharging event:
Pc1=600; %Charging power from charger 1 (kW)
nchgr=0.97; %Charger efficiency
Pchg=Pc1*nchgr; %(kW)

%Energy in battery at a given time:
    for u=1:length(t1)
    if Ptract(u)==0  %this may change when a charger is there.
        Pbatt(u)=Pacc; %Idle
    elseif Ptract(u)<0 && v1(u)>vmin && a1(u)>amax
        Pbatt(u)=Preg(u); %Breaking w/regen
    elseif Ptract(u)<0 && v1(u)<vmin || Ptract(u)<0 && a1(u)<amax
        Pbatt(u)=Pacc; %Breaking wo/regen
    else
        Pbatt(u)=Pdis(u); %Driving mode
    end
    end

%Plot tractive energy and energy in battery:
%Pbatt1=importdata('Pbatt3.mat');
figure;
fig6=plot(t1/60,Pbatt, 'Color', [0.8500, 0.3250, 0.0980]);
%hold on
%fig7=plot(t1/60,Ptract);
set(gca,'fontsize',20);
grid minor;
xlabel('Time (min)', 'FontName', 'Calibri','FontSize',20);
ylabel('Power (kW)', 'FontName', 'Calibri','FontSize',20);
xlim([0 130]);
%ylim([-4500 1700]);

%State of charge calculaption:
Ebatt=275.4; %<-case 1,2 case 3,4=200, Battery capacity, kWh
soc1(1)=Ebatt*0.8; %<-case1 case 2,3,4=0.7 Initial energy in battery, kWh

for j=2:length(t1)
    soc1(j)=soc1(j-1)-(Pbatt(j-1)/3600); %SOC in kWh
end

%Determination of SOC for measurement 1 and 3:
SOC1=soc1./Ebatt; %SOC in % for mes. 1
SOC3=importdata('SOC3.mat'); %SOC in % for mes.3, wo/charging stations
%SOC1=importdata('SOC1case1.mat'); case 1, wo/charging stations

%Input data for measurement 3:
t3=0:length(SOC3)-1;
v3=importdata('v3.mat');

%Plot state of charge in %:
figure;
fig8=plot(t1/60,SOC1*100);
```

```matlab
hold on
fig9=plot(t3/60,SOC3*100);
set(gca,'fontsize',16);
set(fig8,'LineWidth',3);
set(fig9,'LineWidth',3,'color',[0.9290, 0.6940, 0.1250]);
for u=1:length(t1) %marks on stops along route, mes 1
    if v1(u)==0
        U(u)=SOC1(u)*100;
    else
        U(u)=nan;
    end
end
for o=1:length(t3) %marks on stops along route, mes 3
    if v3(o)==0
        O(o)=SOC3(o)*100;
    else
        O(o)=nan;
    end
end
fig10=plot(t1/60,U); %plot stops along route, mes 1
hold on
fig11=plot(t3/60,O); %plot stops along route, mes 3
set(fig10,'LineWidth', 4, 'Color', [0.8500, 0.3250, 0.0980]);
set(fig11,'LineWidth', 4, 'Color', [0.8500, 0.3250, 0.0980]);

grid minor;
xlabel('Time (min)', 'FontName', 'Calibri','fontsize',20)
ylabel('SOC (%)','FontName', 'Calibri','fontsize',20);
legend('Measurement 1', 'Measurement 3','Stop','FontName','Calibri','fontsize',20);
xlim([0 130]);

%Calculating current in NMC li-ion battery:
Umaxcell=4.1; %Maximal voltage in one cell, V
Uterminal=3.6; %Terminal voltage in one cell, V
Qbatt=Ebatt*1000/Uterminal; %Total battery capacity, Ah
Umaxtot=600; %Total maximal voltage, V
cellnumber=Umaxtot/Umaxcell; %Number of cells in parallel

%Determining VOC in battery:
%soct1=importdata('soctcase1wcharging.mat')/Ebatt; %SOC w/charging stations
soct1=SOC1; %SOC wo/charging stations;
%soct1=importdata('SOC1tnewcase1.mat')/100; %SOC w/charging stations;

e=3.5;
b=-0.0334;
c=-0.106;
d=0.7399;
M=1.402;
n=2;
lg=(-log(soct1));
lgg=lg.^(M);
```

```matlab
Voc=e+b*lg+c.*soct1+d*exp((n)*(soct1-1)); %open circuit voltage, V
Vtot=Voc*cellnumber; %Total VOC in battery pack, V

%Determining current in battery:
chargeload=importdata('ploadgrid1case1.mat'); %Load on battery w/charging stations
ploadtot=plus(-chargeload,Pbatt); %Load on battery w/charging stations
Vmax=cellnumber*Umaxcell; %Total maximum battery voltage, V
ploadtot=[ploadtot 0];
%I1=ploadtot*1000/Vmax; %W/charging stations, -I = discharge mode

%Pbatt=[Pbatt 0]; %Wo/charging
I1=Pbatt*1000/Vmax; %Wo/charging stations

%Determining the total terminal voltage in the battery:
R0=0.01; % Internal resistance, ohm
Vterminal1=Vtot-R0*I1;
Vtest1=importdata('Vtest1.mat'); %Vtot+R0*I1
c=(Pchg*1000/Uterminal)/Qbatt; %Charging rate (c-rate)

%Plot current in battery:
Vterminal3=importdata('Vterminal3.mat'); %wo/charging stations
Voc3=importdata('Voc3.mat');
I3=importdata('I3.mat'); %wo/charging stations

figure;
tt=0:1:length(t1);
fig12=plot(t1/60,I1);
%hold on
%fig13=plot(t3/60,I3);
grid minor;
%set (gca, 'xdir', 'reverse' ); %for use when plotting according to SOC
%set(fig13,'color',[0.9290, 0.6940, 0.1250]);
xlabel('Time (min)', 'FontName', 'Calibri','Fontsize',20);
ylabel('Current (A)','FontName', 'Calibri','FontSize',20,'Color','k');
set(gca,'fontsize',20);
xlim([0 130]);
ylim([-2000 3500]);
%legend('Measuremet 1', 'Measurement 3','fontsize',20,'FontName','calibri');

%Plot voltage in battery:
figure;
fig14=plot(t1/60,Vterminal1);
%hold on
%fig15=plot(t3,Vterminal3);
%set (gca, 'xdir', 'reverse' ); %for use when plotting according to SOC
grid minor;
%set(fig15,'color',[0.9290, 0.6940, 0.1250]);
xlabel('Time (min)', 'FontName', 'Calibri','Fontsize',20);
ylabel('Terminal voltage (V)','FontName', 'Calibri','FontSize',20,'Color','k');
set(gca,'fontsize',20);
%legend('Measuremet 1', 'Measurement 3','fontsize',20,'FontName','calibri');
```

```matlab
xlim([0 130]);
%xlim([38 80]);

%Plot voc according to soc:
% figure;
% fig16=plot(SOC1*100,Voc);
% hold on
% fig17=plot(SOC3*100,Voc3);
% set(fig16, 'linewidth',1.5);
% set(fig17,'linewidth',1.5);
% grid minor;
% set (gca, 'xdir', 'reverse' ); %for use when plotting according to SOC
% set(fig17,'color',[0.9290, 0.6940, 0.1250]);
% xlabel('SOC (%)', 'FontName', 'Calibri','Fontsize',20);
% ylabel('VOC (V)','FontName', 'Calibri','FontSize',20,'Color','k');
% set(gca,'fontsize',20);
% xlim([38 80]);
% legend('Measuremet 1', 'Measurement 3','fontsize',20,'FontName','calibri');
```

## C. DATA FOR SUBSTATIONS AT GRORUD AND SNARØYA

Data used with permission from Werner Kalusen, contact person in Hafslund Nett As. Red box indicates which substation that was mentioned in the study.

### Snarøya

Rundt Snarøya endeholdeplass er det i dag 3 nettstasjoner som ligger relativt nært. Disse heter B1773, B1699 og B1460. Høyspenningsnettet er klassifisert som 11 kV med en faktisk spenning på 10 300 V.

#### Nettstasjon 1773 (kiosk)

| Beskrivelse | Verdi |
| --- | --- |
| Transformatorstørrelse i dag | 315 kVA |
| Maksimal transformatorstørrelse | 500 kVA |
| Teoretisk belastning tilkoblet i dag (ca.) | 275 kVA |
| Lavspenning | 230 V |

#### Nettstasjon 1699 (kiosk)

| Beskrivelse | Verdi |
| --- | --- |
| Transformatorstørrelse i dag | 200 kVA |
| Maksimal transformatorstørrelse | 500 kVA |
| Teoretisk belastning tilkoblet i dag (ca.) | 175 kVA |
| Lavspenning | 230 V |

#### Nettstasjon 1460 (kiosk)

| Beskrivelse | Verdi |
| --- | --- |
| Transformatorstørrelse i dag | 500 kVA |
| Maksimal transformatorstørrelse | 500 kVA |
| Teoretisk belastning tilkoblet i dag (ca.) | 385 kVA |
| Lavspenning | 230 V |

### Om lastberegninger

Lastberegninger er basert på teoretiske uttak av strøm hos hver kunde. Tallet sier f.eks. ikke noe om forbrukstopper eller tap i transformator og forsyningskabler.

---

Disse tallene er hentet ut 2019-04-12.

### Grorud

Rundt Grorud endeholdeplass er det i dag 4 nettstasjoner relativt nært. Disse heter 2910, 0196, 3335 og 5355 (se kart). Høyspenningsnettet er klassifisert som 11 kV med en faktisk spenning på 10 500 V.

#### Nettstasjon 2910 (kiosk)

| Beskrivelse | Verdi |
| --- | --- |
| Transformatorstørrelse i dag | 300 kVA |
| Maksimal transformatorstørrelse | 315 kVA |
| Teoretisk belastning tilkoblet i dag (ca.) | 200 kVA |
| Lavspenning | 230 V |

#### Nettstasjon 0196 (kiosk)

| Beskrivelse | Verdi |
| --- | --- |
| Transformatorstørrelse i dag | 800 kVA |
| Maksimal transformatorstørrelse | 800 kVA |
| Teoretisk belastning tilkoblet i dag (ca.) | 245 kVA |
| Lavspenning | 400 V |

#### Nettstasjon 3335 (kiosk)

| Beskrivelse | Verdi |
| --- | --- |
| Transformatorstørrelse i dag | 300 kVA |
| Maksimal transformatorstørrelse | 500 kVA |
| Teoretisk belastning tilkoblet i dag (ca.) | 235 kVA |
| Lavspenning | 230 V |

#### Nettstasjon 5355 (rom i bygg, 2 transformatorer)

| Beskrivelse | Verdi |
| --- | --- |
| Transformatorstørrelse i dag | 1600 kVA / 1600 kVA |
| Maksimal transformatorstørrelse | Rom i bygg* |
| Teoretisk belastning tilkoblet i dag (ca.) | 1300 kVA / 300 kVA |
| Lavspenning | 230 V / 230 V |

*Hvor stor og hvor mange transformatorer en nettstasjon av typen tom i bygg kan ha varierer veldig med størrelsen på rommet, døren inn, ventilasjon osv.

## D. MATLAB SCRIPTS OF OPTIMIZATION MODEL

**Main script containing optimization model:**

```matlab
close all;
clear;
clc;
% % % Script code by Rikke Helene Bækken, 24.05.2019

%Information:x=Pchg;

%Data of bus:
Ebatt=275.4;%<-case1,2,3 case4=200 %Battery capacity, kWh
sl=0.8;%<-case1,2 case3,4=0.7     %Initial level of battery
ul=0.8;                           %Upper limit of battery
ll=0.1;                           %Lower limit of battery
e_init = Ebatt*sl;                %Initial energy in battery, kwh
Pacc=15;                          %Assesory load, kW
socend=0.8;%<-case1,2 case3,4=0.7 %desired energy level at the end of the route
Pacc=15;                          %Assesory load, kW

%Data of chargers:
P1=600;%<-case1,2,3 case4=500     %Maximal charging power, kW
nchg=0.97;                        %Efficiency of charger
P1chg=P1*nchg;                    %Charging power corrigated by efficiency, kW

%Data of battery and tractive power(measurement1):
SOC1=importdata('SOC1case1.mat'); %SOC w/Pacc acorrding to time
Ptract1=importdata('Ptract1case1.mat');  %Tractive power w/Pacc according to time
Pbatt1=importdata('Pbatt1case1.mat');    %Battery power wo/Pacc when stopping
according to time
Pbattorg1=importdata('Pbattorg1case1.mat'); %Battery power w/Pacc according to time

%Time stopped at each stop along route:
T=Ptract1;
T(1)=1;
T(Ptract1<0)=1;
T(Ptract1>0)=1;
T(Ptract1==0)=0;
T(end+1) = 1;
locrise = find([0 diff(T == 0) > 0]);
locFall = find([diff(T==0) < 0 0]);
locRise = [1,locrise];
nstop=length(locrise);
n=ones(1,nstop);
locnum = locFall-locrise;
locT=n./locnum;
for i = 1:numel(locrise)
   T(locrise(i):locFall(i)) = locT(i);
end
T(T==1) = [];
T=1./T;
y = cumsum(Ptract1==0 | [true,Ptract1(1:end-1)==0]);
```

```matlab
Psum = abs(nonzeros(accumarray(y(:),Pbatt1(:))));
z=Ptract1==0;
Start = strfind([0,z],[0 1]);
End = strfind([z,0],[1 0]);
stopt= End - Start + 1;
T=stopt;            %Time stopped at a stop i
nstop=length(T);    %Number of stops

%Reducing regulation time to 10 minutes:
r=10*60; %<-case1,3,4 case2=7*60 Regulation time, s
a=ones(1,length(T)+2);
a(27)=(T(27)-r);
a(71)=(T(end)-r);
a(a==1)=T;
a(28)=r;
a(end)=r;
T=a; %New stop time that may be used to charge, s
b=ones(1,length(Psum)+2);
b(27)=0;
b(71)=0;
b(b==1)=Psum;
Psum=b; %New Psum as a result of new stop time, kWs

%Upper and lower bounds:
x0 = ones(size(T));         %Guessing the charging power
lb = zeros(size(x0));       %Lower bound is zero kW
ub = P1chg*ones(size(x0)); %Upper bound is maximum charging power, kW
ub(27)=0;                   %The first minutes at Snarøya is not possible to charge
ub(71)=0;                   %The first minutes at Grorud T is not possible to charge

%Optimization - fmincon:
options=optimset('Algorithm', 'active-set');
[x,fval]=fmincon(@(x) obj(x),x0,[],[],[],[], lb, ub, @(x)
cons(x,Ebatt,ll,sl,ul,T,Psum,Pacc,socend),options);

%Optimization - ga:
%x=optimvar('x','LowerBound',0,'UpperBound',1,'Type','integer');
%options=optimoptions('ga');
%[x,fval]=ga(@(x) obj(x,T),count,[],[],[],[], lb, ub,@(x)
cons(x,Ebatt,ll,sl,Pmec,P,P1chg,ul),1:count,options);

%Relax x:
      X=x;
  for k = 1:length(x)
    if x(k) <= 1e-10
       X(k) = 0;
    else
       X;
    end
```

```matlab
    end

 %Energy in battery according to stop:
 E(1)=Ebatt*sl; %-(T(1)*Pacc/3600);
 for j=2:length(T)+1
     E(j)=min(E(j-1)+(X(j-1)*T(j-1)-Pacc*T(j-1))/3600,Ebatt)-(Psum(j-1)/3600); %SOC
in kWh
 end
 SOCnew=E./Ebatt*100; %SOC in %

%Transform x according to bus stops to x according to time:
for i =1:length(T)
    if X(i)>0
        Tt(i)=T(i)-1;
    else
        Tt(i)=T(i);
    end
end

XX=repelem(X,T);
xx=Ptract1;
xx(Ptract1==0)=XX;
xx(Ptract1>0)=0;
xx(Ptract1<0)=0;

%Energy in battery according to time:
Et(1)=Ebatt*sl;
 for jj=2:length(Pbattorg1)+1
 Et(jj)=min(Et(jj-1)+(xx(jj-1))/3600,Ebatt)-(Pbattorg1(jj-1)/3600); %SOC in kWh
 end
SOCtnew=(Et./Ebatt)*100; %SOC in %

%Power load on battery and grid:
ploadbatt=xx;                     %Load on battery due to charging, kW
ploadgrid=xx/nchg;                %Load on grid due to charging, kW
figure;
area(ploadgrid);

%Validation process:
Erq=(Ebatt*ll-SOC1(end));    %Minimum required energy for the bus, kWh
Erc=dot(x,T)/3600;           %Energy charged, kWh

%Simple plot of SOC in kWh:
figure;
i=0:1:length(E)-1; %sec according to stop
ii=0:1:length(Et)-1; %sec accoridng to stop
plot(i,E);
%hold on
%plot(ii,Et);
```

```matlab
 end
%Energy in battery according to stop:
E(1)=Ebatt*sl; %-(T(1)*Pacc/3600);
for j=2:length(T)+1
    E(j)=min(E(j-1)+(X(j-1)*T(j-1)-Pacc*T(j-1))/3600,Ebatt)-(Psum(j-1)/3600); %SOC
in kWh
end
SOCnew=E./Ebatt*100; %SOC in %

%Transform x according to bus stops to x according to time:
for i =1:length(T)
    if X(i)>0
        Tt(i)=T(i)-1;
    else
        Tt(i)=T(i);
    end
end
XX=repelem(X,T);
xx=Ptract1;
xx(Ptract1==0)=XX;
xx(Ptract1>0)=0;
xx(Ptract1<0)=0;
%Energy in battery according to time:
Et(1)=Ebatt*sl;
 for jj=2:length(Pbattorg1)+1
 Et(jj)=min(Et(jj-1)+(xx(jj-1))/3600,Ebatt)-(Pbattorg1(jj-1)/3600); %SOC in kWh
 end
SOCtnew=(Et./Ebatt)*100; %SOC in %

%Power load on battery and grid:
ploadbatt=xx;                    %Load on battery due to charging, kW
ploadgrid=xx/nchg;               %Load on grid due to charging, kW
figure;
area(ploadgrid);

%Validation process:
Erq=(Ebatt*ll-SOC1(end));    %Minimum required energy for the bus, kW
Erc=dot(x,T)/3600;           %Energy charged, kWh

%Simple plot of SOC in kWh:
figure;
i=0:1:length(E)-1; %sec according to stop
ii=0:1:length(Et)-1; %sec accoridng to stop
plot(i,E);
%hold on
%plot(ii,Et);

%Plot optimization:
SOC1tnew=SOCtnew; %importdata('SOC1tnewcase1.mat');
```

```matlab
pload11=ploadgrid; %importdata('ploadgrid1case1.mat');
% SOC1tnew=importdata('SOC1tnewcase1reg7.mat'); %for regulation time 7 min
% pload11=importdata('ploadgrid1case1reg7.mat'); %for regulation time 7 min
v11=importdata('v1.mat');
pload1=[pload11 0];
v1=[v11 0];
t1=0:1:length(SOC1tnew)-1; %time,sec

fig=figure;
set(fig,'defaultAxesColorOrder',[0 0 0 ;[0.4660, 0.6740, 0.1880]]);
graph(1)=plot(t1/60,SOC1tnew); %min
set(graph(1),'LineWidth',3,'color',[0, 0.4470, 0.7410]);
hold on
for u=1:length(t1) %plot stop
    if v1(u)==0
        U(u)=SOC1tnew(u);
    else
        U(u)=nan;
    end
    if pload1(u)>0.01 %plot load
        p(u)=Et(u)/Ebatt*100;
    else
        p(u)=nan;
    end
end
graph(2)=area(t1/60,p); %plot stop
set(graph(2),'Facecolor',[0.4660, 0.6740,
0.1880],'FaceAlpha',0.4,'edgecolor','none');
graph(3)=plot(t1/60,U); %plot load
set(graph(3),'LineWidth', 4, 'Color', [0.8500, 0.3250, 0.0980]);
grid minor;
xlabel('Time (min)', 'FontName', 'Calibri','fontsize',20)
ylabel('SOC (%)','FontName', 'Calibri','fontsize',20);
xlim([0 130]);
ylim([20 90]);
hold on

yyaxis right
graph(4)=area(t1/60,pload1);
set(graph(4),'LineWidth', 1.5, 'FaceAlpha', 1,
'edgecolor','none','FaceColor',[0.4660, 0.6740, 0.1880]);
ylabel('Charging power (kW)', 'FontName','Calibri', 'Color',[0.4660, 0.6740,
0.1880],'fontsize',20);
legend(graph(1:3),'Driving mode','Charging mode','Stopping
mode','FontName','Calibri','fontsize',20);
an = annotation('textbox','String','hei','FontName',
'Calibri','Fontsize',18,'EdgeColor','none','Color',[0.4660, 0.6740, 0.1880]);
set(gca,'fontsize',20);
ylim([0 1300]);
```

**Sub script containing objective function:**

```matlab
function f=obj(x)
% % % Script code by Rikke Helene Bækken, 24.05.2019
f=sum(x);
```

**Sub script containing constraint functions:**

```matlab
function [c, ceq]=cons(x,Ebatt,ll,sl,ul,T,Psum,Pacc,socend)
% % % Script code by Rikke Helene Bækken, 24.05.2019
% Side constraint (c) written as something that should be <= 0
% Side constraint (ceq) written as something that should be = 0

E(1)=Ebatt*sl; %Inital energy in battery
 for j=2:length(T)+1
     E(j)=min(E(j-1)+(x(j-1)*T(j-1)-Pacc*T(j-1))/3600,Ebatt)-(Psum(j-1)/3600); %SOC
in kWh

     %Inequality constraints:
     c(1)=Ebatt*ll-E(j-1);     %Energy should never exceed the lower limit, kWh
     c(2)=Ebatt*socend-E(end); %Desired energy in the end of the route, kWh
     c(j)=E(j)-Ebatt*ul; %If a charging stations is placed, the
     %energy should never be above the upper limit, kWh

     %Equality constraints:
     if E(j-1)>ul*Ebatt
        ceq(j)=-x(j-1); %A charging stations should not be placed if the energy in
the battery is too high, kWh
     else
        ceq(j)=0;
     end
 end
 end
```

### E. VERYFING THE OPTIMIZATION MODEL

For the verification process of the optimization model DriveCat was used as the drive cycle analysis tool and a driving cycle from Braunschweig city, Germany was selected [57]. The characteristics of the driving pattern and route specifications are presented in Table 11 and the driving cycle according to time is shown in Figure 40.

*Table 11. Braunschweig city driving cycle; urban bus driving with frequent stops [57]*

| Parameter | Value | Unit |
|---|---|---|
| Time | 29 | Minutes |
| Distance | 10.88 | Km |
| Max speed | 58.26 | Km/h |
| Average speed (including stops) | 22.53 | Km/h |
| Average driving speed | 30.09 | Km/h |
| Stops | 29 | # |
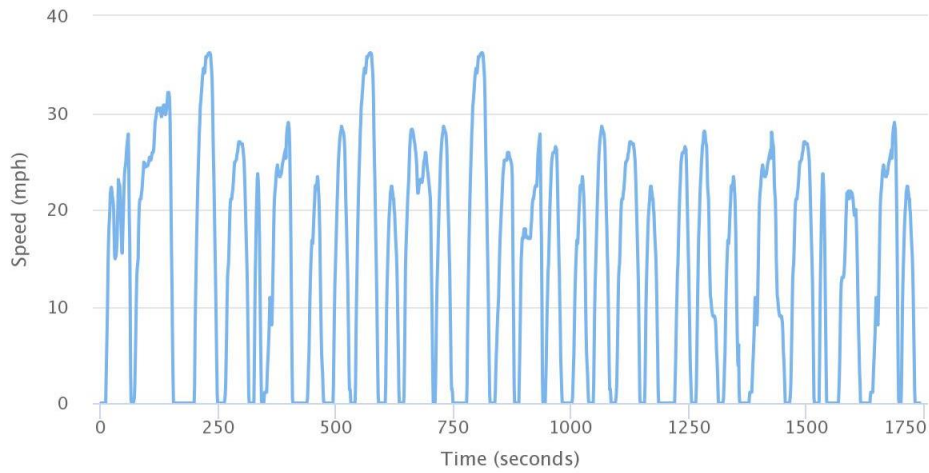


*Figure 40. Driving cycle for a transient bus in Braunschweig city*
*© 2019 NREL [57]*

## F. VELOCITY AND ALTITUDE PROFILE FOR THE MEASUREMENTS

Driving cycle for measurement 2:
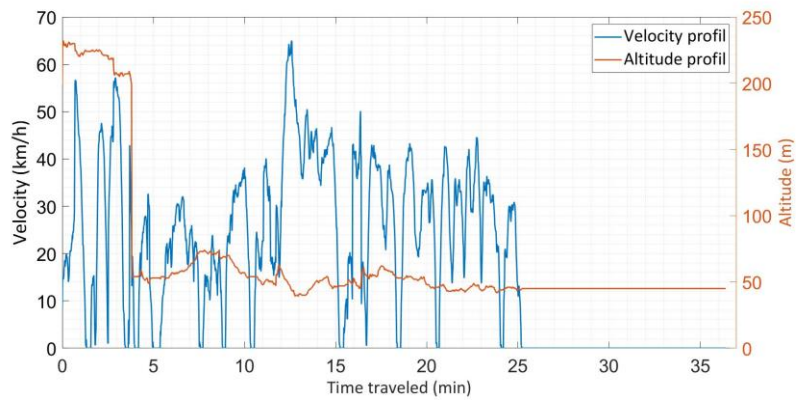
*Figure 41. Driving cycle for measurement 2 for bus line 31 according to time*
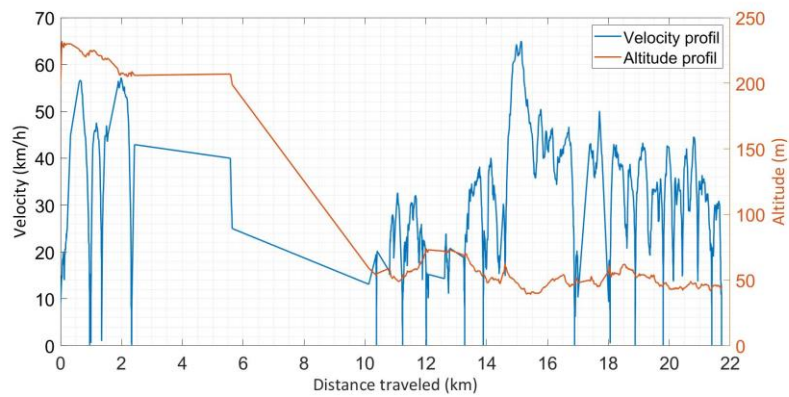
*Figure 42. Driving cycle for measurement 2 for bus line 31 according to distance*

Driving cycle for measurement 1 and 3 according to distance:
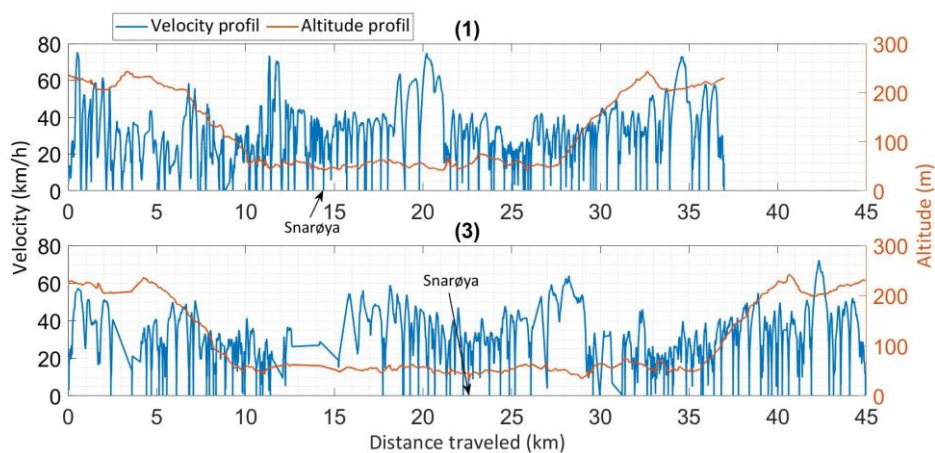
*Figure 43. Driving cycle for measurement 1 and 3 for bus line 31 according to distance*

## G. CALCULATED VALUES FOR DETERMINING SOC

Acceleration without corrections for measurement 3:
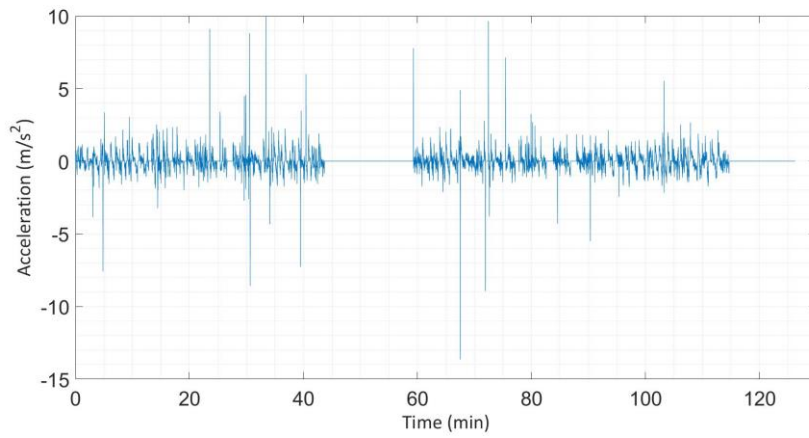


*Figure 44. Acceleration for measurement 3 without correction on the high acceleration values*

Calculations for measurement 1:
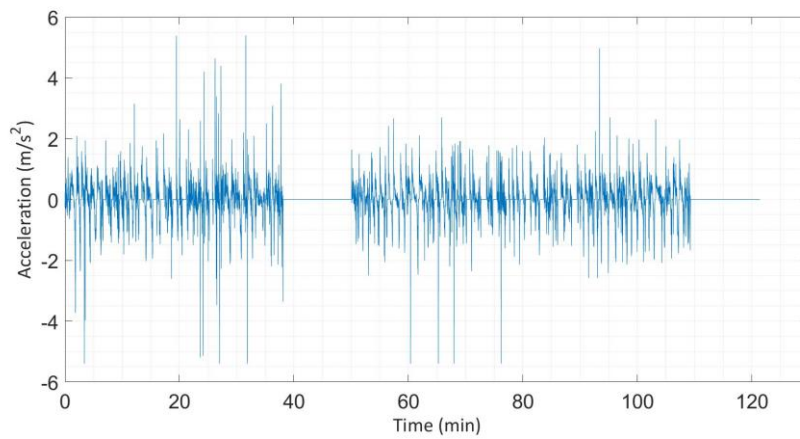


*Figure 45. Acceleration for measurement 1 with corrections regarding high acceleration values*
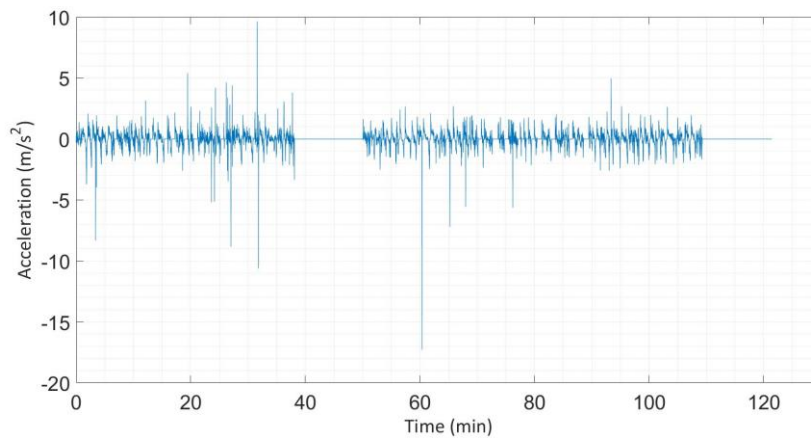


*Figure 46. Acceleration for measurement 1 without correction on the high acceleration values*
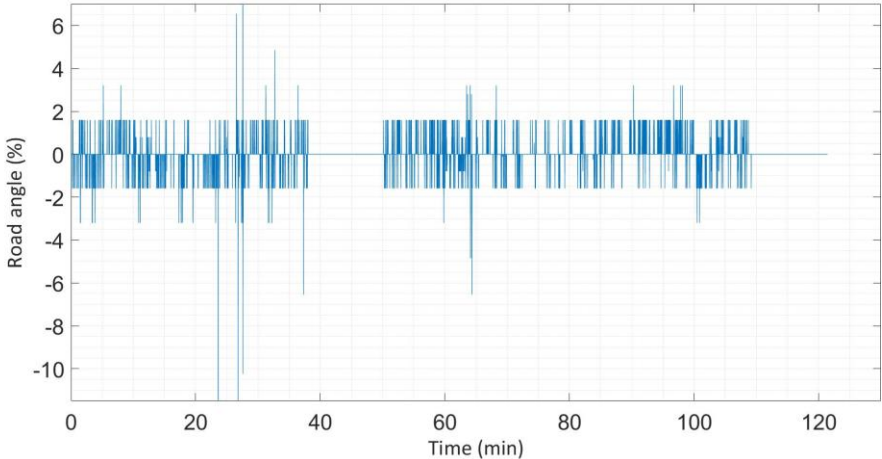
*Figure 47. Road angle for measurement 1*
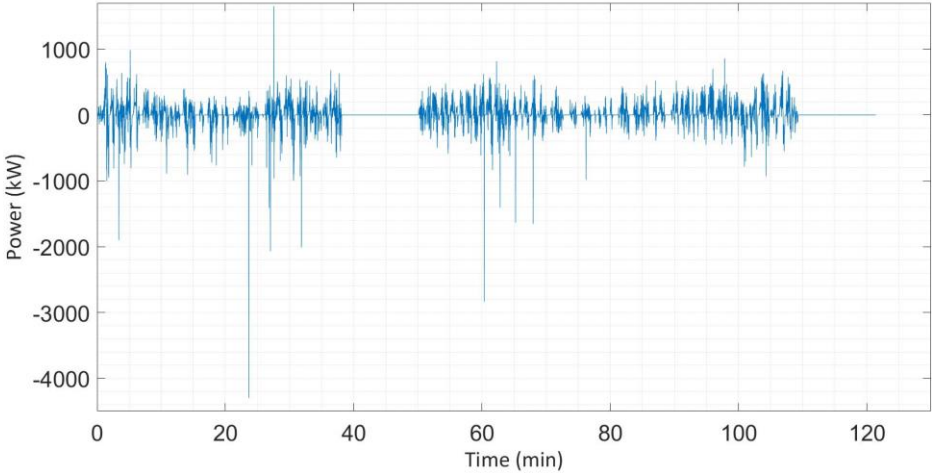


*Figure 48. Tractive power for measurement 1*
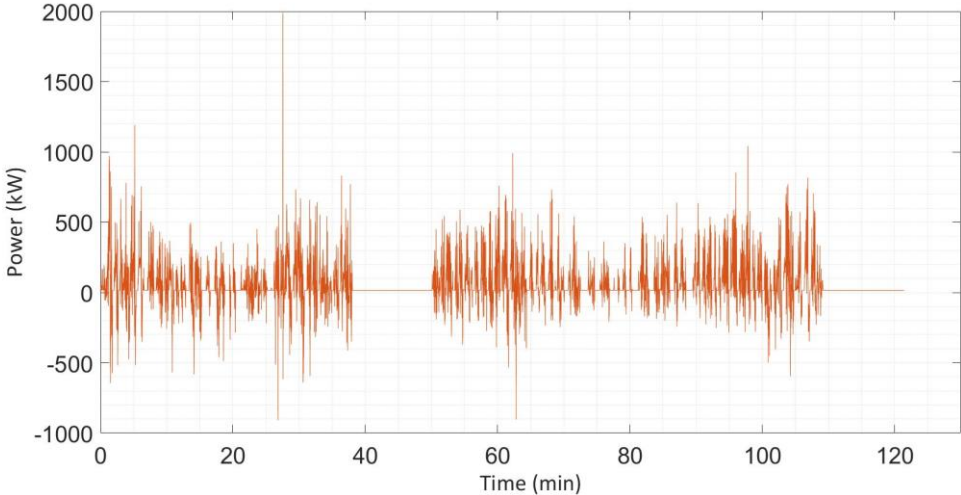


*Figure 49. Battery power for measurement 1*

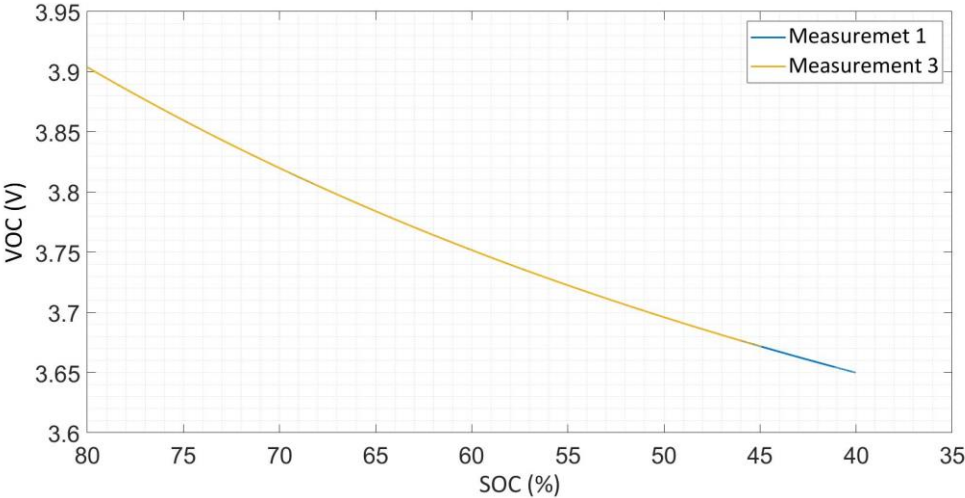## H. OPEN CIRCUIT VOLTAGE FOR MEASUREMENT 1 AND 2



*Figure 50. Open circuit voltage for one NMC battery cell according to SOC*

Note that the open circuit voltage curve in Figure 50 for measurement 1 is covered by the open circuit voltage for measurement 3 as they are identical.

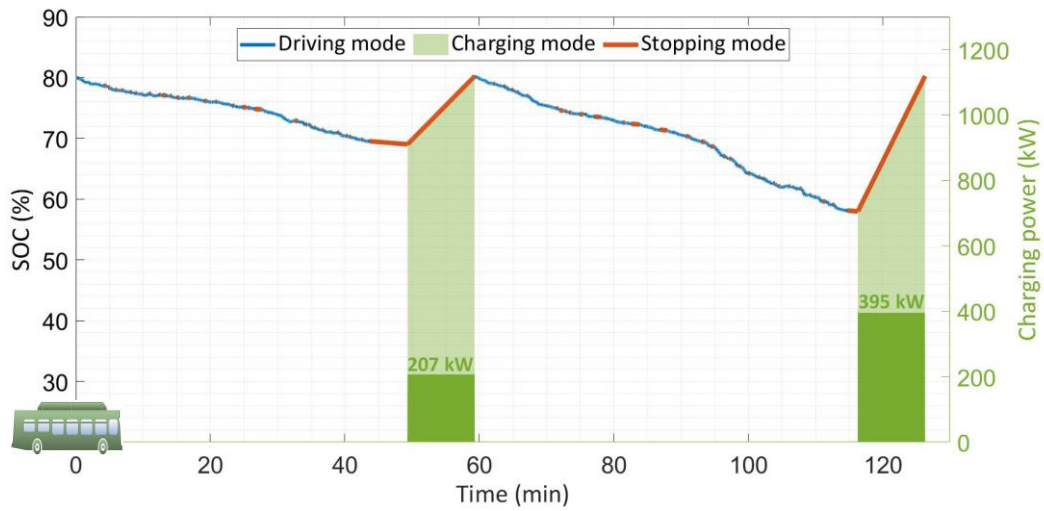## I. OPTIMIZATION OF MEASUREMENT 3 FOR CASE 1, 2 AND 3

Case 1:



*Figure 51. Optimization of measurement 3, case 1*

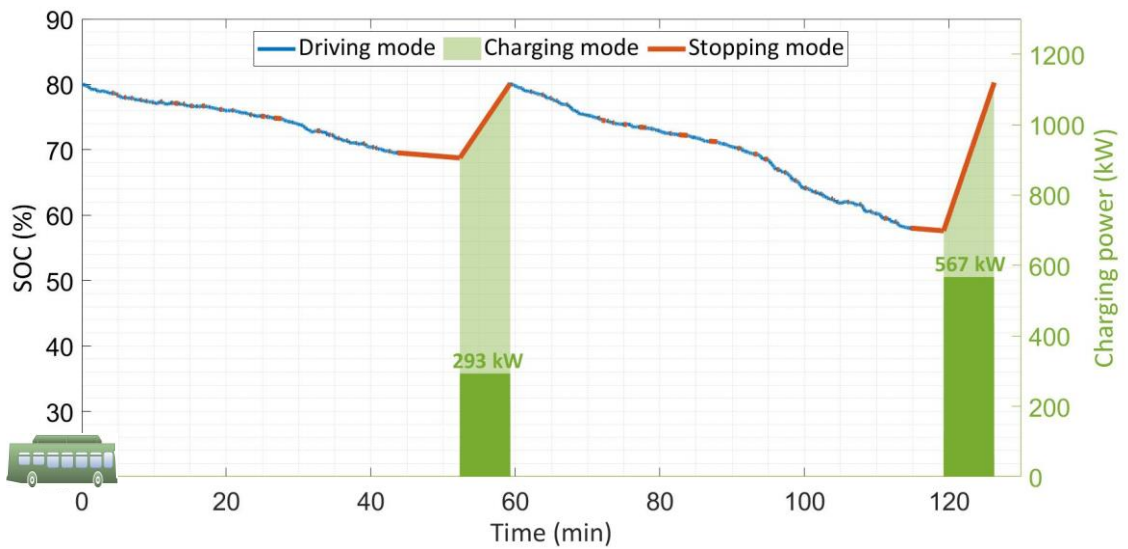Case 2, regulation time of 7 minutes:



*Figure 52. Optimization of measurement 3, case 2*
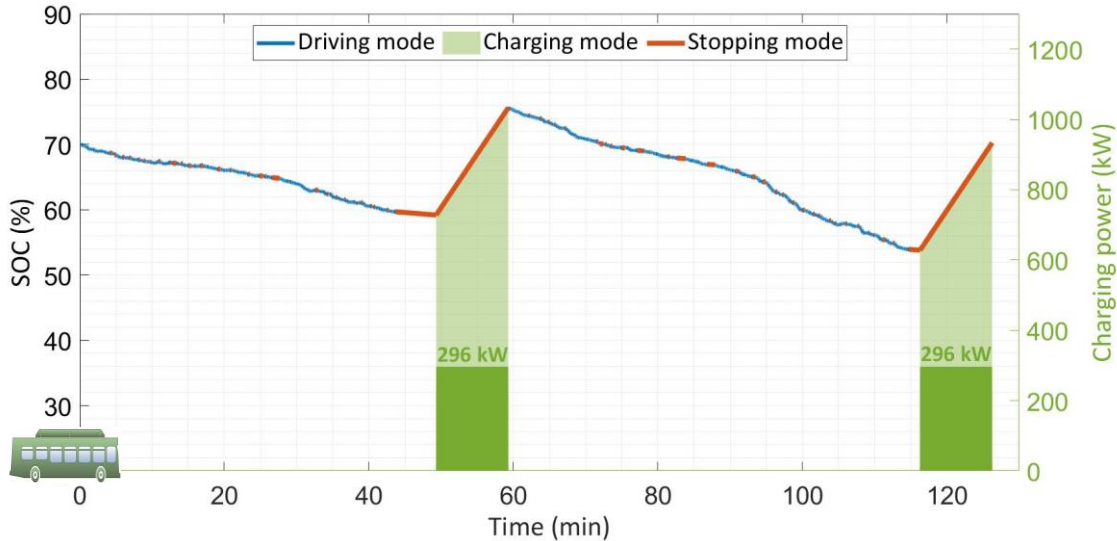
Case 3, initial and end energy in battery at 70 % battery capacity:

*Figure 53. Optimization of measurement 3, case 3*